Shock-wave propagation in the nonuniform interstellar medium

G. S. Bisnovatyi-Kogan

Space Research Institute, 84/32 Profsoyuznaya, Moscow 117810, Russia

S. A. Silich

Main Astronomical Observatory of the National Academy of Sciences of Ukraine, 252650 Kiev, Golosiiv, Ukraine

The development of different analytical and approximate numerical methods for calculations of shock-wave propagation in the inhomogeneous interstellar medium is reviewed. The models of ultracompact H II regions, nonspherical supernova remnants, bubbles produced by stellar winds of hot stars, and expanding supershells are discussed on the basis of these calculations.

CONTENTS

I. INTRODUCTION

Interaction of shock waves with the surrounding gas is a fundamental problem in astrophysics. Shock waves are common in the interstellar medium (ISM) because of a great variety of supersonic motions and energetic events, such as cloud-cloud collisions, bipolar outflow from young protostellar objects, powerful mass loss by massive stars in a late stage of their evolution (stellar winds), supernova (SN) explosions, correlated SNe explosions in OB associations and the central parts of "star burst" galaxies; shock waves are also associated with spiral density waves, radio galaxies, and quasars.

A study of shock-wave propagation is essential for an understanding of the structure, evolution, and energy budget of the interstellar medium. Spiral and irregular galaxies, including the Milky Way, display a variety of large-scale interstellar structures identified as holes and shells in the neutral hydrogen distribution (see reviews by Tenorio-Tagle and Bodenheimer, 1988; Brinks, 1990; Silich, 1990). These objects were first discovered in the Small Magellanic Cloud (SMC) by Hindman (1967) and later were recognized as a characteristic feature of the interstellar medium in our own galaxy by Heiles (1979), who presented a photographic compilation of the neutral hydrogen distribution over a number of small velocity intervals $\Delta V = 2 - 8\,\mathrm{km\,s^{-1}}$. These "snapshots" reveal a number of shells and "supershells" with dimensions of several hundred parsecs and a complex morphology. An infrared shell which is probably connected with the Be 87 association has been discovered by Lozinskaya and Repin (1990). It was suggested this shell might be a result of action on the interstellar gas medium by the stellar wind of Wolf-Rayet and O_f stars.

Later the same structures were discovered in the nearby spirals M31 (Brinks and Bajaja, 1986), M33 (Deul and Hartog, 1990), NGC 55 (Graham and Lawrie, 1982), and irregulars IC 10 (Shostak and van Woerden, 1983), Ho II (Puche *et al.*, 1992), and other galaxies. A program to study the shell structure in dwarf galaxies was recently undertaken by Puche *et al.* (1992; Puche and Westpfahl, 1995). Eight dwarf galaxies of the M81 group—NGC 4214, 3077, UGC 3974, 5666, 4305, 5139, SEXTANS A, and M81DWA—were observed in the radio band with the Very Large Array (VLA). These data show many ex-

 0034-6861/95/67(3)/661(52)/$14.80

panding shells of neutral hydrogen. In the largest dwarfs, traces of induced star formation stimulated by the expansion and collision of the shells are observed. A space correlation of star-forming regions with the edges of the greatest holes in the neutral hydrogen distribution has been observed in the Large Magellanic Cloud (LMC) by Dopita *et al.* (1985). Observational evidence for the initiation of the star-formation process by expanding shells on different spatial scales has been discussed by Elmegreen (1992). In the low-mass dwarf galaxies one large bubble structure dominates the ISM (Puche and Westpfahl, 1995). Spectral evidence for a powerful mass loss (superwind) from the blue compact galaxy SBS0948+532 has been presented by Izotov *et al.* (1994). A spectacular line-emitting bubble of diameter $\approx 1\,\mathrm{kpc}$, with violent gas motion that ranges over $2000\,\mathrm{km\,s^{-1}}$, has been observed in the nuclear region of the galaxy NGC 3079 by Veilleux *et al.* (1994).

In the LMC expanding shells of ionized hydrogen have been revealed by means of H_α images analyzed by Meaburn (1980). In some cases H_α shells coincide with the neutral hydrogen one and represent its inner part ionized by embedded luminous stars.

The largest shells have diameters much greater than the characteristic scale of the gas distribution in the Z direction of the galactic disk and sometimes reach ~ 1 kpc and more. Supershells are also subject to a large-scale galactic shear due to differential rotation of the galactic disk and therefore have a complicated three-dimensional (3D) morphology.

The strongest shock waves in galaxies, apart from the violent phenomena in active galactic nuclei, are produced by supernova explosions. Investigations of supernovae remnants (SNR), which are the observational manifestations of SN shocks, give valuable information about the energetics of the supernova event as well as about the properties of the interstellar medium, where these shocks propagate.

Supernovae are responsible for formation of the hot ($T \sim 10^6\,\mathrm{K}$) rarefied-gas regions in galaxies, representing cavities formed by the SN shock waves. The existence of a hot galactic gas phase in addition to warm ($\sim 10^4\,\mathrm{K}$) and cold ($\sim 100\,\mathrm{K}$) phases was established by McKee and Ostriker (1977).

SNRs are the sources not only of thermal emission of hot gas in optical, UV, and x-ray regions, but also of very strong radio emission, resulting from synchrotron radiation of the relativistic electrons in the magnetic field. That means that SNRs are also accelerational devices in which particles reach relativistic energies $E \gg mc^2$ and thus are important sources of cosmic rays. Particle acceleration in SNR shocks, as well as interstellar shock structure, comprise very broad areas of investigation, which will not be considered here (see Fedorenko, 1983; the reviews of Eilek and Hughes, 1990; and Draine and McKee, 1993).

Shocks from a single supernova and multiple supernovae in OB associations are thought to be important in acceleration of interstellar clouds, as was emphasized by Cowie *et al.* (1981). Now it becomes obvious that the interaction of blastwaves with interstellar clouds plays an important role in the fundamental astrophysical process of star formation. Progress on this complex problem has been made in recent years by Klein *et al.* (1990), Elmegreen (1992), Mac Low *et al.* (1994), and others. The first numerical results were summarized by Klein *et al.* (1994). But many questions remain to be answered.

Recent high-resolution and high-sensitivity radio observations have shown that supernova remnants themselves generally do not posses spherical symmetry. Many SNRs have limb-brightened cylindrical or barrel-like structure, with two regions of low intensity near the top and bottom of the axis of symmetry and with a gradient of radio brightness along the shell. Kesteven and Caswell (1987) have even suggested that the majority of SNRs fall into this category. A number of x-ray and optical remnants show different features of this morphology as well.

Formation of shocks may have resulted not only from explosions, like those of supernovae, but also from long-term continuous acceleration, produced by radiation pressure or hot stellar winds, of coronal origin. Shocks are formed on the boundary between the hot wind and the interstellar gas pushed by it. This boundary may propagate outward or become stationary, probably like that between the solar corona and interstellar gas near the orbit of Pluto (Weigert and Wendker, 1989). Rings around the most luminous stars—such as the O supergiants and Wolf-Rayet stars—are the observational appearance of these interactive shocks (Lozinskaya, 1992). Less intensive shocks also exist around solar-type stars having coronal outflows.

The phenomena observed in newborn stars indicate the existence around these objects of shocks with complicated geometrical structure. Newborn stars, formed after the collapse of rotating gas clouds, are surrounded by discs with the angular momentum of the parent cloud and are strongly convective, producing very strong coronal heating. These conditions lead to the formation of strong nonspherical winds containing jets, which produce a complicated system of shock waves.

The most energetic phenomena in space are probably connected with active galactic nuclei and quasars. In the presence of strong magnetic fields and rotation, explosions accompanied by huge increases in the radiation flux and the flux of relativistic particles lead to formation of directed eruptions observed as jets in many quasars and active galactic nuclei.

The bipolar outflow from protostar objects (see the review of Lada, 1985) and bow shocks surrounding ultracompact H II regions (Mac Low *et al.*, 1991) represent the lower range of the scale for shock-wave phenomena in the inerstellar medium.

The characteristic feature of all these phenomena is their complicated nonspherical morphology. An adequate physical model for them has to include both 2D

and 3D numerical simulations. An accurate description of such events usually requires numerical calculations, which have made progress in recent years. However, the current two-dimensional schemes are very complicated due to the nonlinear character of the hydrodynamical equations and the importance of radiative cooling and gravity for the late stages of an interstellar shock-wave's evolution. The three-dimensional codes that have appeared in the last few years are even more complicated and require long computation times even on the most powerful computers. Therefore we need methods that are easy to work with and could give reasonable accuracy, at least in simulating the shape and dynamics of complex two- and three-dimensional shock waves, although it is true that such approximate methods are usually only valid over a limited parameter regime. Approximate methods may also be useful for assessing the accuracy of more complicated full 2D and 3D calculations.

The description of these semianalytic and approximate methods for calculating shock-wave propagation in the nonuniform interstellar medium, as well as the description of their application to different astrophysical problems, is the main purpose of this review.

II. SPHERICALLY SYMMETRIC SHOCKS

A. Self-similar solutions

1. Equations and conditions for self-similarity. Sedov solution

The basic relations we need to discuss for self-similar problems are the hydrodynamical equations of continuity, motion, and energy conservation (Landau and Lifshitz, 1953; Zeldovich and Raizer, 1966):

$$\begin{aligned}
&\frac{\partial\rho}{\partial t}+\operatorname{div}(\rho\mathbf{u})=0,\\
&\frac{\partial\mathbf{u}}{\partial t}+(\mathbf{u}\nabla)\mathbf{u}=-\frac{1}{\rho}\nabla P+\mathbf{g},\\
&\frac{\partial}{\partial t}\left(\frac{\rho\mathbf{u}^2}{2}+\epsilon\right)=-\operatorname{div}\left[\rho\mathbf{u}\left(\frac{\mathbf{u}^2}{2}+\omega\right)\right]+\rho Q,
\end{aligned}\tag{2.1}$$

where $\mathbf{u}$ is the fluid velocity, ρ and P are the gas density and pressure, t is the time, $\mathbf{g}$ is the gravitational acceleration, ϵ is the internal energy per unit volume, ω is the enthalpy, and Q is the energy supply rate per unit mass from the external energy sources. As a rule we assume the equation of state for a perfect gas

$$P=R\rho T,\tag{2.2}$$

where T is the gas temperature and R is the gas constant.

Equations (2.1), like any others, can be written in nondimensional form with scaling of time t, coordinates r, and mass M. Scaling of all other physical quantities is done using the power functions of t, r, M having corresponding dimensions (Sedov, 1958),

$$P=\frac{a}{r^{k+1}t^{s+2}}\tilde{P}\,,\quad \rho=\frac{a}{r^{k+3}t^{s}}\tilde{\rho}\,,\quad u=\frac{r}{t}\tilde{u},\tag{2.3}$$

where a is a parameter with dimension $[a]=ML^kT^s$, and $\tilde{P},\tilde{\rho},\tilde{u}$ are the dimensionless pressure, density, and velocity. According to the π theorem of the theory of dimensions (Sedov, 1958; Korobeinikov, 1985), any functional relation, independent of the system of units, between $(n+1)$-dimensional variables can be rewritten as a relation between $(n+1-k)$-nondimensional variables, where k is the number of variables with independent dimensions. There are only three main scaling units in hydrodynamics; thus according to the π theorem the number of independent parameters in dimensionless hydrodynamic equations is three fewer than their number in the dimensional ones. When the number of independent variables in the dimensionless equations can be reduced to one, there is a self-similar solution. For one-dimensional flows, this happens when the number of independent dimensional parameters does not exceed two.

The hydrodynamical equations for one-dimensional motion with spherical $(\lambda=2)$, cylindrical $(\lambda=1)$, or plane $(\lambda=0)$ symmetry can be written

$$\begin{aligned}
&\frac{\partial\rho}{\partial t}+\frac{1}{r^\lambda}\frac{\partial(\rho u r^\lambda)}{\partial r}=f_m\,,\\
&\frac{\partial u}{\partial t}+u\frac{\partial u}{\partial r}+\frac{1}{\rho}\frac{\partial P}{\partial r}=f_p\,,\\
&T\frac{\partial s}{\partial t}+Tu\frac{\partial s}{\partial r}=f_e\,.
\end{aligned}\tag{2.4}$$

Here $s=c_V\ln(P/\rho^\gamma)$ is the specific entropy, while f_m, f_p, f_e are the sources of mass, momentum, and energy. For a uniform medium, parameter a may be taken as the ambient gas density ρ_0. Then $s=0, k=-3$, and the self-similar solution may be presented in the form (Sedov, 1958; Zeldovich and Raizer, 1966)

$$u=\frac{r}{t}\,\tilde{v}(\xi)\,,\quad \rho=\rho_0\,\tilde{g}(\xi)\,,\quad \frac{P}{\rho_0}=\frac{r^2}{t^2}\,\tilde{\tau}(\xi)\,,\tag{2.5}$$

with the independent nondimensional variable

$$\xi=\frac{r}{At^\alpha}.\tag{2.6}$$

For these variables the dimensionless self-similar equations may be expressed as (Zeldovich and Raizer, 1966)

$$\begin{aligned}
&\xi\tilde{v}'+(\tilde{v}-\alpha)\,\xi\frac{\tilde{g}'}{\tilde{g}}=-(\lambda+1)\,\tilde{v}+\xi\tilde{\phi}_m\,,\\
&(\tilde{v}-\alpha)\xi\tilde{v}'+\xi\tilde{\tau}'+\tilde{\tau}\xi\frac{\tilde{g}'}{\tilde{g}}=-2\tilde{\tau}-\tilde{v}(\tilde{v}-1)+\tilde{\phi}_p\,,\\
&\xi\frac{\tilde{\tau}'}{\tilde{\tau}}-(\gamma-1)\,\xi\frac{\tilde{g}'}{\tilde{g}}=-2\frac{\tilde{v}-1}{\tilde{v}-\alpha}+\frac{\xi}{\tilde{v}-\alpha}\tilde{\phi}_e\,,
\end{aligned}\tag{2.7}$$

where

$$\tilde{\phi}_m=\frac{f_m t}{\tilde{g}\rho_0}\,,\quad \tilde{\phi}_p=\frac{f_p}{At^{\alpha-2}}\,,\quad \tilde{\phi}_e=\frac{(\gamma-1)f_e}{A^2t^{2\alpha-3}\tilde{\tau}}.\tag{2.8}$$

The similarity index α is determined by the requirement that the time dependence drop out of the right side of Eqs. (2.7).

For zero $\tilde{\phi}_m$, $\tilde{\phi}_p$, and $\tilde{\phi}_m$ there exists an integral of adiabaticy in the form

$$(\tilde{v}-\xi)^{\lambda}\ \tilde{\tau}^{\lambda+1}\ \tilde{g}^{(\lambda-2)/3}\ \xi^{(\lambda+2)(\lambda+1)} = \tilde{C}_1^{-1}, \qquad (2.9)$$

which is obtained by combining the first and the last equations in (2.7). In the general case we have to complement Eqs. (2.7)–(2.9) with the initial and boundary conditions in dimensionless form.

The classical example of the self-similar solution is that of an adiabatic blastwave caused by a point explosion in a cold ($P_{\rm ext}=0$), homogeneous, uniform medium, which has been found by Sedov (1946) and Taylor (1950). There are only two parameters with independent dimension in this problem: the energy of explosion E_0 and the density of the ambient gas ρ_0. The only nondimensional composition formed by E_0, ρ_0, and the independent variables t, r is

$$\xi = r\left(\frac{\rho_0}{\xi_0 E_0 t^2}\right)^{1/5}, \qquad (2.10)$$

where $\xi_0 = 2.025\,97$ for $\gamma = 5/3$ is a constant which follows from the energy integral and the solution of the self-similar equations (Sedov, 1958). Taking the nondimensional coordinate of the shock ξ_s equal to 1, we get the radius of the shock front R_s as a function of time,

$$R_s = \left(\frac{\xi_0 E_0}{\rho_0}\right)^{1/5} t^{2/5}. \qquad (2.11)$$

The velocity of a strong spherical shock is then given by

$$V_s = \frac{dR_s}{dt} = \frac{2}{5}\frac{R_s}{t}. \qquad (2.12)$$

For the case of a strong spherical shock the self-similar equations can be solved analytically (Sedov, 1946). Figure 1 shows the distribution of the hydrodynamic quantities inside the spherical remnant that follows from the Sedov (1946) solution, on which the majority of the approximate methods are based. Two main features of the Sedov-Taylor solution follow from this figure. They are

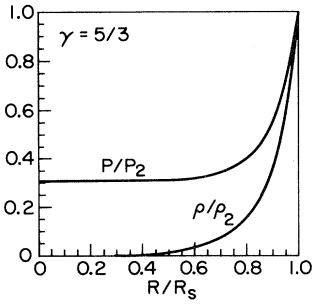

FIG. 1. Distribution of dimensionless density and pressure behind an adiabatic shock front initiated by a point explosion in a homogeneous interstellar medium.

the concentration of the swept-up gas in a thin layer near the shock boundary and the almost uniform distribution of the gas pressure inside the cavity, with the exception of a small region behind the shock front.

While the internal structure of the blastwave at time t is related to that at any other time through simple scaling, the properties mentioned above are present at least during the adiabatic phase of the shock's evolution. The mass concentration behind the shock front becomes even more prominent at the radiative phase, when the swept-up gas collapses into a thin cold shell that expands with almost the same speed as the shock front itself.

2. Solutions for a point explosion with heat conductivity and cloud evaporation

The spherical shock from a point explosion has been successfully applied to explain a variety of features of the observed SNRs. However, theoretical studies (Bychkov and Pikelner, 1975; McKee and Ostriker, 1977; Cowie *et al.*, 1981) and observational evidence (Long and Helfand, 1979; Lozinskaya, 1992) indicate that evaporation of matter from small dense clouds that are engulfed by a shock front and are embedded into a hot tenuous gas might strongly affect the evolution of SNRs and multisupernova shells (Kunze *et al.*, 1992).

An analytical approximation to describe the evolution of spherical SNRs with evaporating clouds has been proposed by McKee and Ostriker (1977; Ostriker and McKee, 1988). A detailed numerical model of spherical SNR evolution in a cloudy ISM has been developed by Cowie *et al.* (1981). Tsunemi and Inoue (1980) carried out a numerical analysis of the evolution of clouds trapped in a hot SNR cavity and of their influence on the spectrum of the Cygnus loop. The results of analytical and numerical studies of the evolution of spherical SNRs in a three-phase ISM have been summarized by McKee (1982).

In a quasistationary state, the values of the total flux L (heat conductivity plus advection) and mass flux $\dot{m}$ are constant (Landau and Lifshitz, 1959; Bisnovatyi-Kogan, 1967; Cowie and McKee, 1977):

$$\dot{m}\left(\frac{u^2}{2}+\frac{5}{2}{a_i}^2\right)+4\pi r^2 q = L, \qquad (2.13)$$

$$4\pi r^2 \rho u = \dot{m}. \qquad (2.14)$$

Here ${a_i}^2 = kT/\mu$ is the isothermal sound speed, and μ is the mean mass per particle. The heat flux q is conducted by the electrons, and the classical thermal conductivity in a fully ionized equilibrium hydrogen plasma (Spitzer, 1962),

$$\kappa = \frac{1.84\times10^{-5}T^{5/2}}{\ln\Lambda}\ \mathrm{ergs\,s^{-1}\,deg^{-1}\,cm^{-1}}, \qquad (2.15)$$

is based on the diffusion approximation, that is, on the assumption that the mean free path of the electrons is less than the characteristic scale of the temperature gradient

$l_T = T/\mid \nabla T \mid$. Here T is the intercloud gas temperature, while $\ln\Lambda$ is the Coulomb logarithm. But when the mean free path of the electrons becomes comparable to the temperature scale height in the cloud, the heat flux is no longer $q = -\kappa \nabla T$. In such a case it depends on some characteristic velocity $v_{\rm ch}$ that is of the order of the electron thermal velocity, $q = \frac{3}{5} n_e k T_e v_{\rm ch}$. Cowie and McKee (1977) estimated $v_{\rm ch}$ as $v_{\rm ch} = \left(\frac{8kT}{9\pi m_e}\right)^{1/2}$ and have called this effect "saturation." The saturated heat flux is given by

$$q_{\rm sat} = 0.4 \left(\frac{2kT_e}{\pi m_e}\right)^{\frac{1}{2}} n_e k T_e. \tag{2.16}$$

Cowie and McKee (1977) argued that the upper limit on the saturated heat flux should take the form

$$q_{\rm sat} = 5\Phi_s \rho {a_i}^2, \tag{2.17}$$

where Φ_s is a parameter less than, or of order of, unity, which depends on cloud geometry, presence and configuration of the magnetic field, etc.

In addition to the quasistationarity condition, Cowie and McKee (1977) set the total energy flux to be zero: $L = 0$ in (2.13). Then the solution of Eq. (2.13) gives the mass loss rates from the cloud in these two cases as

$$\dot{M}_{\rm clas} = 2.75\times10^4 {T_a}^{5/2} r_{\rm pc}\ {\rm g\,s^{-1}},\quad 0.03 < \sigma < 1, \tag{2.18}$$

$$\dot{M}_{\rm sat} = 3.75\times10^4 {T_a}^{5/2} r_{\rm pc} \Phi_s \sigma^{-5/8}\ {\rm g\,s^{-1}},\quad \sigma > 1, \tag{2.19}$$

where $r_{\rm pc}$ is the cloud radius in parsec units, T_a is the temperature of the surrounding hot gas, and

$$\sigma = \left(\frac{T_a}{1.54\times10^7}\right)^2 \frac{1}{n r_{\rm pc} \Phi_s}. \tag{2.20}$$

These results have been further studied recently by Dalton and Balbus (1993). Doroshkevich and Zeldovich (1980) have analyzed the nonstationary structure of the interface between hot and cold gas in the case of nonlinear conductivity and volume energy loss.

Chieze and Lazareff (1981) looked for a similarity solution for a supernova remnant expansion into a two-component interstellar medium containing high-density clouds and low-density intercloud gas. They suggested that due to thermal conductivity (classical case) the mean cloud evaporation rate has the form

$$f_m = \Omega(T^{5/2}) \tag{2.21}$$

used in the first equation of (2.4), with $f_p = f_e = 0$. To make the problem of self-similar type, the external gas density distribution was taken as

$$\rho(r) = \delta r^{-5/3} \Omega^{1/3} E_0^{2/3}, \tag{2.22}$$

where δ is a dimensionless parameter. Then only four-dimensional parameters remain: r, t, Ω, and the explosion energy E_0. The unique dimensionless combination of these parameters is

$$\xi = r\Omega^{1/10} E_0^{-1/10} t^{-3/5}. \tag{2.23}$$

It follows from this equation that the shock radius is in direct proportion to $t^{3/5}$ and the shock velocity varies as $t^{-2/5}$.

A similarity solution for shock-wave evolution in a cloudy medium in the case of saturated evaporation has been found by White and Long (1991). This solution is applicable to a young (less than $\approx$ 20000 yr) supernova remnant. It was applied by Long *et al.* (1991) to SNRs 3C400.2 and W28. They assumed that the clouds are much denser than the intercloud medium and uniformly distributed, with a small volume filling factor. Then clouds that have been engulfed by a shock wave are still cold and do not acquire a significant velocity. The dense cloud material is then evaporated and mixed with post-shock hot intercloud gas. It is assumed that the clouds lose gas having zero internal energy and zero velocity. This gas extracts energy from the shock-heated intercloud medium to reach the intercloud gas parameters. The relative kinetic energy of the newly ejected and post-shock mass is converted into the thermal energy of the gas mixture. Then the right sides of the hydrodynamical equations (2.4) for a spherically symmetric SNR may be expressed as (Mathews and Baker, 1971; White and Long, 1991)

$$f_m = j, \tag{2.24}$$

$$f_p = -\frac{u}{\rho} j, \tag{2.25}$$

$$f_e = c_v T \frac{j}{\rho}\left[\frac{1}{2}(\gamma-1)\frac{\rho u^2}{P} - \gamma\right], \tag{2.26}$$

where j is the integrated cloud evaporation rate per unit volume. To find a similarity solution, we have to make the usual substitutions: $P = P_s f(\xi)$, $f(1) = 1$, $\rho = \rho_s g(\xi)$, $g(1) = 1$, $u = u_s h(\xi)$, $h(1) = 2/(\gamma+1)$, $j = j_s k(\xi)$, $\xi = r/R_s$, where P_s, ρ_s, u_s, and j_s are the values of the gas pressure, density, velocity, and cloud evaporation rate at the shock front. The existence of a similarity solution demands the combination $C = j_s r_s/u_s\rho_s$ to be constant. This implies that the cloud evaporation rate at the shock front has to be in inverse proportion to the time t evolved: $j_s \sim 1/t$. This dependence of the cloud evaporation rate $\dot{m}$ on t is in fact very close to that expected for saturated conduction (Cowie and McKee, 1977), which is usually correct for a young SNR. White and Long (1991) introduced a simple approximate form for the cloud evaporation rate that follows from Cowie and McKee's (1977) result (2.19) and the similarity condition $j_s \sim 1/t$:

$$\dot{m} = \frac{m_c}{\alpha t}\left(\frac{P}{P_s}\right)^{5/6}, \tag{2.27}$$

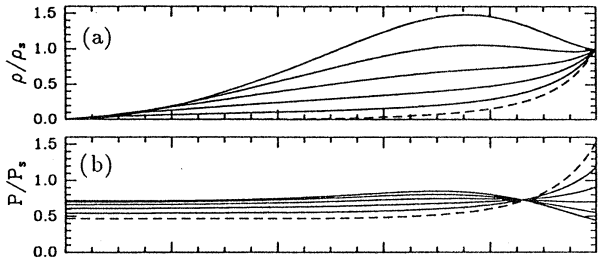

FIG. 2. Distribution of the dimensionless density (a) and pressure (b) behind the shock front initiated by a point explosion in an inhomogeneous cloudy medium, in terms of α, the dimensionless constant that determines the evaporation (see text), and $\beta = \rho_{\rm cl}/\rho_g$. $\alpha = 2$; $\beta = 0$ (dashed lines), 2, 4, 6, 8, 10. From White and Long, 1991.

where m_c is the mass of the cloud, t is the time, and α is a dimensionless constant that describes the rate of cloud evaporation. For $\alpha \gg 1$ clouds evaporate slowly, for $\alpha \ll 1$ quickly.

This model has two more parameters than the Sedov solution: α and $\beta = \rho_{\rm cl}/\rho_g$, where ρ_g is the intercloud gas density and $\rho_{\rm cl}$ is the contribution of the clouds to the mean ISM density.

The main effect of cloud evaporation is to increase and to smooth the density distribution (due to the strong $T^{5/2}$ dependence of the evaporation mass-loss rate on the temperature) and to decrease the temperature inside the remnant. The density, pressure, and temperature distributions inside the remnant that follow from the White and Long (1991) model for different values of α and β are presented in Fig. 2. It follows from this picture that density may even be peaked near the center of the cavity, but only in the case of large β, when the bulk of the ISM is concentrated in the cold cloud component. In the more reasonable case $\beta \approx 1$, the most mass is concentrated behind the shock front.

3. Blast wave initiated by a strong burst of radiation

Bisnovatyi-Kogan and Murzina (1995) have examined the reaction of a uniform gas to the action of a short light pulse. This problem is important, in particular, in considering possible mechanisms for the origin of gamma-ray bursts (Prilutski and Usov, 1975; Paczynski, 1986). The influence of a burst of light on the ambient gas may be described as a δ-like source of momentum and energy on the right sides of Eqs. (2.4). For Thompson scattering of the photons on electrons in a pure hydrogen plasma, Eqs. (2.4) may be used with

$$f_m = 0, \quad f_p = \frac{b'}{r^\lambda}\delta(t-t_0),$$

$$f_e = \frac{b}{r^\lambda}\delta(t-t_0), \qquad (2.28)$$

$$b = cb' = \frac{Q}{\Theta}\frac{\sigma_T}{m_p},$$

where t_0 is the moment that the signal arrives at a layer with coordinate r; Q, with dimension [ergs/cm$^{2-\lambda}$], is the energy production; $\Theta = 1, 2\pi, 4\pi$ for $\lambda = 0, 1, 2$; σ_T is the Thompson cross section; and m_p is the mass of the proton. A self-similar solution of this problem takes the form (Zeldovich and Raizer, 1966)

$$r = R(t)\,\xi\,, \quad u = \dot{R}(t)\,v(\xi)\,, \qquad (2.29)$$

$$\rho = \rho_0(t)\,g(\xi)\,, \quad \frac{P}{\rho} = \dot{R}^2(t)\,\tau(\xi)\,,$$

with a signal that moves as $r_0 = R(t)\xi_0$ and $R(t) = At^\alpha$, for a uniform medium $\rho_0(t) = \rho_0 = \text{const}$. The self-similar equations of the problem may then be written as follows:

$$v' + (v-\xi)\frac{g'}{g} + \lambda\frac{v}{\xi} = \phi_m = \frac{f_m\,t}{\alpha g \rho_0}\,,$$

$$\frac{\alpha-1}{\alpha}v + (v-\xi)v' + \tau' + \tau\frac{g'}{g} = \phi_p = \frac{f_p}{\alpha^2 A t^{\alpha-2}}\,,$$

$$2\frac{\alpha-1}{\alpha} + (v-\xi)\left(\frac{\tau'}{\tau} - (\gamma-1)\frac{g'}{g}\right) = \phi_e = \frac{(\gamma-1)f_e}{\alpha^3 A^2 t^{2\alpha-3}\tau}\,. \qquad (2.30)$$

Self-similar solutions exist when the right sides of Eqs. (2.30) do not depend on t, that is,

$$\alpha = \frac{1}{1+\lambda}, \qquad (2.31)$$

$$\alpha = \frac{2}{2+\lambda}.$$

So for a real light pulse propagating with constant speed c, a similarity solution exists only in plane geometry. For spherical and cylindrical motion at $b = cb'$, self-similar solutions exist for heating or pushing out separately; for $b = V_0(t)b'$ [where $V_0(t) = \dot{r}_0(t)$ is the speed of the signal], both heating and pushing can be taken into account. Note that the self-similar variables (2.5) and (2.29) are connected by simple relations

$$\tilde{v} = \frac{\alpha}{\xi}v\,, \ \tilde{g} = g\,, \ \tilde{\tau} = \frac{\alpha^2}{\xi^2}\tau\,, \qquad (2.32)$$

$$\tilde{\phi}_m = \alpha\phi_m\,, \ \tilde{\phi}_p = \alpha^2\phi_p\,, \ \tilde{\phi}_e = \alpha^3\phi_e.$$

Substituting the first equation (2.30), with zero on the right side, into Eq. (2.32) gives the integral of adiabaticity in the form

$$(v-\xi)^{\lambda}\ \tau^{\lambda+1}\ g^{\frac{\lambda-2}{3}}\ \xi^{\lambda^2}\ =\ C_1^{-1}\ . \tag{2.33}$$

The conservation laws taking account of pushing out and/or heating, for a discontinuity propagating through a cold uniform gas at rest, lead to the following relations between the density ratio Δ, nondimensional constant B, and self-similar coordinate of the discontinuity ξ_0:

$$\Delta = \frac{\frac{5}{2} \pm \sqrt{\frac{9}{4} - \frac{8B}{\xi_0^2}}}{1+2B/\xi_0^2},\ B'=0,$$

$$\Delta = \frac{\frac{5}{2}\left(1-\frac{B}{\xi_0^2}\right) \pm \sqrt{\frac{9}{4} - \frac{41B}{2\xi_0^2} + \frac{25B^2}{4\xi_0^4}}}{1+2B/\xi_0^2},\ B'=B, \tag{2.34}$$

$$B = \frac{b}{\alpha^2 \xi_0^{\lambda}\, A^{2+\lambda}}.$$

When the light front is ahead of the discontinuity, the discontinuity disappears at $B=0$, so a minus sign must be chosen here. It follows from Eqs. (2.34) that, for a self-similar solution to exist with the shock behind the heating front, it is necessary to have

$$B\ <\ 9/32\xi_0^2 \tag{2.35}$$

for the case with heating only, and

$$B\ <\ \frac{41}{25}\left(1-\sqrt{1-\frac{225}{1681}}\right)\xi_0^2\ \simeq\ 0.1137\xi_0^2, \tag{2.36}$$

when both heating and pushing are included. Physically this means that sound speed must not exceed the speed of the signal. This requirement is violated when the power of the signal exceeds the critical one.

Any spherical or cylindrical pulse initially causes infinite pressure at the center, which inevitably produces an expanding shock wave—by contrast to a rarefaction wave in a plane flow. The shock wave is formed behind the signal moving through a cold gas at rest. The results of numerical integration for a spherical light pulse are presented in Fig. 3 (Bisnovatyi-Kogan and Murzina, 1995). One can see from Fig. 3 that the family of spherical geometry solutions, which are of the most physical interest, possesses some special features, which, for post-shock flow, are very close to each other for all values of the parameter $\tilde{B} = B/\xi_0^2$. This means that the shock propagation behavior is defined primarily by the initial heating at the center, while the influence of the signal velocity on the process is small. The velocity of the shock-wave propagation almost does not depend on the ξ_0. So the shock-wave expansion $r = \xi_{\rm sh} A t^{\alpha} = \xi_{\rm sh} b^{1/4}\sqrt{t}$ is almost the same for all the values of the signal speed,

$$r\ \simeq\ 2.1\left(\frac{Q\,\sigma_T}{4\pi\, m_p}\right)^{1/4}\sqrt{t}\ =\ 0.75 Q^{1/4}\sqrt{t}(cm).$$

Thus, in the spherical case, the light pulse could lead to a shock formation that might generate in a dense cloud a luminous ring, visible in optical or radio frequencies. The numerical calculations of the hydrodynamics accompanying light-pulse propagation (Timochin and Bisnovatyi-Kogan, 1995) are in good agreement with this self-similar solution.

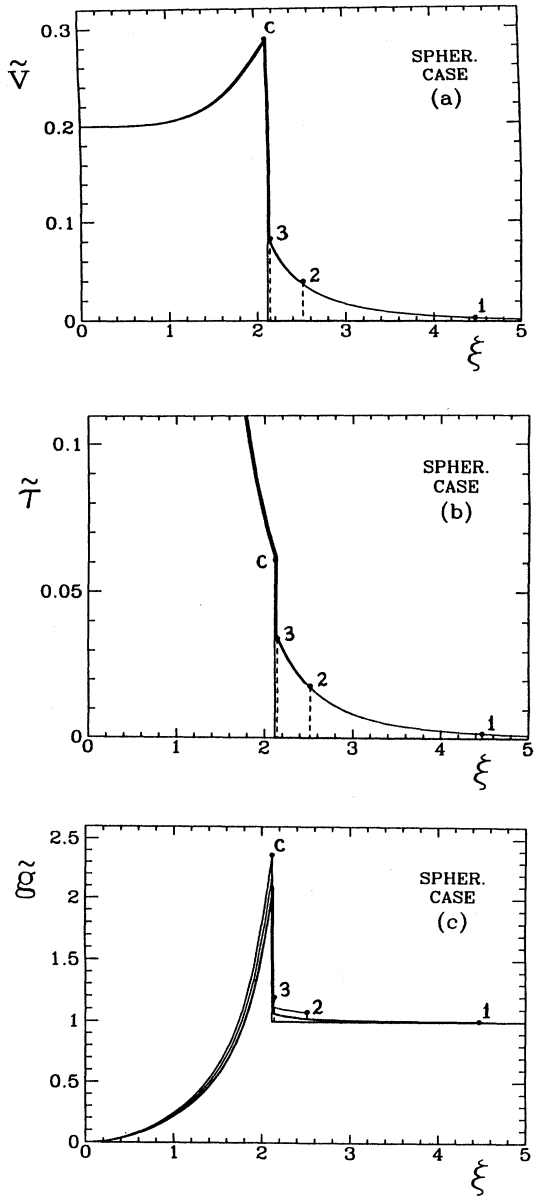

FIG. 3. Solutions for self-similar values of velocity $\tilde{v}$, temperature $\tilde{\tau}$, and density $\tilde{g}$ as functions of ξ for different values of $\tilde{B} = B/\xi_0^2$ [see Eq. (2.34)]: 0.01 (1); 0.1 (2); 0.19 (3); and 0.1994 (c). The last value corresponds to the critical $\tilde{B}$, when the shock wave merges with the light front. Light-front positions are indicated by points. From Bisnovatyi-Kogan and Murzina, 1995.

B. The virial theorem approach

In this section we consider the analytic approach of Ostriker and McKee (1988), based on the generalization of the virial theorem applied to a thin shell, with allowance for its variable mass. Ostriker and McKee (1988) allowed also the expansion of the ambient gas and took into account the effects of cloud evaporation and the cloud drag friction.

Let us consider for simplicity shock-wave propagation in a homogeneous (cloudless) interstellar medium, when gas motion can be described by Eqs. (2.4) with $f_m = f_p = 0$. Here R_s and $u_s = \dot{R}_s$ are the shock-front radius and velocity, ρ_1 and u_1 are the gas density and velocity just behind the shock front, ρ and u are the hydrodynamical variables within the shock cavity, and Ω is the volume of the remnant. Consider the identity

$$\frac{d}{dt}\int_0^{R_s} r\rho u d\Omega = 4\pi R_s^3 \rho_1 u_s u_1 + \int_0^{R_s} r\frac{\partial}{\partial t}(\rho u) d\Omega. \quad (2.37)$$

Let us introduce the dimensionless moments of radius and velocity

$$K_{mn} = \int_0^{R_s} \left(\frac{r}{R_s}\right)^m \left(\frac{u}{u_1}\right)^n \frac{4\pi r^2 \rho}{M} dr, \quad (2.38)$$

where $M(t)$ is the mass of the gas within the cavity. Then identity (2.37) may be rewritten, with the aid of the equations of mass and momentum conservation, in the form (Ostriker and McKee, 1988)

$$\frac{d}{dt}(K_{11} M R_s u_1) = 4\pi R_s^3 [\tilde{P} - P_0 + \rho_0 u_0 (u_s - u_0)] + K_{02} M u_1^2 + W. \quad (2.39)$$

Here the index 0 denotes the unperturbed values, $\tilde{P}$ is the mean gas pressure inside the remnant,

$$\tilde{P} = 3R_s^{-3} \int_0^{R_s} P r^2 dr, \quad (2.40)$$

and W is the gravitational energy,

$$W = \int_0^{R_s} \rho g r d\Omega. \quad (2.41)$$

The second basic equation is that of energy conservation:

$$E_{\rm tot} = \frac{1}{2} M u_1^2 K_{02} + \frac{1}{\gamma - 1}\tilde{P}\Omega + W, \quad (2.42)$$

where $E_{\rm tot}$ is the total energy of the blastwave, which is equivalent to the total injected energy if the blastwave is assumed to be adiabatic, and the ambient gas is stationary and cold. We have $E_{\rm tot}$ =const for a point explosion, and $E_{\rm tot}$ is a function of time for a stellar wind or multiple supernovae.

Let us consider a shock-wave expansion in a cold ($P_0 = 0$), stationary ($u_0 = 0$) medium without gravity ($W = 0$). Then combining Eqs. (2.39) and (2.42) gives the following basic equation for blastwave motion:

$$\frac{d}{dt}(K_{11} M R_s u_1) = 3(\gamma - 1) E_{\rm tot} - \frac{3\gamma - 5}{2} K_{02} M u_1^2, \quad (2.43)$$

where the post-shock velocity u_1 for a strong shock wave is

$$u_1 = \frac{2}{\gamma + 1}\dot{R}_s. \quad (2.44)$$

The moments K_{mn} are constants in the case of a self-similar blastwave (Ostriker and McKee, 1988). For a point explosion with $E_{\rm tot} = E_0 = $ const, Eq. (2.43) has a power-law solution $R_s = At^\eta$. It is easy to find by simple substitution that

$$R_s = \left(\frac{\xi_0 E_0}{\rho_0}\right)^{1/5} t^{2/5}, \quad (2.45)$$

where

$$\xi_0 = \frac{45(\gamma^2 - 1)}{16\pi\left[K_{11} + \frac{6\gamma - 10}{5(\gamma + 1)} K_{02}\right]}. \quad (2.46)$$

For a power-law distribution of the ambient gas density

$$\rho = \rho_0 (r/r_0)^k, \quad (2.47)$$

the following kinematic relation is valid (Ostriker and McKee, 1988):

$$K_{n0} = \frac{3 - k + \frac{2n}{\gamma + 1} K_{n-1,1}}{3 - k + n}. \quad (2.48)$$

In order to complete the solution, the moments K_{11} and K_{02} must be found. To get the exact values of K_{11} and K_{02} we have to specify the hydrodynamic variables within the cavity as functions of r and t. An approximate approach to calculating K_{mn}, providing good accuracy, has been described by Ostriker and McKee (1988).

The hydrodynamic quantities $u(r,t)$, $\rho(r,t)$, and $P(r,t)$ in a self-similar blastwave may be written in the form

$$X(r,t) = X_1(t)\tilde{X}(\lambda), \quad (2.49)$$

where $\lambda = r/R_s$ is the independent nondimensional variable and $X_1(t)$ is the post-shock value of the corresponding hydrodynamical variable (see previous section). Ostriker and McKee assumed some $\tilde{X}(\lambda)$ to be a power function of λ. The simplest approximation is a linear velocity approximation, which assumes that the velocity field within the remnant is a linear function of radius r: $u = \dot{R}_s \lambda$. The one-power approximation assumes

$$\tilde{X}(\lambda) = a_x \lambda^l. \quad (2.50)$$

In the two-power approximation we have

$$\tilde{X}(\lambda) = a_x \lambda^{l_1} + (1 - a_x)\lambda^{l_2}. \quad (2.51)$$

TABLE I. Parameters of a self-similar blastwave in a uniform medium: LVA, linear velocity approximation; OPA, one-power approximation; TPA, two-power approximation. From Ostriker and McKee (1988).

	LVA	OPA	TPA	Exact
K_{20}	0.8571	0.8571	0.8367	0.83567
K_{11}	0.8571	0.8000	0.7889	0.78557
K_{02}	0.8571	0.7500	0.7445	0.74042
ξ_0	1.8568	1.9894	2.0175	2.02597

The parameters a_x, l_1, and l_2 are fixed by the integral constraints on $\tilde{X}(\lambda)$ which follow from the conservation laws, or by requiring the derivative of $\tilde{X}(\lambda)$ to be correct at the remnant boundaries.

In the linear velocity approximation there exists a simple relation between the moments:

$$K_{mn} = K_{m+n,0} = K_{0,m+n}. \tag{2.52}$$

This relation, when inserted into Eq. (2.48), gives

$$K_{11} = K_{02} = \frac{1}{1 + \frac{2(\gamma-1)}{(3-k)(\gamma+1)}} \tag{2.53}$$

and completes the solution. For a uniform interstellar medium ($k = 0$),

$$K_{11} = K_{02} = \frac{3(\gamma+1)}{5\gamma+1}, \tag{2.54}$$

and constant ξ_0 is equal to

$$\xi_0 = \frac{75(\gamma^2-1)(5\gamma+1)}{16\pi(11\gamma-5)}. \tag{2.55}$$

A comparison between approximate and exact values for an adiabatic shock wave in a uniform medium with $\gamma = 5/3$ is presented in Table I from Ostriker and McKee (1988).

Koo and McKee (1990) have extended this method for the expansion of an adiabatic shock wave in a medium with a finite total mass, where the mass of the shell may reach its maximum value and the motions of the shell and accelerating shock wave have to be treated separately. The method is applied to different cases of astrophysical interest in the review of Ostriker and McKee (1988).

C. Thin-layer approximation

As has been shown in the previous paragraphs, in a spherical adiabatic shock wave almost all swept-up intercloud gas is concentrated in a thin layer behind the shock front. The intercloud gas density distributions inside the blastwave, with and without evaporated clouds, are similar when the cloud component does not include most of the interstellar matter. The concentration of the mass near the shock front becomes even more pronounced in the radiative phase, when radiative cooling becomes important and swept-up gas collapses into a cool dense shell expanding with nearly the velocity of the shock front. The gas pressure is almost uniform within the cavity, where the gas temperature is high, and the average interior sound speed is much greater than the shell's expansion velocity.

The thin-shell approximation is based on two main simplifications. First, it is assumed that all swept-up intercloud gas accumulates into an infinitely thin shell just behind the shock front and moves with the post-shock velocity u_1. Second, the pressure distribution inside the cavity $P(r,t)$ is approximately taken with a specified space profile, so that only one parametric dependence $P_{\rm in}(t)$ remains. It is taken to be uniform in all cases where magnetic field is negligible.

There is one kinematic inconsistency in this approach. If all swept-up gas is concentrated in the thin shell behind the shock front, then it must move with the velocity u_s of the shock front, rather than the post-shock velocity u_1. This contradiction vanishes for radiative blastwaves when the ratio of specific heats $\gamma \to 1$ and the post-shock velocity approaches the blastwave speed. Nevertheless, numerical calculations for axial symmetry made by Falle *et al.* (1984), Mac Low and McCray (1988), and Bisnovatiy-Kogan *et al.* (1989) have shown that this approximation is sufficiently good not only for spherically symmetric shocks, but also for blastwaves with a more complicated morphology. Of course, in this approximation we lose information about the distribution of the hydrodynamic quantities within the remnant and use only the average value for the inner gas pressure $P_{\rm in}$. However it is possible to describe such important shell properties as shape, expansion velocity, and surface density distribution. The thin-layer approximation is well known in plasma physics (Imshennik, 1977), and its astrophysical applications in 2D and 3D cases are described in subsequent sections of this review.

For the spherically symmetrical case and a smooth background medium without clouds, the equations of mass and momentum conservation may be expressed as follows (Cherny, 1957; Bisnovatiy-Kogan and Blinnikov, 1982):

$$M = M_0 + 4\pi \int_0^R \rho(r) r^2 dr, \tag{2.56}$$

$$\frac{d}{dt}(Mu) = 4\pi R^2 (P_{\rm in} - P) + Mg, \tag{2.57}$$

where M is the mass of the shell, M_0 is the ejected mass, R is the shock radius, and u is the gas velocity behind the shock; $\rho(r)$ and P are the density and the pressure of the ambient gas, while g is the external gravitational field. The equations describing the energy balance in the remnant and the relation between the shell velocity u and $\dot{R}$ depend on physical conditions. For an adiabatic blastwave without gravity,

$$\frac{dR}{dt} = \frac{\gamma+1}{2} u, \tag{2.58}$$

$$E_0 = E_{\rm th} + \frac{1}{2}Mu^2, \tag{2.59}$$

where $E_0 = \text{const}$ is the energy of the explosion, $E_{\rm th} = \frac{4\pi}{3(\gamma+1)}P_{\rm in}R^3$ is the thermal energy of the blastwave, and γ is the ratio of the specific heats (adiabatic power). For a radiative blastwave,

$$\frac{dR}{dt} = u, \tag{2.60}$$

$$\frac{dE_{\rm th}}{dt} = -4\pi R^2 P_{\rm in} u. \tag{2.61}$$

Equations (2.56)–(2.59) have a simple solution for a homogeneous interstellar medium without gravity if the swept-up mass is much greater than the ejected one (see also Zeldovich and Raizer, 1966):

$$R = \left[\frac{\xi_0 E_0}{\rho_0}\right]^{1/5} t^{2/5}, \tag{2.62}$$

where (Chernyi, 1957; Andriankin *et al.*, 1962)

$$\xi_0 = \frac{75(\gamma-1)(\gamma+1)^2}{16\pi(3\gamma-1)}. \tag{2.63}$$

Kinetic and thermal energy remain constant during shock propagation and are equal to

$$E_{\rm th} = \frac{\gamma+1}{3\gamma-1}E_0, \quad E_{\rm kin} = 2\frac{\gamma-1}{3\gamma-1}E_0. \tag{2.64}$$

Taking into account that the shock speed dR/dt is connected with the pressure behind the shock P_s by the relation

$$\frac{dR}{dt} = \sqrt{\frac{\gamma+1}{2}\frac{P_s}{\rho_0}}, \tag{2.65}$$

we find

$$P_s = (\gamma-1)\frac{2(\gamma+1)}{3\gamma-1}\frac{E_0}{\Omega}, \quad \Omega = \frac{4\pi}{3}R^3. \tag{2.66}$$

The average pressure inside the bubble is

$$P_{\rm in} = (\gamma-1)\frac{E_{\rm th}}{\Omega} = (\gamma-1)\frac{\gamma+1}{3\gamma-1}\frac{E_0}{\Omega}, \tag{2.67}$$

which gives in this approximation $P_s/P_{\rm in} = 2$. Thus two methods [the virial theorem, Eqs. (2.45) and (2.55), and the thin-layer approximation, Eqs. (2.62) and (2.63)] give similar results for a shock-wave expansion that are in a good agreement with the Sedov-Taylor self-similar solution. Equations (2.56)–(2.59) allow us to calculate both the adiabatic ($M \gg M_0$) and the earlier stages of supernova remnant evolution when the ejected mass is similar to or even greater than the swept-up mass.

D. Shock waves in gravitating media

The action of gravity on the motion of interstellar gas is one of the characteristic features of interstellar hydrodynamics. The gravitational influence is the most marked for gas motion in the vicinity of relativistic objects, for dynamics of large-scale galactic structures, or in regions with strong concentrations of stars like the circumnuclear regions of galaxies (Oort, 1978).

It is not possible to extend the self-similar method to these problems, because allowance for the contribution of gravitational force introduces a third parameter with an independent dimension. Assuming that the main simplifications of the thin-layer approximation are correct, we shall consider the propagation of a strong spherical shock in a stationary medium that consists of stellar and gas components with a power-law density distribution (Silich, 1985; Pas'ko and Silich, 1986),

$$\rho_g(r) = \rho_{0g}(r/R_0)^{-n}, \tag{2.68}$$

$$\rho_s(r) = \rho_{0s}(r/R_0)^{-m}. \tag{2.69}$$

For a strong shock we can neglect the ambient gas pressure and set $P_0 = 0$; then, for density distribution (2.68), Eqs. (2.56)–(2.59) may be rewritten as

$$\begin{aligned} M_g &= \frac{4\pi}{3-n}\rho_{0g}R^3(R_0/R)^n, \\ M_s &= \frac{4\pi}{3-m}\rho_{0s}R^3(R_0/R)^m, \\ \frac{d}{dt}(M_g u) &= 4\pi R^2 P - \frac{GM_s M_g}{R^2}, \\ E &= \frac{4\pi}{3(\gamma-1)}PR^3 + \frac{1}{2}M_g u^2 + E_G, \\ u &= \frac{2}{\gamma+1}\dot{R}. \end{aligned} \tag{2.70}$$

Here γ is the adiabatic index of the gas, G is the gravitational constant and E_G is the work done by the hot remnant interior against the gravitational field of the stellar component of the medium, to compress the gas with a smooth density distribution (2.68) into an infinitely thin shell.

Equations (2.70) may be reduced to one linear differential equation for a shock-wave velocity (Silich, 1985),

$$u_{\rm sh}^{(a)}(R) = D_0\left[1 - K\left(\frac{R}{R_0}\right)^{5-m-n}\right]^{\frac{1}{2}}\left(\frac{R_0}{R}\right)^{\frac{3-n}{2}}, \tag{2.71}$$

where

$$D_0 = \left[\frac{3(\gamma+1)(\gamma^2-1)}{9\gamma-3-n(\gamma+1)}\frac{E}{M_{0g}}\right]^{\frac{1}{2}}, \tag{2.72}$$

$$K = \frac{(2A+n-3)(2+3\gamma-n-m)}{3(\gamma-1)(2A+2-m)(5-m-n)}\frac{GM_{0g}M_{0s}}{R_0 E}. \tag{2.73}$$

Here M_{0g} and M_{0s} are the masses of the gas and of the

stars inside the radius R_0 [see Eq. (2.70)]. In the absence of gravity ($K = 0$), for $n = 0$, Eq. (2.71) gives for the shock-wave expansion in a uniform medium the Sedov-Taylor solution in the form (2.62) and (2.63).

The adiabatic phase of the remnant's evolution persists until radiative cooling of the hot compressed gas behind the shock front becomes important and a thin, dense, cold shell is formed, enclosing a low density hot gas within the cavity (Cox, 1972; Chevalier, 1974). Then the radiative stage of blastwave evolution begins. New portions of the swept-up interstellar gas cool so quickly that all thermal energy of the gas crossing the shock is radiated, and the cavity does not gain any energy during expansion. The rarefied hot cavity expands adiabatically, pushing away the surrounding dense shell, so that $PR^{3\gamma} = C_r$. Numerical calculations (Chevalier, 1974; Falle, 1981) have shown that, during the short transition phase from an adiabatic to a radiative blastwave, almost half of the remnant's thermal energy is carried away by radiation. By contrast to the thermal energy, the kinetic energy of the remnant (and the velocity of the shell) does not suffer significant change. By the same substitution $\dot{R}^2 = y$, Eqs. (2.56)–(2.57), (2.60)–(2.61), and (2.68)–(2.69) may be reduced to a single linear differential equation, whose solution can be presented in the form (Pas'ko and Silich, 1986)

$$u_{\rm sh}^{(r)}(R) = \frac{2D_c}{\gamma+1}\left(\frac{R_c}{R}\right)^{3-n} \times\left[\xi+\xi_1\left(\frac{R}{R_c}\right)^{6-3\gamma-n} -\xi_2\left(\frac{R}{R_c}\right)^{8-2n-m}\right]^{\frac{1}{2}}. \tag{2.74}$$

Here R_c and D_c are the radius and the shock-wave velocity at the beginning of the radiative phase (Cox, 1972; Blinnikov *et al.*, 1982; Falle *et al.*, 1984). The constants ξ, ξ_1, and ξ_2 are

$$\xi = \frac{4}{(\gamma+1)^2} + \xi_2 - \xi_1,$$

$$\xi_1 = \frac{2B}{6-3\gamma-n}\frac{R_c^{n-3\gamma}}{{D_c}^2}, \tag{2.75}$$

$$\xi_2 = \frac{2B_1}{8-2n-m}\frac{R_c^{2-m}}{D_c^2}. \tag{2.76}$$

The requirement of finite mass at the center of the explosion and finite work done by the hot interior against the gravitational forces constrains the exponents n and m to the values $n < 3$, $m < 3$, $n + m < 5$. Then the absolute value of the negative terms in Eq. (2.74) always increases with R faster than the positive term. This results in an abrupt (faster than power-law) velocity decrease and shock-wave damping. This possibility is illustrated in Fig. 4, where the dependence of the shock-wave velocity on radius R is shown for a uniform system with parameters similar to those of the circumnuclear region of the Milky Way Galaxy (see Oort, 1977): $m = -1.8$, $R_0 = 1\,\mathrm{kpc}$, $M_s(R_0) = 10^{10}M_\odot$, $M_g(R_o) = 10^8 M_\odot$. Here the dashed line represents shock-wave expansion when the gravitational action of stars is negligible. Gravity remains ineffective when $|\xi_2/\xi| \ll 1$. Then the term $(R_c/R)^{3-n}$ is more important, and the expression in the brackets of Eq. (2.74) becomes equal to zero after shock-wave damping, i.e., when $u_{\rm sh}^{(r)}(R)$ becomes less than the speed of sound in the ambient interstellar gas.

E. Dynamics of shells driven by radiation pressure from field stars

Very large shells having diameters of the order of a kiloparsec and expansion velocities of 10–30 $\mathrm{km\,s^{-1}}$ have been observed during the last decade in our own (Heiles, 1979) and nearby galaxies (Meaburn, 1980; Brinks and Bajaja, 1986; Deul and Hartog, 1990; Puche *et al.*, 1992; Puche and Westpfahl, 1995).

Two main physical mechanisms for the creation of such shells are considered in current research. The first is multiple supernovae explosions from OB-association

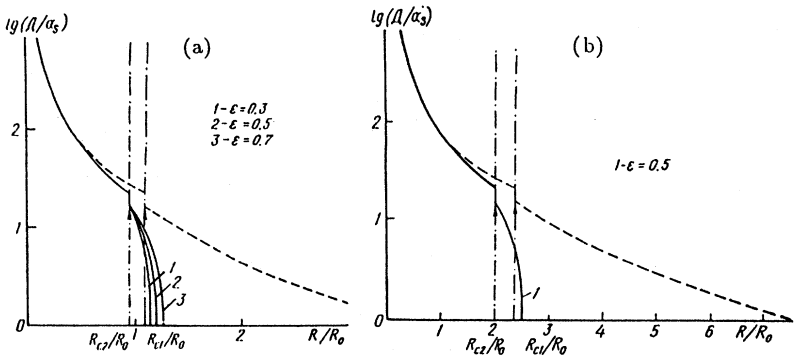

FIG. 4. Shock-wave expansion in a gravitating medium with the parameters of the circumnuclear region of the galaxy. Dashed lines represent shock-wave expansion if the external gravitational field is negligible, ε is the part of the thermal energy that is carried away by radiation during a short transition from the adiabatic to the radiative phase. (a) Explosion energy $E = 10^{56}$ ergs; (b) Explosion energy $E = 10^{57}$ ergs. From Pas'ko and Silich, 1986.

stars (Bruhweiler *et al.*, 1980; Tomisaka *et al.*, 1981; McCray and Kafatos, 1987). The second is collision of massive high-velocity clouds with the galactic plane (Tenorio-Tagle, 1980, 1981; Tenorio-Tagle *et al.*, 1986; Comeron and Torra, 1992).

Elmegreen and Chiang (1982) have proposed an alternative mechanism. They assume that supershells reach their huge sizes developing from smaller shells around O and B stars in OB associations under the influence of radiation pressure from field stars in the rarefied interior of a supernova remnant.

They suggest that initial perturbations produce a cavity in the gas with a dense shell. Absorption inside the cavity is small, and radiation flux from the stars becomes anisotropic due to dilution. The dense swept-up layer absorbs the photon momentum, which leads to creation of a radiative force—"radiation pressure." This radiation pressure accelerates the grains in the shell, which transmit this force to the gas by grain-gas collisions and by the ambient magnetic field. Thus starlight energy may be transferred under these circumstances to the kinetic energy of the shell motion. The radiation pressure from the field stars exerted on a thin shell is given by

$$P_r = \frac{\Delta F}{c}[1 - \exp(-Q_m \tau)], \tag{2.77}$$

where ΔF is the excess of the radiative flux from the cavity, c is the light speed, and τ is the optical depth of the shell. $Q_m = 0.74$ is the wavelength-averaged momentum absorption efficiency factor. If the initial state of the interstellar medium is uniform, then the resulting radiative flux contributed by all stars (inside and outside the cavity) exerting pressure on the shell is equal to the difference between the flux from a cleared cavity and one filled with gas at the mean interstellar density. This difference for a uniform spherical volume with mean isotropic emissivity inside the cavity j_c, outside the remnant j_0, and wavelength-averaged linear extinction coefficient K [for our galaxy $K \approx 1.51 \times (n/1.2\ \mathrm{cm}^{-3})\ \mathrm{kpc}^{-1}$], may be expressed as follows (Elmegreen and Chiang, 1982):

$$\Delta F = \Phi(j_c, 0, R) - \Phi(j_0, K, R), \tag{2.78}$$

where R is the shell radius,

$$\Phi(j, K, R) = 2\pi j \int_0^{\pi/2} \sin\Theta \cos\Theta d\Theta \times \int_0^{2R\cos\Theta} \exp(-Kr) dr. \tag{2.79}$$

Elmegreen and Chiang (1982) have shown that Eq. (2.77) can be written as

$$P_r \approx 0.8 U x\,[\Gamma(x) - 0.26]\,[1 - \exp(-x/4)]\,, \tag{2.80}$$

where

$$\Gamma(x) = 1 - \frac{3}{4x}\left[1 + \frac{1}{2x^2}\left[(1 + 2x)\exp(-2x) - 1\right]\right]. \tag{2.81}$$

Here $x = RK$ is the dimensionless radius of the shell having the physical sense of the optical depth of the unperturbed gas along the cavity radius.

Expansion of a spherically symmetric self-gravitating shell in a uniform medium, with density $\rho_e = \frac{14}{11} m_H n$ and pressure P_e, obeys the equation (Elmegreen and Chiang, 1982; Pas'ko and Silich, 1988)

$$\frac{d}{dt}\left(\frac{4}{3}\pi\rho_e R^3 u\right) = 4\pi R^2 (P_r - P_e) - \frac{1}{2}\frac{G}{R^2}\left(\frac{4}{3}\pi\rho_e R^3\right)^2. \tag{2.82}$$

Here G is the gravitational constant and u is the shell velocity. This equation may be rewritten in dimensionless form for $M = u/a_0$, $a_0{}^2 = P_0/\rho_e$, time $T = t a_0 K$, and dimensionless parameters $\beta = 2.5U/P_0$, $\alpha = 2\pi G \rho_e^2 / 3K^2 P_0$, $\xi = P_e/P_0$ (for $P_0 \approx 1.7 \times 10^{-12}\ \mathrm{ergs\,cm}^{-3}$ we have $\alpha \approx 2.2$), as

$$\frac{dM}{dT} = -\frac{3(M^2 + \xi)}{x} + \beta\,[\Gamma(x) - 0.26] \times [1 - \exp(-x/4)] - \alpha x. \tag{2.83}$$

Here the optical depth τ of a thin spherical shell, formed from a uniform cavity gas with linear absorption coefficient K, is $\tau = \frac{KR}{3}$, and Q_m is taken as approximately 0.75, so as to allow for analytical solution. The numerical solution of this equation with $\alpha = 0$ was studied by Elmegreen and Chiang (1982). Three types of solutions emerged from their calculations. For small initial radius, external pressure exceeds radiative pressure throughout the evolution, and the shell decelerates steadily to zero velocity. For greater initial radius x_0, deceleration is replaced by an acceleration phase. The turnaround point for $\beta \approx 1$ and $x_0 = 2.25$ corresponds to approximately 10^8 yr. For large initial radius x_0, radiative pressure P_r exceeds external gas pressure P_e from the very beginning. In this case the shell expands with increasing speed up to its breakup by Rayleigh-Taylor or Jeans instability.

Self-gravity of the shell has been taken into account by Pas'ko and Silich (1988), who have found an analytic solution for Eq. (2.83) with an arbitrary parameter α. The shell is accelerated if the right-hand side of Eq. (2.83) is positive, that is, if

$$0 < M < \left[\beta x[\Gamma(x) - 0.26]\left(1 - \frac{\exp(-x/4)}{3}\right) - \frac{\alpha x^2}{3} - \xi\right]^{1/2}. \tag{2.84}$$

Equation (2.84) shows that the expansion velocity may increase only if parameter β lies above the curve,

$$\beta = \frac{\alpha x^2 + 3\xi}{x[\Gamma(x) - 0.26][1 - \exp(-x/4)]}. \tag{2.85}$$

For any external pressure P_e (parameter ξ), the curve (2.85) has a minimum. Figure 5 shows that there is a

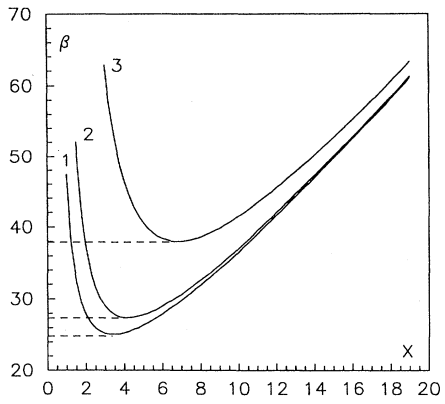

FIG. 5. Curves $\beta(x)$ for different values of ξ: (1) $\xi = 0$; (2) $\xi = 1$; (3) $\xi = 30$. From Pas'ko and Silich, 1988.

critical value $\beta_c \simeq 25$. The expansion velocity may increase only if $\beta > \beta_c$. This condition is necessary but not sufficient for shell acceleration. Whether the shell accelerates or not (for $\beta > \beta_c$) depends on the initial values of M_0, shell radius x_0, and external pressure P_e. For a given P_e, inequality (2.84) defines the region in the M, x plane where dM/dT is positive (if $\beta > \beta_{\min}$). This region lies between the abscissa and the curve,

$$M = \{\beta x[\Gamma(x) - 0.26][1 - \exp(-x/4)]/3 - \alpha x^2/3 - \xi\}^{\frac{1}{2}}. \quad (2.86)$$

In our galaxy the ratio of radiation energy density U to mean gas pressure P_0 is such that $\beta \approx 1$ (Elmegreen and Chiang, 1982). This value is much less than the critical one, $\beta_c \approx 25$. Thus we cannot test in our galaxy the hypothesis that the largest expanding neutral hydrogen shells may be produced by radiation pressure of the field stars.

F. Interstellar bubbles

Strong stellar winds with terminal velocities of about $1000\,\mathrm{km\,s^{-1}}$ from stars of early spectral type were discovered by Morton (1967). Earlier Gershberg and Scheglov (1964) observed peculiar gas motions with velocities of some dozen kilometers per second in the Orion, NGC 6618, and NGC 6523 nebulae. Johnson and Hogg (1965) have drawn attention to a new class of circle nebulae and suggested that they might be caused by the action of strong stellar winds from the central Wolf-Rayet stars. Such winds cause the ejection of gas with a large amount of kinetic energy into the medium around progenitors of type-II supernovae. SN 1987A provides an example of such a process [see the reviews of Imshennik and Nadyozhin (1989) and McCray (1993)]. Extensive observational evidence of the interaction of stellar wind with the ambient interstellar gas medium has been collected by Lozinskaya (1992). Dopita *et al.* (1994) have published an atlas of the ring nebulae around Wolf-Rayet stars in the Magellanic Clouds. The origin of extensive gaseous envelopes around Wolf-Rayet stars has been discussed by Bisnovatyi-Kogan and Nadyozhin (1972).

The principal model for the interaction of a stellar wind with the circumstellar gas medium has been described by Pikel'ner (1968), Pikel'ner and Shcheglov (1968), Avedisova (1971), Dyson and de Vries (1972), and Dyson (1973). They have shown that the evolution of a wind-driven bubble is very similar to the evolution of a supernova remnant. There is a short initial phase of free expansion, an adiabatic phase, and a radiative or snowplow phase when, due to the increasing importance of radiative cooling, the swept-up interstellar gas collapses into a thin cold shell. A comprehensive model for the evolution of a wind-driven interstellar bubble has been advanced by Castor *et al.* (1975) and Weaver *et al.* (1977). A schematic view of a radiative wind bubble is shown in Fig. 6. The bubble has a four-zone structure: (a) free-expansion stellar wind zone with the constant expansion velocity V_w which is surrounded by the inner shock surface; (b) hot, almost isobaric region occupied by the shocked interstellar gas evaporated from the dense shell and stellar wind gas; (c) dense, cold shell containing most of the swept-up interstellar gas separated from region (b) by contact discontinuity; and (d) undisturbed interstellar gas region separated from region (c) by the outer shock wave. The large temperature gradient between the hot rarefied interior and the cold expanding shell causes the shell to evaporate and add mass inside the cavity. The process of shell evaporation is similar to that of the clouds inside a supernova remnant, described in Sec. II.A.2. In order to illustrate this process Castor *et al.* (1975) have

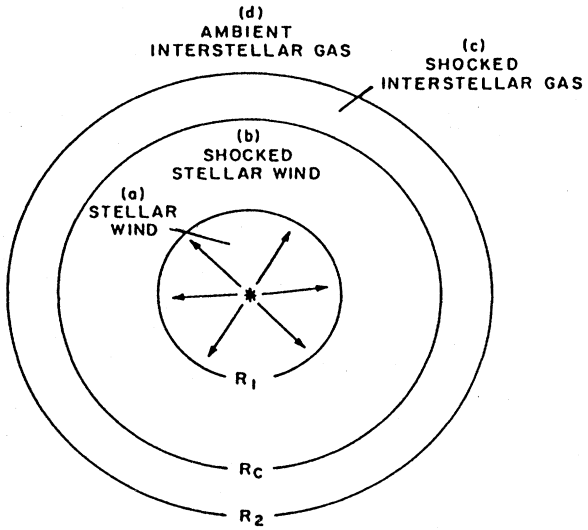

FIG. 6. Schematic sketch of a radiative bubble driven by stellar wind.

examined a time-independent plane-parallel solution for the mass-loss rate,

$$\dot{M}_b = 4\pi\rho u R_s^2, \tag{2.87}$$

where R_s is the shell radius, and ρ and u are the density and velocity in region (b). Assuming that radiative cooling is negligible in the transition zone, we can write the equation of energy conservation in the form

$$\nabla\,[\rho u(\tfrac{1}{2}u^2 + \tfrac{5}{2}a^2) + q] = 0, \tag{2.88}$$

where $a^2 = kT/\mu$, T is the temperature, μ is the mean mass per particle, $q = -\kappa \nabla T$. The thermal conductivity is given by $\kappa = CT^{5/2}$, $C = 6.0 \times 10^{-7}$ ergs cm^{-1} s^{-1} K$^{-7/2}$. Integration of this equation gives

$$\frac{5}{2}a^2\dot{M}_b\left(1 + \frac{1}{5}\frac{u^2}{a^2}\right) - 4\pi R_s^2\kappa\frac{dT}{dz} = A, \tag{2.89}$$

where $z = R_s - r$ is the distance from the shell to the center of the remnant. The integration constant A represents the difference between the inward enthalpy flux and the outward heat flux and approximately equals zero. Since the motion in region (b) is subsonic, we can neglect the second term in the brackets and solve Eq. (2.89) separately from the equation of motion with two boundary conditions: $T = 0$ at $z = 0$ and $T = T_b$ near the center of region (b):

$$T(r) = T_b(1 - r/R_s)^{2/5}, \tag{2.90}$$

where

$$T_b = \left(\frac{25k}{16\pi\mu}\frac{\dot{M}_b}{CR_s^2}\right)^{2/5}. \tag{2.91}$$

Then mass flux due to evaporation of the dense cold shell may be expressed as a function of central temperature T_b and shell radius R_s:

$$\dot{M}_b = \frac{16\pi\mu}{25k}CT_b^{5/2}R_s. \tag{2.92}$$

The distribution of gas number density $n(r)$ follows from the condition $n(r)T(r) = n_bT_b$,

$$n(r) = n_b(1 - r/R_s)^{-2/5}. \tag{2.93}$$

Comparison with the nonstationary spherically symmetric solution (Weaver *et al.*, 1977) shows that this approximation is valid within a factor of 2.

The motion of the bubble shell follows from the equations of mass, momentum and energy conservation (Castor *et al.*, 1975) and is similar to that of a radiative shock wave from a point explosion:

$$M = \frac{4}{3}\pi\rho_0 R_s^3, \tag{2.94}$$

$$\frac{d}{dt}(Mu_s) = 4\pi R_s^2 P_b, \tag{2.95}$$

$$\frac{dE_b}{dt} = L_0 - 4\pi R_s^2 P_b u_s, \tag{2.96}$$

$$\frac{dR_s}{dt} = u_s, \tag{2.97}$$

$$P_b = (\gamma - 1)\frac{3E_b}{4\pi R_s^3}. \tag{2.98}$$

Here ρ_0 is the density of the ambient gas, R_s and u_s are the radius and velocity of the shell, M is the mass of the swept-up interstellar gas, $L_0 = \frac{1}{2}\dot{M}_w V^2$ is the wind energy supply rate, P_b is the pressure of the hot interior gas, and E_b is the total thermal energy of this gas. Substitution of M and u_s from Eqs. (2.94) and (2.97) into Eqs. (2.95) and (2.96), then P_b from Eq. (2.95) into (2.98) and E_b from Eq. (2.98) into (2.96) yields the one differential equation:

$$\frac{d^2}{dt^2}(R^3\dot{R}) + (3\gamma - 2)R^{-1}\dot{R}\frac{d}{dt}(R^3\dot{R}) = \frac{9(\gamma - 1)L_0}{4\pi\rho_0}\frac{1}{R}. \tag{2.99}$$

It is easy to see by simple substitution that this equation has a power-law solution (Castor *et al.*, 1975; Avedisova, 1971),

$$R_s = \left[\frac{375(\gamma - 1)}{28(9\gamma - 4)}\frac{L_0}{\pi\rho_0}\right]^{1/5}t^{3/5}, \tag{2.100}$$

$$u_s = \frac{3}{5}\frac{R_s}{t}, \tag{2.101}$$

$$P_b = 7\rho_0\left[\frac{3(\gamma - 1)}{700(9\gamma - 4)}\frac{L_0}{\pi\rho_0}\right]^{2/5}t^{-4/5}. \tag{2.102}$$

Integration of Eq. (2.93) by the bubble volume gives the mass of the gas in region (b):

$$M_b = \frac{125\pi}{39}\mu n_b R_s^3. \tag{2.103}$$

Assuming that the pressure inside the bubble P_b is approximately uniform and equals kn_bT_b, the interior mass M_b may be expressed as function of time and central temperature T_b,

$$M_b = \frac{125\pi\mu}{39k}\frac{P_bR_s^3}{T_b}, \tag{2.104}$$

where R_s and P_b are defined by Eqs. (2.100) and (2.102). Combining derivatives of Eq. (2.104) with respect to t with Eq. (2.92), we get the differential equation that defines T_b as function of time. This equation has a power-law solution (Castor *et al.*, 1975) which allows us to define T_b as a function of the energy input rate L_0 and bubble radius R_s:

$$T_b = \left[\frac{128125(\gamma - 1)}{5824(9\gamma - 4)\pi}\frac{L_0}{CR_s}\right]^{2/7}. \tag{2.105}$$

The equation of state $P_b = kn_bT_b$ and Eqs. (2.100) and

(2.102) then give the central gas number density,

$$n_b = \frac{15(\gamma-1)}{4\pi(9\gamma-4)}\frac{L_0 t}{kT_b R_s^3}. \quad (2.106)$$

This theory has been applied by McCray and Kafatos (1987) to the dynamics of supershells caused by stellar winds and coherent supernovae explosions in OB associations. It was assumed that most massive stars are born in compact groups containing some dozens or hundreds stars. A typical OB association in our galaxy has 20–40 stars of spectral type earlier than B3 (Heiles, 1987). The combined action of these stars will create an expanding bubble with radius given by Eq. (2.100), which may be rewritten in astrophysical quantities as

$$R_s = 267(L_{38}/n_0)^{1/5} t_7^{3/5} \text{ pc}, \quad (2.107)$$

where L_{38} is the energy input rate in 10^{38} ergs s^{-1} units, t_7 is time in units of 10^7 yr, and n_0 is the particle number density of the ambient gas.

Thus the combined action of stellar winds in a typical OB association may create a bubble with a radius of some dozens of parsecs before the first supernova explosion. But the main growth of supershells with radii of hundreds of parsecs is driven by the subsequent supernova explosions in the OB association.

The main sequence lifetimes of massive stars are given approximately by $\tau_{\rm OB} \approx 3\times10^7(M/10M_\odot)^{-1.6}$ yr for $7 \le M \le 30M_\odot$ (Stothers, 1972) and $\tau_{\rm OB} \approx 9\times10^6(M/10\,M_\odot)^{-0.5}$ yr for $30 \le M \le 80\,M_\odot$ (Chiosi *et al.*, 1978). Then for the initial mass function $dN/dM = M^{-(1+\beta)}$, $\beta = 1.6$, supernovae will release energy with the average rate

$$L_{\rm SN} = 6.3\times10^{35}(N_{\rm OB}E_{51}) \text{ ergs s}^{-1}, \quad (2.108)$$

where $N_{\rm OB}$ is the number of massive ($M > 7\,M_\odot$) stars in the OB association and E_{51} is the explosion energy in units of 10^{51} ergs. Mac Low and McCray (1988) have shown that after the first 5–10 star explosions discrete supernovae may be treated as events with a continuous energy input rate $L_{\rm SN}$. Then the radius and velocity of an expanding bubble may be expressed by Eqs. (2.100)–(2.101) (McCray and Kafatos, 1977):

$$R_{\rm sh} = 97(N_{\rm OB}E_{51}/n_0)^{1/5} t_7^{3/5} \text{ pc}, \quad (2.109)$$

$$V_{\rm sh} = 5.7(N_{\rm OB}E_{51}/n_0)^{1/5} t_7^{-2/5} \text{ km s}^{-1}. \quad (2.110)$$

The distortion of the largest shells by the gas density gradient and galactic disk shear will be discussed in Secs. III.G and III.H.

Chu and Mac Low (1990), Wang and Helfand (1991), and Chu *et al.* (1993) have found enhanced diffuse x-ray emission from some H II regions of the Large Magellanic Cloud containing OB associations. Most of these complexes have simple shell-like morphology. Their x-ray luminosities range from 7×10^{34} ergs s^{-1} to 7×10^{36} ergs s^{-1}. A classical H II region has too low a temperature ($\sim 10^4$ K) to be a source of x-ray emission. But as has been shown in this subsection the combined effect of strong stellar winds from massive stars belonging to OB associations may produce an expanding bubble filled by a hot ($\sim 10^6$ K) rarefied mixture of shocked stellar wind and interstellar gas evaporated from the cold thin shell. Thus we may assume that x-ray/H II complexes in the Large Magellanic Cloud represent an early stage of superbubble evolution. The x-ray luminosity from a hot bubble interior is given by the integral

$$L_x = 4\pi\int_0^{R_s} n_i^2(r)\Lambda_x(T(r))r^2dr, \quad (2.111)$$

where distributions of the ion number density $n_i(r) = \frac{11}{24}n(r)$ and temperature $T(r)$ inside the remnant are given by Eqs. (2.90), (2.93), (2.105), and (2.106). The x-ray emissivity falls quickly for temperatures below the critical one, $T_c \simeq 5\times10^5$ K, so the outer region of a hot bubble interior will not add to the total x-ray luminosity. Chu and Mac Low (1990) have estimated that over the temperature range 2.5×10^6–10^8 K the x-ray emissivity Λ_x within the Einstein energy band of 0.2–4 keV is almost independent of temperature. It may be approximated within a 25% accuracy by the constant value

$$\Lambda_x \approx 9\times10^{-24}\xi \text{ ergs cm}^3\text{ s}^{-1}, \quad (2.112)$$

where ξ is metallicity. Then integration of Eq. (2.111) with density and temperature distributions (2.90) and (2.93) gives (Chu and Mac Low, 1990)

$$L_x = 3.29\times10^{34}\xi I(\tau)L_{37}^{33/35} \times n_0^{17/35}t_6^{19/35} \text{ ergs s}^{-1}, \quad (2.113)$$

where $\tau = T_c/T_b$, $I(\tau)$ is the dimensionless integral

$$I(\tau) = \frac{125}{33} - 5\tau^{1/2} + \frac{5}{3}\tau^3 - \frac{5}{11}\tau^{11/2}. \quad (2.114)$$

Chu and Mac Low (1990; Chu *et al.*, 1993) have shown that for N51D and N44 complexes, x-ray luminosities estimated from Eq. (2.113) fall an order of magnitude below the observed value. They proposed a mechanism for an off-center supernova explosion, which will be considered in Sec. III.F.3. Wang and Helfand (1991) have reached the same conclusion based on more detail analysis of the x-ray observations.

Franco *et al.* (1993) have examined the interaction of small clumps ejected during supernova explosions with the multisupernova shell. At early times the contrast between the density of ejected fragments and that of gas in the bubble interior remains low, and clumps move almost freely. Then reverse shock begins effectively to erode the fragments. If the ejected fragments can survive until they collide with the bubble shell (which is possible during the first few 10^6 years of the remnant's evolution) they will reshock some fraction of the previously cold shell and reheat it to temperatures of about 10^6 K. Thus during

the first few 10^6 years of evolution the remnant should be highly inhomogeneous, with a series of local bright x-ray spots indicating the places where ejected fragments impacted with the shell.

A similar view on the origin of the powerful x-ray emission from SN1986j was proposed by Chugai (1993). In this model x-ray emission is associated with shocked clouds compressed by the dynamic pressure of supernova ejecta.

Bochkarev and Lozinskaya (1985) have calculated the expected x-ray emission from eight ring nebulae around Wolf-Rayet and O_f stars. They also used a model (Castor *et al.*, 1975) for bubble structure and data (Raymond and Smith, 1977) for the x-ray emissivity, and took into account the x-ray absorption as consistent with model A from Ride and Walker (1977). The spectral density of the x-ray flux was written

$$F_\nu = \frac{R_s^3 n_b^2}{r^2} \exp(-\tau_\nu) \int_0^1 x^2 (1-x)^{-4/5} \Lambda_x(T) dx, \tag{2.115}$$

where $x = R/R_s$ is a dimensionless coordinate in the bubble interior, r is the distance to the nebula, and τ_v is the optical depth. Integral (2.115) was calculated numerically. The expected x-ray fluxes fell in the interval 10^{-15}–10^{-11} ergs cm^{-2} s^{-1}.

Bochkarev (1985) has calculated the spectra of x-ray-emitting bubbles in the equilibrium-ionization approximation and compared them with the spectra of the isothermal gas plasma. The isothermal bubble spectra are generally harder but have a steeper low-frequency cutoff. Calculations of the soft (0.1–0.4 keV) x-ray emission for six strong stellar wind nebulae—NGC 6888, S 119, S 308, NGC 2359, NGC 3199, and NGC 7635—were improved by Bochkarev and Zhekov (1990), who took into account the deviation of the hot gas ionization state from equilibrium. They showed that this effect decreases the estimated x-ray fluxes and the central bubble temperature by several times but enhances the hard ($h\nu \geq 1$ keV) part of the nebula spectra.

Soft x-ray emission from the nebula NGC6888, formed by the stellar wind of the central Wolf-Rayet star HD192163, was discovered by Bochkarev (1988) after processing of the Einstein observatory data. The x-ray flux in the 0.2–3.0-keV band was estimated to be 1×10^{-12} ergs cm^{-2} s^{-1}. This value is an order of magnitude lower than that predicted by the model of Castor *et al.* (1975), but agrees well with the calculations of Bochkarev and Zhekov (1990).

III. TWO-DIMENSIONAL SHOCKS

A. Kompaneets approximation

1. Propagation of an adiabatic shock wave in an exponential atmosphere

The first analytic discussion of two-dimensional shock waves was presented by Kompaneets (1960). He considered propagation of adiabatic shock waves from a point explosion in a plane-stratified exponential atmosphere with the gas density distribution

$$\rho(z) = \rho_0 \exp(-z/Z_0). \tag{3.1}$$

There are three independent dimensional parameters in the problem: the midplane density ρ_0, the characteristic scale height of the gas density inhomogeneity Z_0, and the energy of the explosion E_0. Thus it is not possible to extend the self-similar method to describe shock-wave propagation in this case.

The main idea of the Kompaneets approach is to calculate the smoothed, averaged parameters of the hot gas within the remnant only, and not to consider possible space variations of the thermodynamical variables.

It is assumed that the pressure in the shocked gas is uniform and equal to

$$P_{\rm sh} = (\gamma - 1)\frac{\lambda E_0}{\Omega}, \tag{3.2}$$

where γ is the ratio of specific heats. Here the constant λ describes deviation of the post-shock pressure from the mean value and the fraction of the explosion energy that is converted into the thermal energy of the hot interior gas. We consider here an axially symmetric problem in cylindrical coordinates (r, ϕ, z). The volume Ω of the remnant is defined by the integral

$$\Omega(t) = \pi \int_{z_1}^{z_2} r^2(z,t) dz, \tag{3.3}$$

where z_2 and z_1 are the coordinates of the remnant top and bottom.

The physical reasons for this simplification are the high temperature and great sound speed in the shocked gas, which permit redistribution of the internal energy to a nearly isobaric state before the shock front moves an appreciable distance. The Kompaneets approximation assumes also that the shock is strong, i.e., the ambient gas pressure is negligible. Then Hugoniot conditions determine the normal component of the expansion velocity at any point in the shock front as function of time:

$$D_n = \sqrt{\frac{\gamma+1}{2}\frac{P_{\rm sh}(t)}{\rho}}, \tag{3.4}$$

where $\rho(z)$ is the density of the ambient interstellar gas.

Let us define the surface of the shock front as $f(r,z,t) = 0$. The time derivative of this function is

$$\frac{df}{dt} = \frac{\partial f}{\partial t} + \frac{\partial f}{\partial z} D_z + \frac{\partial f}{\partial r} D_r = 0. \tag{3.5}$$

The component of the arbitrary vector $\mathbf{D}$ which is normal to this surface may be expressed as

$$D_n = n_z D_z + n_r D_r = \frac{1}{|\nabla f|}\left(\frac{\partial f}{\partial r} D_r + \frac{\partial f}{\partial z} D_z\right). \tag{3.6}$$

Then combination of Eqs. (3.5) and (3.6) gives an expression for the shock-wave velocity in the form (see also Shapiro, 1979)

$$D_n = -\frac{\partial f/\partial t}{|\nabla f|}. \tag{3.7}$$

Assuming that the equation of the shock surface may be written in the evident form $r = r(z,t)$ and equating (3.7) to (3.4), we get an equation for the evolution of the shock front,

$$\left(\frac{\partial r}{\partial y}\right)^2 - \exp(z/Z_0)\left[\left(\frac{\partial r}{\partial z}\right)^2 + 1\right] = 0. \tag{3.8}$$

Here y is a transformed time variable,

$$y = \int_0^t \sqrt{\frac{\gamma^2-1}{2}\frac{\lambda E_0}{\rho_0 \Omega}}\,dt, \tag{3.9}$$

and it has been taken into account that

$$|\nabla f| = \sqrt{\left(\frac{\partial f}{\partial r}\right)^2 + \left(\frac{\partial f}{\partial z}\right)^2} = \sqrt{1 + \left(\frac{\partial r}{\partial z}\right)^2}. \tag{3.10}$$

Equation (3.8) may be solved analytically by separation of the variables (Stepanov, 1958):

$$\frac{\partial r}{\partial y} = \xi, \quad \frac{\partial r}{\partial z} = \pm\sqrt{\xi^2 \exp(-z/Z_0) - 1}, \tag{3.11}$$

$$r = \xi y \pm \int_0^z \sqrt{\xi^2 \exp(-z/Z_0) - 1}\,dz + b(\xi), \tag{3.12}$$

$$\frac{\partial r}{\partial \xi} = y \pm \int_0^z \frac{\xi \exp(-z/Z_0)}{\sqrt{\xi^2 \exp(-z/Z_0) - 1}}\,dz + \frac{\partial b}{\partial \xi} = 0, \tag{3.13}$$

where ξ is a parameter. The function $b(\xi)$ is defined by the initial conditions and is equal to zero, for shocks that are spherical at the initial time (small y). Elimination of the parameter ξ from Eqs. (3.12) and (3.13) then yields the expression for the shape of the shock front:

$$r = 2Z_0 \arccos\left\{\frac{1}{2}\exp\left(\frac{z}{2Z_0}\right)\left[1 - \frac{y^2}{4Z_0^2} + \exp\left(\frac{-z}{Z_0}\right)\right]\right\}. \tag{3.14}$$

An equation for the top and bottom of the blastwave follows from Eq. (3.14) if we set r to zero:

$$\exp(-z_{1,2}/2Z_0) = 1 \mp \frac{y}{2Z_0}. \tag{3.15}$$

A solution of Eq. (3.15) exists for $0 \le y < 2Z_0$. When y approaches $2Z_0$ and physical time t also remains finite, the top of the remnant reaches infinity. Physically this means infinite shock acceleration in the z direction due to the strong density gradient. This is an effect of the atmospheric blowout. The bottom of the shock wave

$$z_2 = -2Z_0 \ln 2 \tag{3.16}$$

does not penetrate downward more than ≈ 1.4 scale height in this model, as a consequence of our assumption of uniform pressure within the cavity (see Laumbach and Probstein, 1969). When the shock wave blows out, the remnant volume goes to infinity, while internal gas pressure and downstream velocity drop to zero. The maximum cylindrical radius of the blastwave can be obtained from Eq. (3.14) if $(\partial r/\partial z) = 0$:

$$r_{\max} = 2Z_0 \arccos\frac{y}{2Z_0}. \tag{3.17}$$

This radius cannot exceed the critical value $r_c = \pi Z_0$ for any explosion energy, because a larger fraction of the explosion energy is escaping away from the plane of the explosion $z = 0$ in the direction of the steepest density gradient.

Aside from the exponential atmosphere, the Kompaneets approximation may be used to determine shock-wave expansion initiated by a point explosion in a variety of ambient gas density distributions.

2. Expansion of an adiabatic shock wave in an exponential atmosphere with nonzero asymptotics

The atmospheric blowout phenomenon is the consequence of the specific (pure exponential) gas density distribution. A great variety of astrophysical objects (flat galaxies with extended halos, atmospheres of planets and stars, etc.) have more complicated multicomponent gas density distributions, which in the first approximation may be described as exponential but with a nonzero asymptotic value:

$$\rho = \rho_0 [\exp(-z/Z_0) + \alpha], \tag{3.18}$$

where α is an arbitrary constant, $0 < \alpha < 1$. Silich and Fomin (1983) have extended the Kompaneets method to this problem. If we use Eqs. (3.11)–(3.13) and use instead of ξ the constant $\eta = \xi^{-1}$, we get the basic equations for the evolution of the shock front as follows:

$$r = \eta^{-1}\left(y \pm \int_0^z \sqrt{\exp(-z/Z_0) + \alpha - \eta^2}\,dz\right) + b(\eta), \tag{3.19}$$

$$\frac{\partial r}{\partial \eta^{-1}} = y \pm \int_0^z \frac{\exp(-z/Z_0) + \alpha}{\sqrt{\exp(-z/Z_0) + \alpha - \eta^2}}\,dz + \frac{db}{d\eta^{-1}} = 0. \tag{3.20}$$

The requirement that the shock be spherically symmetric at an early time after the explosion defines the function $b(\eta)$ as zero (Kompaneets, 1960). Then Eqs. (3.19) and (3.20) give

$$r = 2Z_0 \frac{\eta}{\sqrt{\eta^2-\alpha}} \left\{ \arccos\sqrt{\eta^2-\alpha} - \arccos[\exp(z/2Z_0)\sqrt{\eta^2-\alpha}] \right\}, \tag{3.21}$$

$$y = 2Z_0 \left[\sqrt{1+\alpha-\eta^2} - \sqrt{\exp(-z/Z_0)+\alpha-\eta^2} \right] + \alpha\eta^{-1} r, \tag{3.22}$$

in the region

$$z \geq Z_+(y) \geq 0, \qquad \exp(-z/Z_0)+\alpha \geq \eta^2 \geq 0, \tag{3.23}$$

and

$$r = 2Z_0 \frac{\eta}{\sqrt{\eta^2-\alpha}} \left\{ \arccos[\exp(z/2Z_0)\sqrt{\eta^2-\alpha}] - \arccos\sqrt{\eta^2-\alpha} \right\}, \tag{3.24}$$

$$y = 2Z_0 \left[\sqrt{\exp(-z/Z_0)+\alpha-\eta^2} - \sqrt{1+\alpha-\eta^2} \right] + \alpha\eta^{-1} r, \tag{3.25}$$

in the region

$$z \leq Z_-(y) \leq 0, \quad \alpha+1 \geq \eta^2 \geq 0. \tag{3.26}$$

Restrictions (3.23) and (3.26) follow from the requirement that radius of the shock front r and transformed time y have to be real. The functions $Z_+(y)$ and $Z_-(y)$ follow from Eqs. (3.21), (3.22), (3.24), and (3.25) if $\eta^2 = \exp(-z/Z_0) + \alpha$ and $\eta^2 = 1+\alpha$. However, in contrast with the Kompaneets (1960) solution, Eqs. (3.21), (3.22), (3.24), and (3.25) define only the parts of the shock front near the Z axis. The lower boundary of the region (3.23) corresponds to the plane $z = z(t)$, where the derivations $\partial r/\partial z$ change their sign and the shock radius reaches maximum.

In the intermediate zone $Z_+(y) \geq z \geq Z_-(y)$ the function $b(\eta) \neq 0$. One can find it by matching the functions $r(z,\eta)$ and $y(z,\eta)$ in the plane $z = Z_+(y)$. The solution of Eqs. (3.19) and (3.20) then takes the form

$$r = 2Z_0 \frac{\eta}{\sqrt{\eta^2-\alpha}} \left\{ \arccos[\exp(z/2Z_0)\sqrt{\eta^2-\alpha}] + \arccos\sqrt{\eta^2-\alpha} \right\}, \tag{3.27}$$

$$y = 2Z_0 \left[\sqrt{\exp(-z/Z_0)+\alpha-\eta^2} + \sqrt{1+\alpha-\eta^2} \right] + \alpha\eta^{-1} r. \tag{3.28}$$

This is matched with the solution of Eqs. (3.24) and (3.25) automatically.

The motion of the remnant top and bottom ($r = 0$) follows from Eqs. (3.21), (3.22), (3.24), and (3.25) if $\eta \to 0$:

$$z_{\rm top} = \frac{y}{\sqrt{\alpha}} + 2Z_0 \left(1 + \ln \frac{1+\sqrt{1+\alpha^{-1}}}{2} - \sqrt{1+\alpha^{-1}} \right), \tag{3.29}$$

$$z_{\rm bot} = -2Z_0 \ln \frac{y+2Z_0}{2Z_0} + O(\alpha^{1/2}). \tag{3.30}$$

The maximum radius of the remnant $r_m(y)$ and the radius $r_0(y)$ of the remnant in the plane $z = 0$ follow from Eqs. (3.27) and (3.28) if we set $z = Z_+(y)$ or $z = 0$. For large times ($y \gg 2Z_0$) they are

$$r_m(y) = \frac{y}{\sqrt{\alpha}}, \tag{3.31}$$

$$r_0(y) = \frac{y}{\sqrt{\alpha}}. \tag{3.32}$$

It may be assumed from these equations that the expansion velocities of the shock wave in the plane $z = 0$ and far away from it are equal, despite a large density gradient in the z direction for $\alpha \ll 1$. This obvious contradiction vanishes if we take into account that $r_0(y)$ is the radius of intersection of the shock front with the plane $z = 0$, so the motion of this line does not represent the motion of the shock front. This is a phase speed whose large value

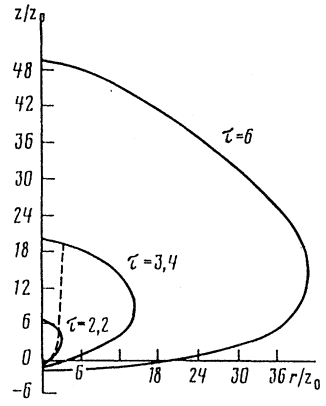

FIG. 7. Shape of the shock wave initiated by a point explosion in an exponential atmosphere with nonzero asymptotics for different "times" $\tau = y/Z_0$. Dashed line represents shape of the shock front in a pure exponential atmosphere ($\alpha = 0$) at the time of blowout $\tau = 2$. From Silich and Fomin, 1983.

is a result of the small angle ϕ between the shock-wave surface and the $z = 0$ plane (Silich and Fomin, 1983),

$$\tan\phi \approx \sqrt{\alpha}. \tag{3.33}$$

The shape of the shock front for different values of y is shown in Fig. 7 . Here the dashed line represents blowout phenomena for $\alpha = 0$.

Thus even a small deviation from the pure exponential distribution (3.1) provides qualitative changes in the shock-wave expansion. The "expansion time" y is no longer constrained by the value $2Z_0$. The cylindrical radius of the shock front is not restricted when the gas density is constant at infinity, in contrast to Kompaneets' (1960) solution with pure exponential gas distribution.

3. Off-center point explosion in a cloud

An off-center point explosion in a medium that is radially stratified has been considered by Korycansky (1992). This work was an attempt to understand the effects of an impact in a deep gaseous envelope, such as might have happened to the planet Uranus early in its history, accounting for its large obliquity.

In polar coordinates (r, Θ), Eq. (3.8) may be rewritten in the form

$$\left(\frac{\partial\chi}{\partial y}\right)^2 = \frac{\rho_0}{\rho(r)}\left[\left(\frac{\partial\chi}{\partial r}\right)^2 + \frac{1}{r^2}\right], \tag{3.34}$$

where the shock-wave surface is defined by the function

$$\psi(r, \Theta, y) = \chi(r, y) - \Theta = 0. \tag{3.35}$$

The density distribution is modeled by a spherically symmetric power law,

$$\rho(r) = \rho_0(r/a)^{-\omega}. \tag{3.36}$$

The explosion occurs on the axis $\Theta = 0$ at the radius $r = a$. Korycansky (1992) proposed to solve Eq. (3.34) by means of a coordinate transformation in which the solution takes spherical form, with the center in the initial blast location. Let us introduce the variables

$$\xi = (r/a)^{\alpha}, \quad \phi = \alpha\chi, \tag{3.37}$$

and choose the constant α to eliminate the density variation outside the brackets in Eq. (3.34). Then Eq. (3.34) is reduced to

$$\left(\frac{\partial\phi}{\partial y}\right)^2 = \frac{1}{y_c^2}\left[\left(\frac{\partial\phi}{\partial\xi}\right)^2 + \frac{1}{\xi^2}\right], \tag{3.38}$$

where the constant y_c is equal to $2a/|2-\omega|$, and $\alpha = (2-\omega)/2$. Equation (3.38) may be considered as an equation for shock-wave propagation in a uniform medium. Thus its solution is a sphere of radius $x = y/y_c$:

$$2\xi\cos\phi = 1 + \xi^2 - x^2. \tag{3.39}$$

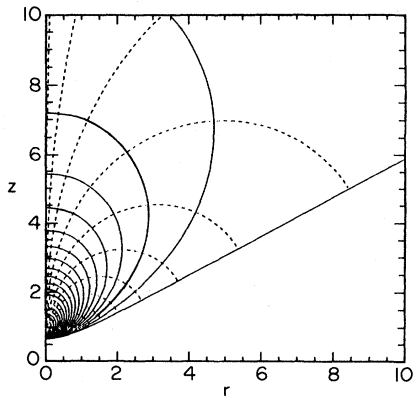

FIG. 8. Shape of the shock wave from an off-center point explosion in a radially stratified cloud. Dashed lines represent paths followed by the points on the shock front. The power-law index in the gas density distribution is $\omega = 5$. From Korycansky, 1992.

In terms of the "real" coordinates r, Θ this equation yields

$$2(r/a)^{\frac{2-\omega}{2}}\cos\left[\frac{(2-\omega)\Theta}{2}\right] = 1 - \frac{y^2(2-\omega)^2}{4a^2} + (r/a)^{2-\omega}. \tag{3.40}$$

The maximum r_+ and minimum r_- radii of the remnant along the Θ axis follow from Eq. (3.40) if we set $\Theta = 0$:

$$r_{\pm} = a\left[1 \mp \frac{y|2-\omega|}{2a}\right]^{\frac{2}{2-\omega}}. \tag{3.41}$$

For $\omega > 2, r_+ \to \infty$ if $y \to y_c$. This does not mean that blowout occurs as in the case of a pure exponential atmosphere because in this case time t goes to infinity in the same limit. The shapes of the shocks for the case $\omega = 5$ is shown in Fig. 8. Here the dashed lines represent the paths followed by points on the shock front. For $\omega > 2$ the intersection of the remnant at large time t by the plane through the symmetry axis, becomes a pair of straight lines that intersect at some angle θ_m. For $\omega > 4$ the value of θ_m is less than π, and the whole remnant is located in the upper half-space.

4. Other applications and comments

The Kompaneets approximation has been widely applied to different astrophysical problems. Lozinskaya (1979) used Eq. (3.14) to interpret the asymmetric shape and velocity field of the supernova remnant IC 443. Kovalenko (1987) found an hourglass solution for the shape of the shock front that appears after an explosion in the gas density distribution

$$\rho = \rho_0[\cosh^{-2}(z/Z_0) + \alpha]. \tag{3.42}$$

This distribution approximates the density stratification in the gaseous disks of spiral galaxies. Schiano (1985) used the Kompaneets approximation to model the form of the cavity produced by wind flow from an active galactic nucleus. Kontorovich and Pimenov (1995) have applied this method for solar bursts.

By "Kompaneets approximation" we denote the method in which (a) the shock velocity at each point is directed normal to the layer. (b) The energy density behind the shock is taken as a constant part of the average total energy of the bubble.

The constant λ in (3.2) is given analytically [Eqs. (2.64)–(2.67)] in the thin-layer approximation, $\lambda = \lambda_1\lambda_2$:

$$\lambda_1 = \frac{\gamma+1}{3\gamma-1}; \quad \lambda_2 = 2; \quad \lambda = 2\frac{\gamma+1}{3\gamma-1}, \tag{3.43}$$

where λ_1 is the ratio of thermal energy to the total energy of the explosion $\lambda_1 = E_{\rm th}/E_0$; and λ_2 is the ratio of the post-shock pressure to the average pressure in the bubble. A more exact value of λ is obtained by comparison of the Sedov and Kompaneets methods for a point explosion in a uniform medium. That gives the expression $\lambda = 32\pi\xi_0/75(\gamma^2-1)$, where ξ_0 from the Sedov solution is defined in Eq. (2.10). For $\gamma = 1; 5/3$ the values from the Sedov (1959) solution are $\lambda = 2; 1.53$, and from (3.43) we have $\lambda = 2; 1.33$.

These two suggestions (Kompaneets, 1960) permit us to reduce the problem to a kinematic one, because when we know the pressure behind the shock, then the velocity of the shock front is found directly from the Hugoniot relation (3.4). The Kompaneets approximation is compared with the results of full numerical calculations (Kestenboim *et al.*, 1974) for a pure exponential atmosphere in Fig. 9. Here dimensionless time $\tau = t/(\alpha_0\rho_0 Z_0^5/E_0)^{1/2}$, where constant $\alpha_0 = 0.851$ for $\gamma = 1.4$ (Sedov, 1959; Kestenboim *et al.*, 1974). Conservation of the thermal energy of the remnant (the value of λ is constant in the Kompaneets approach) and neglect of the pressure gradient within the cavity lead to a faster expansion of the shock front in the upward direction and slower motion in the downward one.

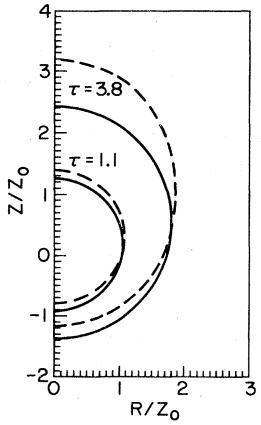

FIG. 9. Comparison of the Kompaneets approximation (dashed lines) with the full 2D calculations (solid lines). $\tau = t/(\alpha_0\rho_0 Z_0^5/E_0)^{1/2}$ is the dimensionless time.

A further improvement of this method, in which dynamic equations for thin-layer motion are solved directly and simplifications (a) and (b) are not used, is discussed below, and we call it "the thin-layer approximation." We stress this difference here, because both methods are sometimes referred to in the literature by the same name, "Kompaneets approximation" (Mac Low and McCray, 1988). In fact, Kompaneets also significantly improved his simplest version (Andriankin *et al.*, 1962), so we use another name for it only to make the description clearer.

B. Thin-layer approximation

The snowplow or thin-shell approximation was developed in plasma physics and hydrodynamics (Leontovich and Osovetz, 1956; Andriankin *et al.*, 1962; Imshennik, 1977) and has been extended to two-dimensional astrophysical problems by Bisnovatyi-Kogan and Blinnikov (1982), Mac Low and McCray (1988), Bisnovatyi-Kogan *et al.* (1989), and others. Different modifications of this method and the Kompaneets method for adiabatic shock waves have been compared with the full 2D calculations by Hnatyk (1987).

We consider here the extension of the thin-layer approximation following the papers of Bisnovatyi-Kogan and Blinnikov (1982) and Bisnovatyi-Kogan *et al.* (1989). As a more general case we consider an ambient gas with density distribution $\rho(z)$, which moves with velocity distribution $\mathbf{V}(\omega, z)$. Let us introduce a cylindrical coordinate system ω, ϕ, z and consider axial symmetry $\partial/\partial\phi = 0$. If $\mathbf{R} = (\omega, z)$ is the Euler radius vector of the shock front, $\mathbf{n}$ is the unit vector normal to the shock surface, and λ is the Lagrangian coordinate along the front, then the mass of the shell per unit Lagrangian coordinate λ and per radian around the symmetry axis Z may be expressed as

$$\mu = \sigma\omega\partial R/\partial\lambda, \tag{3.44}$$

where σ is the surface density of the layer and $\omega\partial R/\partial\lambda \equiv \partial\Sigma/\partial\lambda$ is the surface area per unit Lagrangian coordinate and per radian around the axis of symmetry Z. We assume that all interstellar gas swept up by the shock wave accumulates in a thin shell near the shock front. The time derivative of the momentum of the Lagrangian element is determined by the pressure difference between the hot internal and warm external gases, $\Delta P = P_{\rm in} - P_{\rm ext}$, the action of gravity $\mathbf{g}$, and the additional momentum of the swept-up interstellar gas. Thus equations for the mass and momentum conservation of the Lagrangian element may be written in the form

$$\frac{d\mu}{dt} = \rho(z)\omega\frac{\partial R}{\partial\lambda}(\mathbf{D}-\mathbf{V})\mathbf{n}, \tag{3.45}$$

$$\frac{d}{dt}(\mu\mathbf{U}) = \Delta P\frac{\partial\Sigma}{\partial\lambda}\mathbf{n} + \frac{d\mu}{dt}\mathbf{V} - \mu\mathbf{g}. \tag{3.46}$$

Here $\rho(z) = \rho_0 f(z)$, $\mathbf{U}$ is the gas velocity behind the shock, and $\mathbf{D}$ is the shock-front velocity. In components we have

$$\mathbf{U} = \left(\frac{d\omega}{dt}, \frac{dz}{dt}\right),$$
$$\mathbf{n} = \left(-\frac{\partial z}{\partial\lambda}, \frac{\partial\omega}{\partial\lambda}\right)\left(\frac{\partial R}{\partial\lambda}\right)^{-1}, \tag{3.47}$$
$$\frac{\partial R}{\partial\lambda} = \left[\left(\frac{\partial\omega}{\partial\lambda}\right)^2 + \left(\frac{\partial z}{\partial\lambda}\right)^2\right]^{\frac{1}{2}},$$

$\rho_0 = \eta n_0$ is the mass density of the interstellar medium in the plane of symmetry $z = 0$, and $\eta = (14/11)m_H$ is the mass per particle in a neutral gas with the "normal" chemical composition $n_{\rm He}/n_{\rm H} = 0.1$. The equations of mass and momentum conservation (3.45) and (3.46) are coupled by the relation between gas velocity $\mathbf{U}$ and shock velocity $\mathbf{D}$. Bisnovatyi-Kogan and Blinnikov (1982) distinguished between the normal components of gas and shock velocities and used for the adiabatic shock wave

$$D_n = \mathbf{D}\cdot\mathbf{n} = \frac{\gamma+1}{2}\mathbf{U}\mathbf{n}. \tag{3.48}$$

For a radiative blastwave we use the condition

$$\mathbf{U} = \mathbf{D}, \tag{3.49}$$

which is asymptotically accurate at $\gamma \to 1$. At the beginning of the calculation the remnant is divided into N Lagrangian layers by planes parallel to the plane of symmetry $z = 0$. The motion of every Lagrangian element is followed using the equations of mass and momentum conservation (3.45) and (3.46). The whole system of ordinary differential equations is coupled by the equation of energy conservation and expression for the internal gas pressure

$$P_{\rm in} = (\gamma-1)\frac{E_{\rm th}}{\Omega}, \tag{3.50}$$

where

$$\Omega = \pi\int_{z_{\rm min}}^{z_{\rm max}} \omega^2(\lambda)\left(\frac{\partial z}{\partial\lambda}\right)d\lambda \tag{3.51}$$

is the volume inside the blastwave. The total energy of the adiabatic remnant is defined as the sum of the initially deposited energy E_0, energy input rate $L(t)$, and added kinetic and thermal energies of the swept-up interstellar gas:

$$E_{\rm tot} = E_0 + \int_0^t\left(L(t) + \pi\int_{\lambda_{\rm min}}^{\lambda_{\rm max}}\dot{\mu}(V^2 + 3kT/\eta)d\lambda\right)dt. \tag{3.52}$$

The thermal $E_{\rm th}$ and kinetic E_k energies of the remnant are (Bisnovatyi-Kogan and Blinnikov, 1982)

$$E_{\rm th} = \frac{\pi P_{\rm in}}{\gamma-1}\int_{\lambda_{\rm min}}^{\lambda_{\rm max}}\omega^2(\lambda)\left(\frac{\partial z}{\partial\lambda}\right)d\lambda, \tag{3.53}$$

$$E_k = \pi\int_{\lambda_{\rm min}}^{\lambda_{\rm max}}\mu(U_\omega^2 + U_z^2)d\lambda. \tag{3.54}$$

The equation of energy conservation

$$E_{\rm tot} = E_{\rm th} + E_k + E_g \tag{3.55}$$

then defines the internal gas pressure $P_{\rm in}$. For a cold ambient medium without gravity that is at rest, the energy conservation equation may be written in the simple form

$$E_0 = \frac{\pi P_{\rm in}(t)}{\gamma-1}\int_{\lambda_{\rm min}}^{\lambda_{\rm max}}\omega^2(\lambda)\left(\frac{\partial z}{\partial\lambda}\right)d\lambda + \pi\int_{\lambda_{\rm min}}^{\lambda_{\rm max}}\mu(U_\omega^2 + U_z^2)d\lambda. \tag{3.56}$$

The system of equations (3.45), (3.46), (3.48) or (3.49), and (3.50)–(3.55) then describes the motion of the remnant.

C. Sector approximation

An approximation very similar in spirit to the snowplow model was developed by Laumbach and Probstein (1969). This method was applied to a strong point explosion in a plane-stratified exponential atmosphere. The flow was assumed to be radial, and energy and momentum were conserved in separate radial sectors. Later this was referred to as the "sector approximation." This assumption is equivalent to treating the streamlines as straight and does not take into account the tangential velocities along the shock front that appear in the developed stage of evolution under the influence of front distortion and gravity.

Let us introduce the spherical coordinate system r, ϕ, Θ with the polar angle Θ measured from the vertical axis, which is the axis of symmetry. We assume that an explosion occurs in the center of the coordinate system. Laumbach and Probstein (1969) have used a Lagrangian formulation of the hydrodynamic equations. Then the initial gas density distribution (3.1) can be written as

$$\rho_L(r_L, \Theta) = \rho_0\exp\left(-\frac{r_L}{Z_0}\cos\Theta\right), \tag{3.57}$$

where the Lagrangian coordinate r_L is defined as the position of a particular fluid particle at the time of the explosion. Assuming radial flow, the equation of mass conservation may be written as

$$\rho_L r_L^2 dr_L = \rho r^2 dr. \tag{3.58}$$

The equation of momentum conservation yields (Klimishin, 1984)

$$\frac{\partial^2 r}{\partial t^2} + \frac{r^2}{\rho_L r_L^2}\frac{\partial P}{\partial r_L} = 0. \tag{3.59}$$

The boundary conditions for a strong shock may be written as

$$\rho_{\rm sh} = \frac{\gamma+1}{\gamma-1}\rho_L, \tag{3.60}$$

$$P_{\rm sh} = \frac{2}{\gamma+1}\rho_L D^2, \tag{3.61}$$

where $D = \dot{R}$ is the shock-front velocity and R is the shock-front radius. The independent variables are the Lagrangian coordinate r_L and time t. The equations of momentum (3.59) and energy conservation may be written in integral form consistent with the assumption that mass within a particular solid angle is constant:

$$P(r_L,t,\Theta) - P_{\rm sh}(R,\Theta) = \int_{r_L}^{R}\frac{1}{r^2}\frac{\partial^2 r}{\partial t^2}\rho_L r_L^2 dr_L, \tag{3.62}$$

$$E_0 = 2\pi\int_0^\pi\left[\int_0^R \frac{P}{\gamma-1}r^2 dr + \frac{1}{2}\int_0^R\left(\frac{\partial r}{\partial t}\right)^2 \times\rho_L r_L^2 dr_L\right]\sin\Theta d\Theta. \tag{3.63}$$

Here E_0 is the explosion energy, the first term on the right side of Eq. (3.63) is the internal energy, and the second term is the kinetic energy per unit solid angle. To integrate Eqs. (3.62) and (3.63) we consider the Taylor expansion of the radius $r(r_L,t)$ near the shock front,

$$r(r_L,t) = R + \frac{\partial r}{\partial r_L}(r_L - R) + \frac{1}{2}\frac{\partial^2 r}{\partial r_L^2}(r_L-R)^2 + \cdots. \tag{3.64}$$

Taking into account that near the shock front

$$\left(\frac{\partial r}{\partial r_L}\right)_R = \left(\frac{\rho_L r_L^2}{\rho r^2}\right)_R = \frac{\gamma-1}{\gamma+1}, \tag{3.65}$$

$$\left(\frac{\partial^2 r}{\partial r_L^2}\right)_R = -\frac{2}{\gamma+1}\frac{\ddot{R}}{\dot{R}^2} - \frac{2}{\gamma+1}\left(\frac{1}{P}\frac{\partial P}{\partial r_L}\right)_R, \tag{3.66}$$

and differentiating Eq. (3.64) with respect to time, Laumbach and Probstein (1969) obtained relations for the location, velocity, and acceleration of the shock front r_s $(\partial r/\partial t)_s$ and $(\partial^2 r/\partial t^2)_s$. Approximating $r^{-2}(\partial^2 r/\partial t^2)$ in the integral (3.62) by the values of r and $(\partial^2 r/\partial t^2)$ at the shock front, we get the internal pressure P as a function of r_L, location of the shock front R, polar angle Θ, and a new variable

$$\eta = \frac{R}{Z_0}\cos\Theta. \tag{3.67}$$

To evaluate the energy integral (3.63) it was assumed that all swept-up interstellar mass is concentrated just behind the shock front. In the Laumbach and Probstein (1969) approach this means that, for any radius r different from the shock radius R, the corresponding value of the initial radius r_L is equal to zero. Then $P(r,\Theta,t) = P(0,t)$ and the integral (3.63) may be evaluated by substituting the pressure near the remnant center $P(0,t)$ for $P(r,\Theta,t)$ and replacing $\partial r/\partial t$ by its value at the shock front. Actually this entails the same averaging of internal parameters as in the thin-layer approximation with the additional assumption of straight particle trajectories. After taking into account Eqs. (3.61), (3.64), (3.65), and (3.66) in (3.62) and (3.63), and integrating ρ_L from Eq. (3.57), we get the ordinary differential equation for the evolution of the shock front

$$f(\eta)\frac{d^2\eta}{dt^2} + g(\eta)\left(\frac{d\eta}{dt}\right)^2 = \frac{E}{4\pi\rho_0}\left(\frac{\cos\Theta}{Z_0}\right)^5, \tag{3.68}$$

where the functions $f(\eta)$ and $g(\eta)$ are given by the formula (Laumbach and Probstein, 1969)

$$f(\eta) = \frac{8}{3}\frac{(2\gamma-1)\eta}{(\gamma-1)(\gamma+1)^2} \times\left[1-\exp(-\eta)\left(\frac{1}{2}\eta^2+\eta+1\right)\right], \tag{3.69}$$

$$g(\eta) = \frac{2}{3}\frac{\eta^3\exp(-\eta)}{\gamma^2-1} + \frac{\gamma-1}{2(2\gamma-1)}\left[\frac{7\gamma+3}{(\gamma+1)\eta}-1\right]f(\eta). \tag{3.70}$$

It is easy to see that motion of any part of the shock front may be scaled from a single solution for a definite direction (along the definite angle Θ). In the case of a uniform atmosphere with infinite Z_0, the variable η goes to zero, $\eta = R\cos\Theta/Z_0 \to 0$. In this limit we have instead of Eq. (3.68)

$$\frac{d^2R}{dt^2} + \frac{\gamma(5\gamma+1)}{(2\gamma-1)(\gamma+1)}\frac{1}{R}\left(\frac{dR}{dt}\right)^2 = \frac{9(\gamma-1)(\gamma+1)^2}{16\pi(2\gamma-1)R^4}\frac{E_0}{\rho_0}. \tag{3.71}$$

The solution of this equation gives the shock radius as a function of time

$$R = \left[\xi_0\frac{E}{\rho_0}\right]^{\frac{1}{5}} t^{\frac{2}{5}}, \tag{3.72}$$

where

$$\xi_0 = \frac{225}{32\pi}\frac{(\gamma-1)(\gamma+1)^3}{(4\gamma^2-\gamma+3)}. \tag{3.73}$$

Note that, when neglecting the third term in (3.64), one arrives at the thin-layer approximation in the spherical case. We have instead of (3.71)

$$\frac{d^2R}{dt^2}+\frac{6\gamma}{\gamma+1}\frac{1}{R}\left(\frac{dR}{dt}\right)^2=\frac{9}{8\pi}\frac{\gamma^2-1}{R^4}\frac{E_0}{\rho_0}, \tag{3.74}$$

which gives the solution (2.62), (2.63) instead of (3.72), (3.73). It was mentioned by Laumbach and Probstein (1969) that Eqs. (2.62) and (2.63) give better coincidence with the exact Sedov solution than do (3.72) and (3.73).

Numerical calculations of Falle *et al.* (1984) and Hnatyk (1987) have shown that the Laumbach and Probstein approximation underestimates the size and velocity of the shock. This is a consequence of the assumption that all mass is concentrated near the shock front and is accelerated to the shock-front velocity. Gaffet (1978) has improved this approach by taking into account higher-order terms in the Taylor expansion (3.64). Sakashita and Hanami (1986) have generalized the Laumbach and Probstein approach to a wind-driven bubble. Hnatyk (1988) used a modification of this method based on the approximate formula for shock-wave expansion (Klimishin and Hnatyk, 1981) to calculate adiabatic blastwave evolution in an exponential atmosphere, inside an interstellar cloud, and near a density discontinuity. It was proposed to approximate adiabatic shock-wave expansion in an inhomogeneous medium with the gas density distribution $\rho(R)$ by the formula

$$D(R)=\text{const}[\rho(R)R^{N+1}]^{-\delta}, \tag{3.75}$$

where D is the blastwave velocity, R is the shock-wave location, and $N=0,1,2$ for plane, cylindrical, and spherical shocks, respectively. The constant δ is defined as

$$\delta=\begin{cases}1/2, & \text{if } m(R)\le N+1 \text{ and } D\ge D_a,\\ 1/5, & \text{if } m(R)>N+1 \text{ or } D<D_a,\end{cases} \tag{3.76}$$

where $m(R)=-d\ln\rho/d\ln R$,

$$D_a=\frac{2}{3+N}\left[\frac{E}{\alpha\rho}\right]^{\frac{1}{2}}R^{-\frac{N+1}{2}}, \tag{3.77}$$

and α is the constant to be taken from the Sedov (1946) solution. The location of the shock front in any direction then is determined by solution of two ordinary differential equations:

$$\frac{dR}{dt}=D, \tag{3.78}$$

$$\frac{dD}{dt}=\delta\frac{D^2}{R}[m-(N+1)]. \tag{3.79}$$

Numerical integration of these equations along different rays from the explosion point then reproduces the shock-front evolution. At early stages of expansion, inhomogeneity in the ambient gas distribution leads to a significant anisotropy in the density, temperature, and x-ray luminosity along the shock front, while the shape of the remnant often remains almost spherical, with the center shifted from the center of the explosion. This may explain some supernova remnants, in which sphericity exists along with gradients in the surface brightness.

D. Thin-layer approximation for axial hydromagnetic flows

Regular magnetic fields may be expected to be one of the physical factors leading to axially symmetric hydrodynamical flows and various barrel-like envelopes, from planetary nebulae to superbubbles. Here we consider a generalization of the thin-shell approach for axisymmetric hydromagnetic flows. The basic concept is the definition of a control volume that is neither Eulerian nor Lagrangian. This concept was introduced by Giuliani (1982) and really is a combination of the sector approximation and thin-layer approaches. The control volume, following Giuliani (1982), is not fixed in the coordinate system and not connected with definite gas particles, but is located between two neighboring radius vectors $\mathbf{R}$ and $\mathbf{R}'$ and moves through space with the velocity of the swept-up interstellar gas. The shell is supposed to have a finite half-thickness Δ, and we define the line going through the middle of the shell as the "center line" (see Fig. 10 from Giuliani, 1982). Let us introduce the spherical coordinate system (r,Θ,ϕ) and consider axisymmetric flow. Then function $R(\Theta,t)$ defines the center line, while the $\mathbf{e}_\perp$ and $\mathbf{e}_\parallel$ in Fig. 10 are unit vectors normal and tangent to the center line. The parameter ξ is the angle between the radial vector $\mathbf{R}$ and the normal $\mathbf{e}_\perp$. It is assumed the shell is thin and Δ/R is a small number. The length of the segment along the shell dl is related to the length along the spherical surface $dl_R=Rd\Theta$ by the equation

$$\frac{dl_R}{dl}=\frac{Rd\Theta}{dl}=\cos\xi. \tag{3.80}$$

Taking into account that

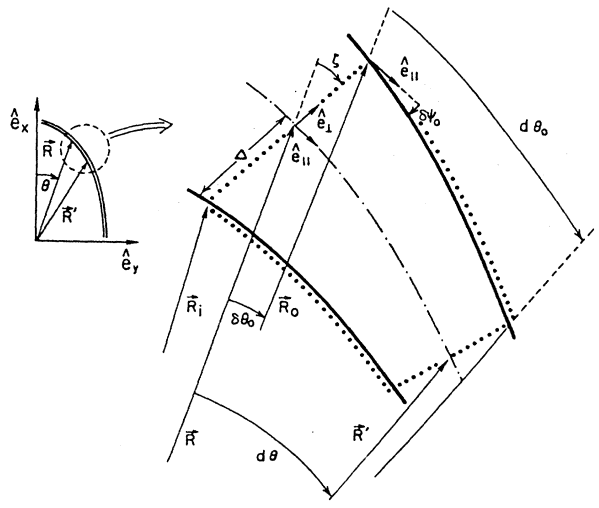

FIG. 10. Schematic sketch of the shell section indicating some of the geometrical quantities used in discussing a magnetized superbubble. From Giuliani, 1982.

$$\sin\xi = \frac{R - R'}{dl}, \tag{3.81}$$

we get

$$\tan\xi = -\frac{1}{R}\frac{\partial R}{\partial \Theta}. \tag{3.82}$$

Thus at a fixed time t the angle ξ is defined by the shape of the remnant, or the shape of the remnant may be restored if one knows the function $\xi = \xi(\Theta)$.

The unit normals $\mathbf{e}_\perp$ and $\mathbf{e}_\parallel$ are connected with the unit vectors $\mathbf{e}_r$ and $\mathbf{e}_\Theta$ along and perpendicular to the radius vector $\mathbf{R}$ by the equations

$$\mathbf{e}_\perp = \mathbf{e}_r \cos\xi + \mathbf{e}_\Theta \sin\xi, \tag{3.83}$$

$$\mathbf{e}_\parallel = -\mathbf{e}_r \sin\xi + \mathbf{e}_\Theta \cos\xi. \tag{3.84}$$

The normal and parallel components of the control volume midpoint (center-line) velocity may then be written

$$u_\perp = \frac{\partial R}{\partial t}\cos\xi, \tag{3.85}$$

$$u_\parallel = -\frac{\partial R}{\partial t}\sin\xi. \tag{3.86}$$

For a strong isothermal shock wave the shell material moves with almost the same velocity as the shell boundaries, and we have

$$v_\perp = u_\perp \tag{3.87}$$

where $\mathbf{v}$ is the shell gas velocity. Taking into account that the length of the shell segment is $dl = Rd\Theta/\cos\xi$ [see Eq. (3.80)], one can get an expression for dV of the control volume:

$$dV = 2\Delta\frac{R^2\sin\Theta}{\cos\xi}d\Theta d\phi. \tag{3.88}$$

The basic magnetohydrodynamic equations include the equations of mass and momentum conservation and the induction equation for the magnetic field $\mathbf{B}$. For a highly conducting medium without viscosity and heat conductivity, these equations may be written in the form (Kulikovskyi and Lyubimov, 1962)

$$\frac{\partial\rho}{\partial t} + \mathrm{div}(\rho\mathbf{v}) = 0, \tag{3.89}$$

$$\frac{\partial\mathbf{v}}{\partial t} + (\mathbf{v}\nabla)\mathbf{v} = -\frac{1}{\rho}\nabla\left(P + \frac{B^2}{8\pi}\right) + \frac{1}{4\pi\rho}(\mathbf{B}\nabla)\mathbf{B}, \tag{3.90}$$

$$\frac{\partial\mathbf{B}}{\partial t} = \mathrm{rot}(\mathbf{v}\times\mathbf{B}). \tag{3.91}$$

The last equation represents the flux freezing condition of the magnetic field, i.e., the conservation of the magnetic flux through the arbitrary Lagrangian surface, which moves with the gas flow.

Let us introduce the column density

$$\sigma = \int_{R_i}^{R_s}\rho d\eta = 2\Delta\bar{\rho}, \tag{3.92}$$

where η is the distance inside the shell along the normal to the center line, R_i and R_s are the shell's inner and outer radii, and $\bar{\rho}$ is the average density across the shell. The variation of mass within the control volume dV is defined by the mass flux due to gas motion across the surface of a control volume and the mass flux due to the motion of the control volume through the background material:

$$\frac{\partial}{\partial t}\oint\rho dV = \oint\rho\mathbf{u}\mathbf{n}dS - \oint\rho\mathbf{v}\mathbf{n}dS, \tag{3.93}$$

where $\mathbf{v}$ is the gas velocity and $\mathbf{u}$ is velocity of the control volume, as defined by Eqs. (3.85) and (3.86). Equation (3.93) may be rewritten in the form

$$\begin{aligned}\frac{\partial}{\partial t}(\sigma A d\Theta d\phi) = {} & [(u_\perp - v_{\perp 0})\rho_0 A d\Theta d\phi]_{R_s} \\ & -[(u_\perp - v_{\perp i})\rho_i A d\Theta d\phi]_{R_i} \\ & +[(v_\parallel - u_\parallel)\sigma R\sin\Theta d\phi]_{\mathbf{R}} \\ & -[(v_\parallel - u_\parallel)\sigma R\sin\Theta d\phi]_{\mathbf{R}'}.\end{aligned} \tag{3.94}$$

Here

$$A = \frac{R^2\sin\Theta}{\cos\xi}, \tag{3.95}$$

and the subscripts 0 and i denote the ambient gas parameters and hydrodynamical variables just behind the inner-shell boundary. The first two terms describe mass flow through the outer and inner surfaces of the control volume, and the last two terms reflect the mass flow through its lateral surfaces.

Thermal conductivity is suppressed across the magnetic field. Therefore, in a magnetized bubble, there is no evaporative mass flux from the shell to the hot bubble interior and one may set the density of the hot gas within the cavity to zero, $\rho_i = 0$. Taking into account that

$$-\frac{\sigma}{A}\frac{\partial A}{\partial t} = -\frac{2\sigma}{R}\frac{\partial R}{\partial t} - \sigma\tan\xi\frac{\partial\xi}{\partial t}, \tag{3.96}$$

one can write the equation of mass conservation (3.89) for a thin shell with $\Delta/R \ll 1$ in the form (Chevalier and Luo, 1994)

$$\begin{aligned}\frac{\partial\sigma}{\partial t} = {} & \rho_0(u_\perp - v_{\perp 0}) - \frac{2\sigma}{R}\frac{\partial R}{\partial t} - \sigma\tan\xi\frac{\partial\xi}{\partial t} \\ & -\frac{1}{A}\frac{\partial}{\partial\Theta}[R\sigma\sin\Theta(v_\parallel - u_\parallel)].\end{aligned} \tag{3.97}$$

In a similar fashion one can rewrite Eq. (3.90) for momentum conservation. For a strong shock wave with

$P_0 + B_0^2/8\pi \ll P_{\rm in} + B_i^2/8\pi$, this equation becomes (Giuliani, 1982)

$$\sigma\frac{\partial \mathbf{v}}{\partial t} = \left[\rho_0(u_\perp - v_{\perp 0})(\mathbf{v}_0 - \mathbf{v}) + \frac{B_{\perp 0}}{4\pi}(\mathbf{B} - \mathbf{B}_0)\right] + \left[\mathbf{e}_\perp\left(P_{\rm in} + \frac{B_i^2}{8\pi}\right) + \frac{B_{\perp i}}{4\pi}(\mathbf{B} - \mathbf{B}_i)\right] + (u_\parallel - v_\parallel)\sigma\frac{\cos\xi}{R}\frac{\partial \mathbf{v}}{\partial \Theta}. \quad (3.98)$$

The terms in the first set of brackets are the sum of the ram pressure and magnetic stress acting on the outer surface of the shell. The next terms are the sum of the thermal and magnetic pressures and magnetic stress acting on the inner shell boundary.

These equations have been used by Chevalier and Luo (1994) to calculate the shape of a self-similar wind bubble in a toroidal magnetic field. A similar set of equations for the average values across the shell of mass M, radial Q_r, and poloidal Q_Θ components of momentum was derived by Ferriere *et al.* (1991) to calculate superbubble expansion in a homogeneous interstellar medium permeated by a uniform magnetic field.

To get a full set of equations Ferriere *et al.* (1991) used the magnetic flux-freezing condition, added boundary conditions on the inner surface of the bubble, and used Rankine-Hugoniot relations at the outer shock surface. The flux-freezing condition implies that the magnetic flux Φ_s through the part of the shell within a cone of constant angle Θ, is equal to a flux Φ_0 of the ambient magnetic field through a disk with the radius $R = R_s \sin\Theta$:

$$2\pi\int_{R_i}^{R_s} B_\Theta \sin\Theta dR = \pi(R_s\sin\Theta)^2 B_0. \quad (3.99)$$

Since the field lines are frozen and lie within the shell, magnetic pressure within a hot bubble interior is assumed to be negligible,

$$\frac{B_{\rm in}^2}{8\pi} = 0. \quad (3.100)$$

Thus at the inner surface of the shell pressure continuity requires

$$P_i + \frac{B_i^2}{8\pi} = kn_{\rm in}T_{\rm in}, \quad (3.101)$$

where $n_{\rm in}$ and $T_{\rm in}$ are the gas number density and temperature within the cavity, and P_i and B_i are the gas pressure and magnetic field at the inner shell boundary. In the radiative phase of the bubble's evolution the equation of energy conservation at the outer shell boundary may be replaced by the relation

$$T_1 = T_s. \quad (3.102)$$

The subscript 1 denotes the hydrodynamical values just behind the radiative shock front; T_s was assumed by Ferriere *et al.* (1991) to be in the range $100\,{\rm K} \le T_s \le 1000\,{\rm K}$. The Rankine-Hugoniot relations express the mass, momentum, and magnetic flux conservation on the shock boundary. For a magnetohydrodynamic discontinuity they may be written in the form

$$\rho_1 v_{1\perp} = \rho_0 V_{s\perp}, \quad (3.103)$$

$$\rho_1 v_{1\perp}^2 + P_1 + \frac{B_1^2}{8\pi} = \rho_0 V_{s\perp}^2 + P_0 + \frac{B_0^2}{8\pi}, \quad (3.104)$$

$$\rho_1 v_{1\perp} v_{1\parallel} - \frac{B_{1\perp}B_{1\parallel}}{4\pi} = \rho_0 V_{s\perp}V_{s\parallel} - \frac{B_{0\perp}B_{0\parallel}}{4\pi}, \quad (3.105)$$

$$B_{1\perp} = B_{0\perp}, \quad (3.106)$$

$$v_{1\perp}B_{1\parallel} - v_{1\parallel}B_{1\perp} = V_{s\perp}B_{0\parallel} - V_{s\parallel}B_{0\perp}. \quad (3.107)$$

Here the subscript 0 refers to the values ahead of the shock front, $\mathbf{V}_s$ is the shock velocity, and $\mathbf{v}_1$ is the gas velocity behind the shock front, calculated in the shock frame of reference.

E. Bow shocks around hot stars

The Infrared Astronomical Satellite (IRAS) all-sky survey of extended sources revealed a number of arc-shaped features with unusually high color temperatures $[I(60\,\mu{\rm m})/I(100\,\mu{\rm m}) > 0.3]$. The 15 most prominent objects were summarized by van Buren and McCray (1988). Most of them (13 of 15) have been identified with a central OB or Wolf-Rayet star. About 20% of the ultracompact H II regions around hot luminous stars embedded in molecular clouds show a similar cometarylike morphology (Mac Low *et al.*, 1991). The prototype of this relatively new class of objects is the nebula G34.3+0.2 (Reid and Ho, 1985). This limb-brightened shell with a luminous head and extended tail has a linear scale of 0.06 pc and is embedded in a dense NH_3 clump. Radio recombination lines of hydrogen show significant broadening and a systematic velocity gradient across the nebula (Garay *et al.*, 1986). Several physical mechanisms may explain these objects: the supersonic expansion of the Stromgren zone (Raga, 1986); the confining pressure of the interstellar magnetic field (Gaume and Mutel, 1987); the champagne flow model that was developed in a series of papers by Tenorio-Tagle and co-workers (Bodenheimer *et al.*, 1979; Tenorio-Tagle, 1979; Yorke *et al.*, 1983); and stellar wind expansion in a medium with a density gradient (Tomisaka and Ikeuchi, 1986; Mac Low and McCray, 1988; Bisnovatyi-Kogan *et al.*, 1989). One of the main theoretical difficulties of the problem is that the dense ionized region is expected to expand in a relatively short ($\approx 10^3$ yr) time due to excess internal pressure if there is no confining mechanism. Van Buren *et al.* (1990) and Mac Low *et al.* (1991) have proposed that confinement is produced by a ram pressure of the surrounding medium if a massive star producing stellar wind moves supersonically through the ambient molecular cloud.

When an early-type star moves supersonically with the speed V_s through the ambient gas, the structure and dynamics of a spherically symmetric bubble, described in Sec. II, should be modified. In the earliest stage of bub-

ble expansion, when the inner shock front is still far away from the outer shell, a shocked stellar wind [region (b) in Fig. 6] remains isobaric irrespective of stellar location, and the star's motion has no effect on the bubble dynamics. But when the inner shock front reaches the outer shell, the dynamics and internal structure of the bubble change drastically. This happens when the expansion velocity of the outer shock becomes comparable to the speed of the star. Since region (b) no longer exists, the shape of the leading edge of the bubble is determined by a balance between ram pressure from the stellar wind and the pressure of the ambient interstellar medium:

$$\rho_w V_{w,n}^2 = \rho_c V_{s,n}^2, \tag{3.108}$$

where $V_{w,n}$ and $V_{s,n}$ are components of the stellar wind normal to the shell and stellar velocities, while ρ_w and ρ_c are densities of the stellar wind ejecta and ambient cloud material. V_w, V_s, and ρ_c are assumed to be constant. The density profile in a freely expanding stationary wind changes as

$$\rho_w = \frac{\dot{M}}{4\pi r^2 V_w}, \tag{3.109}$$

where $\dot{M}$ is the star's mass-loss rate. The flow appears to be similar to the flow around a blunt body in a supersonic stream. This shape remains stationary and has been calculated analytically by Baranov *et al.* (1971) and Dyson (1975). Near the stagnation point the shell curvature of the bubble may be well approximated by a parabola, $y = x^2/3l$, where x and y are coordinates perpendicular and parallel to the direction of motion. The distance between the top of the bow shock and the star l (see Fig. 11) follows from Eqs. (3.108) and (3.109) with

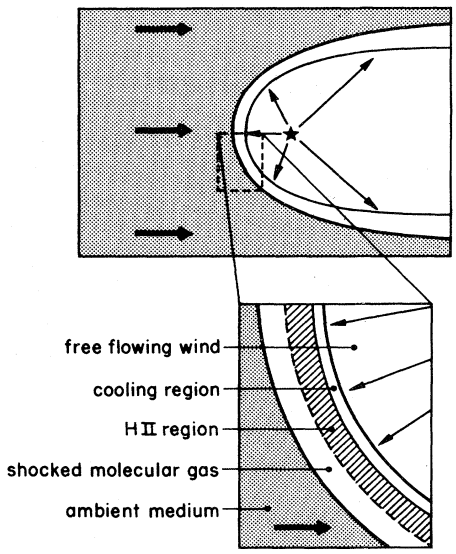

FIG. 11. Structure of an ultracompact H II region produced by strong stellar wind from a supersonically moving star.

$l = r$ as (van Buren and McCray, 1988; van Buren *et al.*, 1990)

$$l = 1.74 \times 10^{19} \dot{M}_6^{1/2} V_{w,8}^{1/2} \rho_c^{-1/2} V_{s,6}^{-1} \text{ cm}. \tag{3.110}$$

Here the star's mass-loss rate is in units of $10^{-6} M_\odot$ per year, wind velocity is in units of 10^8 cm s^{-1}, and star velocity is in units of 10^6 cm s^{-1}. The shell surface density σ, thickness h, and tangential velocity of the swept-up material near the stagnation point may then be estimated from the equations of mass and momentum conservation.

The mass swept up by the bow-shock shell inside the coordinate interval $(0,x)$ is equal to

$$\dot{m}_b(x) = \pi x^2 \rho_c V_s. \tag{3.111}$$

In a stationary flow this mass should be equal to the mass flow along the shell,

$$\dot{m}_{\rm sh}(x) = 2\pi x \sigma u_t(x), \tag{3.112}$$

where $u_t(x)$ is the velocity of the swept-up material tangential to the shell. The tangential component of the equation of momentum conservation leads to (van Buren *et al.*, 1990)

$$u_t(x)\dot{m}_{\rm sh}(x) = \int_0^x V_{s,t} d\dot{m}_b. \tag{3.113}$$

Here the contributions to mass and momentum from the stellar wind were estimated to be negligible in comparison with that of the swept-up gas material, while $V_{s,t}$ is the star's velocity, tangential to the surface of the bow shock. Equating mass input and output rates [Eqs. (3.111) and (3.112)], we get the tangential velocity component in the shell,

$$u_t(x) = \frac{\rho_c}{2\sigma} V_s x. \tag{3.114}$$

Substituting into Eq. (3.113) for $V_{s,t}$ in the vicinity of the stagnation point,

$$V_{s,t} \simeq \frac{2}{3}\frac{x}{l} V_s, \tag{3.115}$$

we get the tangential flow velocity and surface density of the shell in the neighborhood of the stagnation point (Mac Low *et al.*, 1991),

$$u_t(x) = \frac{4}{9} V_s \frac{x}{l}, \tag{3.116}$$

$$\sigma = \frac{9}{8} \rho_c l. \tag{3.117}$$

When the stellar wind material passes through the terminal inner shock it has a high temperature,

$$T_b = \frac{3}{16} \frac{\mu_H m_H}{k} V_w^2. \tag{3.118}$$

However, energy losses are very effective here, and van Buren *et al.* (1990) have shown that evaporation of the

swept-up cloud material reduces the temperature in this zone to values at which cooling becomes important. Velocity shears and the Kelvin-Helmholtz instability may be another mechanism for the effective exchange of mass between swept-up shell and shocked wind region. Dust which enters this region may enhance the cooling rate by a factor of 100. Thus we have to expect rapid cooling and attenuation of the shocked wind layer between terminal shock and contact discontinuity. Then the dynamics of the shell in the vicinity of the stagnation point will be governed by momentum rather than by the energy input from the stellar wind material. A two-dimensional numerical model of a momentum-driven shell surrounding a massive star with strong stellar wind which moves supersonically through a molecular cloud was developed by Mac Low *et al.* (1991). This model is developed analogously to the thin-layer approximation described in Sec. III.B. The shell is divided into a number of cylindrical segments with mass m_j, coordinates r_j, z_j, and velocity $u_j = dr_j/dt$. The coordinate system is connected with the moving star. Then the ambient gas has velocity V_s. The equation of mass conservation takes into account both the mass swept up by the bow shock and the mass ejected by the star as wind material:

$$\frac{d\mu_j}{dt} = \rho_c \Sigma_j (\mathbf{u}_j - \mathbf{V}_s)\mathbf{n}_j + \rho_w \Sigma_j (\mathbf{V}_w - \mathbf{u}_j)\mathbf{n}_j = \dot{m}_c + \dot{m}_w. \tag{3.119}$$

Here Σ_j and vector $\mathbf{n}_j$ are, respectively, the segment area of a Lagrangian element, and the unit normal. The equation of momentum conservation (3.46) for a momentum-driven shell reduces to

$$\frac{d}{dt}(\mu_j \mathbf{u}_j) = \dot{m}_w \mathbf{V}_w - \dot{m}_c \mathbf{V}_s - P_{\rm ext}\Sigma_j \mathbf{n}_j, \tag{3.120}$$

where $P_{\rm ext}$ is the ambient gas pressure, which is important only far downstream from the stagnation point. A spherical shell with radius much smaller than the characteristic scale l, and negligible velocity has been taken as initial conditions. Due to a tangential component of velocity, mass constantly flows away from the head of the remnant and the space resolution near the stagnation point becomes too crude. To maintain sufficient res-

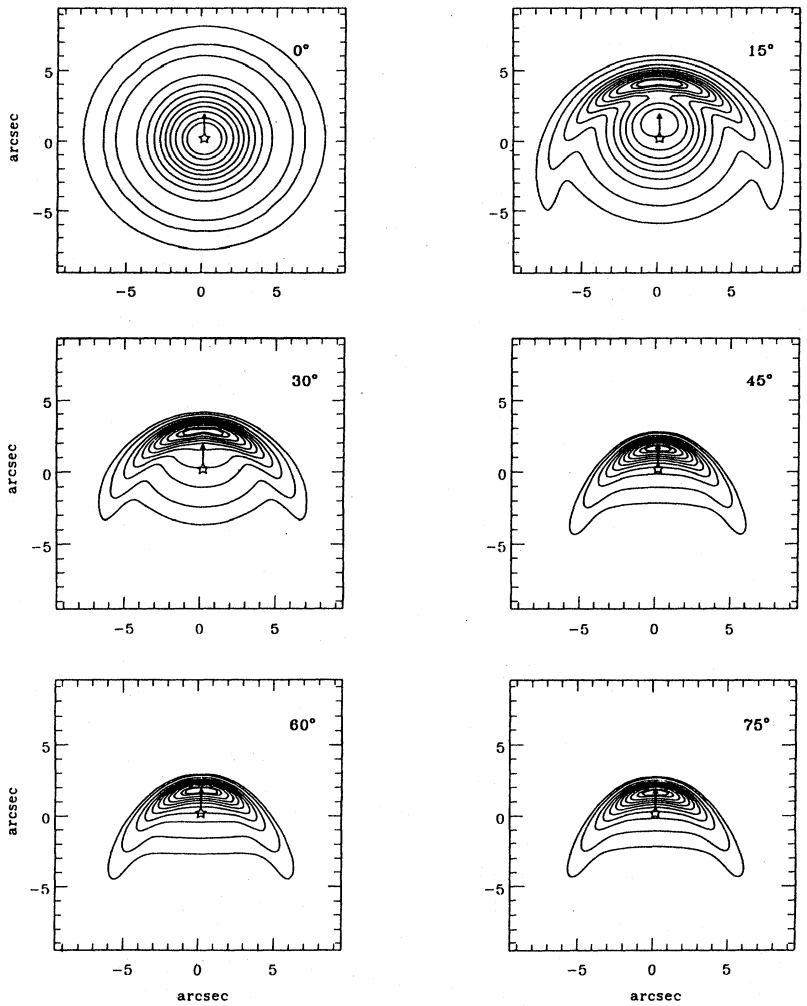

FIG. 12. Surface brightness of an ultracompact H II region, observed with a beam having a full width at half maximum of 1″ at wavelength 2 cm at different viewing angles. From Mac Low *et al.*, 1991.

olution, the Lagrangian grid was restored from time to time.

This algorithm gives two-dimensional shape, velocity, and surface density σ in the bow-shock region. The particle number density n_H in the ionized part of the shell was calculated as $n_H = \rho_c V_s^2/kT$, where the temperature of the ionized layer was assumed to be $T = 10^4$ K. Then the thickness $h = \sigma/\mu_h n_H$ of the particular Lagrangian element and finally the surface brightness S could be calculated (Mac Low *et al.*, 1991). The calculated shapes of the ultracompact H II regions visible from different viewing angles are presented in the Fig. 12. Here a typical O6 star, moving at a velocity of $5\,\mathrm{km\,s^{-1}}$ through a cloud with particle number density $n_c = 10^5\,\mathrm{cm^{-3}}$ was assumed.

F. Axially symmetric supernova remnants

High-resolution and high-sensitivity observations of supernova remnants (SNR) have shown that radio-emitting regions generally do not possess spherical symmetry. The most commonly observed departure from spherical symmetry is the presence of two bright arcs with radio brightness changing gradually along their length, which are located on the opposite sides of the axis of symmetry and are separated on the top and bottom by regions of weak emission (Kesteven and Caswell, 1987; Manchester, 1987). Usually remnants with this type of symmetry are referred to as barrel-like supernova remnants. Storey *et al.* (1992) have made a quantitative analysis of the morphology of SNR G296.5+10.0. Their calculations demonstrate a high degree of axial symmetry, even in the small-scale filamentary features that are seen in both radio arcs. Kesteven and Caswell (1987) have suggested that the majority of SNRs are barrel-shaped. A number of x-ray (Seward, 1990) and optical remnants fall into this category as well. This type of morphology is revealed in both young and old SNRs.

The possible mechanisms for generation of such a structure may be divided into four categories (Bisnovatyi-Kogan *et al.*, 1990; Storey *et al.*, 1992). In the first, the shape of the remnant is dominated by external factors such as large-scale density gradients in the surrounding medium or compression of a preexisting regular interstellar magnetic field, as has been proposed for SNR G327.6+14.6 (the remnant of the historical supernova SN1006) and SNR G296.5+10.0 by Roger *et al.* (1988). In the second mechanism, the remnant's morphology is dominated by the distortion of the ambient interstellar medium by the powerful mass-loss rate of the presupernova wind, as considered by Lozinskaya (1992) and as probably is observed in SN 1987 A (Crotts *et al.*, 1989; Jakobsen *et al.*, 1991; Panagia *et al.*, 1991). The third mechanism is an anisotropic supernova explosion, and the fourth is the interaction of collimated jets of relativistic particles from a central pulsar within the SNR shell.

1. Asymmetric explosion in a uniform medium

Anisotropy of the velocity field and mass distribution with a concentration of the ejected material in the equatorial plane of the progenitor star are the natural consequences of the magnetorotational mechanism of a supernova explosion (Bisnovatyi-Kogan, 1970; Ardelian *et al.*, 1979) or of a thermonuclear explosion of a rotating presupernova star (Bodenheimer and Woosley, 1983; Chechetkin *et al.*, 1989). This mechanism is partially supported by x-ray observations of ringlike structures in several young supernova remnants (Tuohy *et al.*, 1982; Markert *et al.*, 1983), which may be treated as the observational evidence of a highly anisotropic explosion.

Bisnovatyi-Kogan and Blinnikov (1982) have examined the evolution of an initially anisotropic remnant in a uniform ambient medium. In addition to the Kompaneets approximation, where the problem had an analytical solution, they used the thin-layer approximation described in Sec. III.B. At the initial time $t = 0$ the supernova remnant was assumed to be spheroidal,

$$\omega = R_e \sin\Theta, \tag{3.121}$$

$$z = R_p \cos\Theta, \tag{3.122}$$

with an equatorial radius R_e, pole radius R_p, and homogeneous surface density distribution σ_0. The expansion velocity of the remnant was defined as

$$u(\Theta) = u_0(1 - b\cos 2\Theta), \tag{3.123}$$

with the highest velocity at the equator, $U_e = U_0(1+b)$, and the lowest at the pole, $U_p = U_0(1-b)$. The explosion energy E_0 and kinetic energy E_k of the shell, the density of the ambient medium ρ_0, and the mass of ejected material M_0 were considered as additional parameters of the problem. Only adiabatic solutions were considered. A sequence of models with different initial shapes $2 \le R_e/R_p \le 5$, different ratios of the expansion velocities at pole and equator, $1 \le U_e/U_p \le 3$, different masses of ejecta, and different initial kinetic energies were calculated. The spherization of the SNR happened after $\approx 10\tau_0$, where τ_0 is the characteristic time scale,

$$\tau_0 = (\rho_0/E_0)^{1/2} R_e^{5/2}. \tag{3.124}$$

Here "spherization" means low relative difference between the equator and pole radii of the supernova remnant, $0.9 \le R_p/R_e \le 1$. This does not, however, mean the homogeneity of the remnant. A large inhomogeneity may still exist in the surface density distribution, with differences in the surface density near the pole and equator of a factor 2–3. Bisnovatyi-Kogan and Blinnikov (1982) have proposed that this effect may explain the observations of the Cas A remnant (Fabian *et al.*, 1980), in which spherical morphology is accompanied by great differences in surface brightness distribution.

2. Barrel-like supernova remnants

Radio maps of the two best known barrel-shaped supernova remnants, SN 1006 (G327.6+14.6) and G296.5+10.0, from the paper of Roger *et al.* (1988), are shown in Fig. 13. Both of the remnants lie at relatively high distances above the galactic plane ($z = 450$ pc for SNR 1006 and $z = 260$ pc for G296.5+10.0). Thus the low density of the ambient gas may be the reason for the rather long-time influence of the ejected material on the subsequent evolution of the remnant. Kirshner *et al.* (1987) have estimated from optical observations of SN 1006 a shock velocity in the range 2800–3900 $\mathrm{km\,s^{-1}}$. An x-ray image of SNR 1006 with a circular limb-brightened shell has been obtained via the Einstein Observatory by Pye *et al.* (1981). At the distance $z = 450$ pc from the galactic plane the number density of the diffuse ambient gas must be $n_0 \leq 0.1\,\mathrm{cm^{-3}}$, that is, close to the value $n_0 = 0.05\,\mathrm{cm^{-3}}$ obtained by Hamilton *et al.* (1986) from the x-ray model of SN 1006.

Helfand and Becker (1984) have detected x-ray emission from both wings of G296.5+10.0 and revealed a compact centrally located x-ray source. Storey *et al.* (1992) have shown the high degree of axial symmetry of this remnant and argued the importance of the ejected matter and energy input produced by the explosion in the formation of the observed remnant morphology. The mean ambient gas density near G296.5+10.0 was estimated from the x-ray data to be 0.24–0.08 $\mathrm{cm^{-3}}$.

Bisnovatyi-Kogan *et al.* (1990) have provided numerical simulations of the evolution of these two remnants based on the thin-layer approximation. The following parameters were used for the calculations: the explosion energy E_0, temperature and density distribution of the ambient gas, stellar mass M_{ej} ejected during the explosion, and its ratio to the swept-up interstellar mass M_0, the fraction of the kinetic energy E_k in the total explosion energy E_0. A spherical shell of radius

$$R_e = \left(\frac{3}{4\pi}\frac{M_{\mathrm{ej}}}{\rho_0}\frac{M_0}{M_{\mathrm{ej}}}\right)^{1/3} \tag{3.125}$$

and constant expansion velocity

$$U_0 = (2E_k/M_{\mathrm{ej}})^{1/2} \tag{3.126}$$

were assumed at the beginning of the calculations; ρ_0 is the ambient gas density at the point of the explosion. The anisotropy of the explosion was included by the inhomogeneity of the surface density σ_{ej} of the ejected material along the remnant:

$$\sigma_{\mathrm{ej}} = \sigma_0(A\sin^2\Theta + B\sin\Theta + C), \tag{3.127}$$

where polar angle Θ is defined as

$$r = R_e\sin\Theta, \quad z = R_e\cos\Theta. \tag{3.128}$$

Here r and z are the remnant coordinates at the beginning of the calculations. If one adopts normalization $A + B = 1$, the constant C can be expressed by the ratio of the surface densities σ_p and σ_e at the pole and the equator of the remnant:

$$C = \frac{\sigma_p/\sigma_e}{1 - \sigma_p/\sigma_e}. \tag{3.129}$$

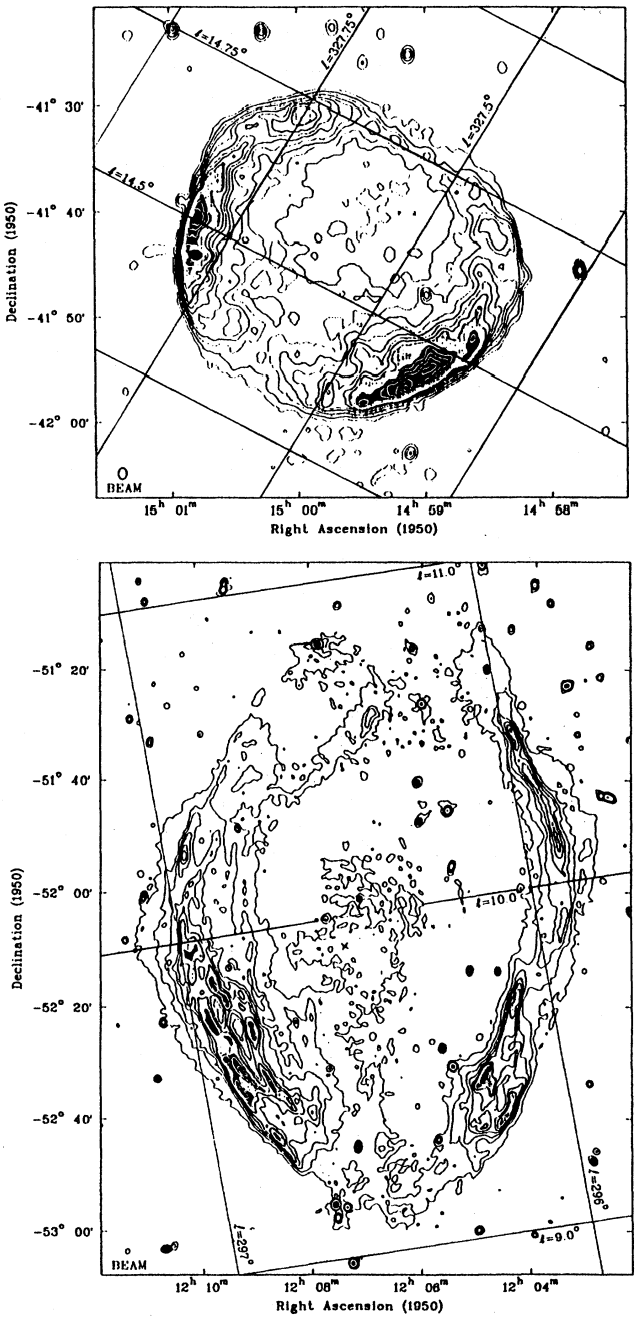

FIG. 13. The 843 MHz radio maps of supernova remnants (a) G327.6+14.6 (SNR 1006) and (b) G296.5+10.0. From Roger *et al.*, 1988.

The constant σ_0 then may be expressed through the mass of ejecta M_{ej} as

$$\sigma_0 = \frac{M_{ej}}{4\pi R_c^2(\frac{2}{3}A + \frac{1}{4} + C)}, \tag{3.130}$$

and the constant A determines the distribution of the surface density along the shell.

The explosion energy E_0 was assumed to be 10^{51} ergs. The ratio of the surface densities on the remnant's pole and equator at $t = 0$ was taken to be in the range $\sigma_p/\sigma_e = 0.1$–0.2. The ejected mass $M_{ej} = 2M_\odot$ was 250–1000 times greater then the initial swept-up interstellar mass M_0. These parameters correspond to an initial radius of 0.5–1.0 pc.

The best-fit model to the morphology of SNR 1006 corresponds to an anisotropic supernova explosion in a plane-stratified gas distribution,

$$n(z) = n_0\left[1 + \frac{2(1-\alpha)}{\pi(1+\alpha)}\arctan\frac{z}{z_0}\right], \tag{3.131}$$

where $n_0 = 0.05\,\mathrm{cm}^{-3}$, $\alpha = 3$, and $z_0 = 1\,\mathrm{pc}$. Such a density distribution can be related to the local inhomogeneity of the interstellar medium. The shape of the remnant and surface density distribution after 980 years of evolution are shown in Fig. 14. The shape of the remnant is close to spherical, but applelike features are present. This is a consequence of the initial surface density, and consequently of the initial momentum distribution, with the maxima of the Z component of the momentum being in the intermediate regions between the poles and the equator of the remnant. The radius of the remnant is equal to 6 pc and it is in the transition phase from free to adiabatic expansion. The shock velocities at the poles are $3900\,\mathrm{km\,s}^{-1}$ (on the top) and $2700\,\mathrm{km\,s}^{-1}$ (on the bottom). At the equator, the expansion velocity is equal to $5100\,\mathrm{km\,s}^{-1}$. These values are in good agreement with the data of Kirshner *et al.* (1987) and with the estimation of the expansion velocities of ejected material in the central part of the remnant (Wu *et al.*, 1983). The radius of the remnant 6–7 pc, implies a distance to the remnant of 1.4–1.6 kpc.

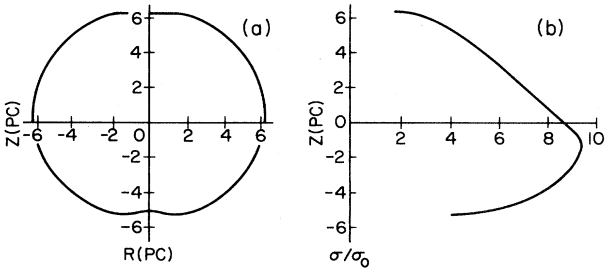

FIG. 14. Simulations of SNR 1006 by an anisotropic explosion on the edge of the gas layer. (a) The shape of the remnant; (b) the surface density distribution in the remnant. $E_0 = 10^{51}$ ergs, $M_{ej} = 2M_\odot$, the remnant age $t = 980$ yrs, $\sigma_p/\sigma_e = 0.1$ at the beginning of calculations. From Bisnovatyi-Kogan *et al.*, 1990.

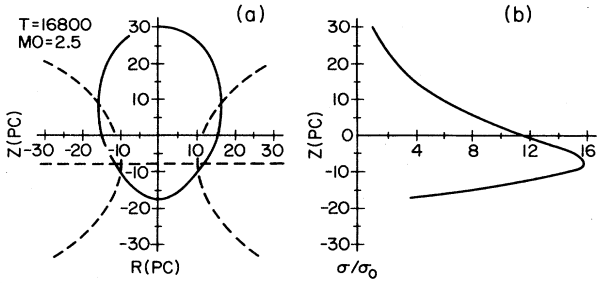

FIG. 15. Simulations of SNR G296.5+10.0 by an explosion of energy $E_0 = 10^{51}$ ergs in a gas tunnel. (a) The shape of the remnant. (b) The surface density distribution in the remnant. $M_{ej} = 2.5M_\odot$, the remnant age $t = 16800$ yrs. Dashed lines represent the shape and the plane of symmetry of the ambient gas density distribution. From Bisnovatyi-Kogan *et al.*, 1990.

Numerical simulations of the evolution of G296.5+10.0 (Bisnovatyi-Kogan *et al.*, 1990) have shown that it is impossible to obtain the observed shape and great contrast in the surface density distribution by an asymmetric explosion in a uniform medium. The morphology of SNR G296.5+10.0 could be explained if a spherical explosion occurred in the gas near the bridge between two old supernova remnants and was produced by their merging. The results of calculations are presented in Fig. 15, where dashed lines represent the shape and symmetry plane of the gas density distribution. The maximum number density in the plane of symmetry is $n_0 = 1\,\mathrm{cm}^{-3}$. The characteristic scale of the density gradient along the Z axis is $H = 10$ pc. The point of the explosion is shifted up from the symmetry plane by $z_0 = 7.5$ pc. The age of the remnant is about 17 000 years, but it is still in the adiabatic stage. The velocities of the shock are equal to $1100\,\mathrm{km\,s}^{-1}$ on the top, $440\,\mathrm{km\,s}^{-1}$ on the bottom, and $250\,\mathrm{km\,s}^{-1}$ in the midplane of the ambient gas density distribution.

3. Supernova explosion inside a wind-driven cavity

The massive progenitors of Type-II and Ib supernovae undergo a significant mass loss during their red and blue giant phases prior to explosion. This stellar wind modifies the ambient density distribution and creates an expanding shell, as was shown in Sec. II. Chu (1981), Lozinskaya and Sitnik (1988), Dufour (1989), Lozinskaya (1992); and Dopita *et al.* (1994) have presented numerous examples of optical shells around Wolf-Rayet and O_f stars. Similar structures are observed in different wavelength bands as well as in the nearby galaxies (Rosado, 1989; Laval *et al.*, 1992). Asymmetric shapes of planetary nebulae are often observed (Balick, 1987). On the

other hand, a number of observational (Hamilton, 1985; Danziger and Bouchet, 1989; Lozinskaya, 1992; Chugai, 1993) and theoretical papers (see Arnett *et al.*, 1989) indicate that supernova ejecta are not smooth flowing but contain a great number of dense fast fragments. As a first approach to the problem, consider the expansion of a blast wave in a gas with power-law density distribution. The first application of a self-similar solution to an explosion in a spherically symmetric preexisting cavity was carried out by Cox and Franco (1981). Cox and Edgar (1983) included the effects of thermal conduction. Krol' and Fomin (1978) considered shock-wave expansion in a medium disturbed by a previous shock wave. The later evolution of a SNR, however, depends strongly on the details of the expelled gas thermalization in the early stage of the expansion. Chevalier (1982) and Nadyozhin (1985) have found a self-similar solution for outgoing and reverse shocks assuming power-law density distributions for both the ejecta and the ambient medium. Detailed 1D and 2D numerical simulations of the interaction of the ejected material, containing high-density fragments, with the ambient gas were performed by Franco *et al.* (1991; see also the application of approximate methods by Chevalier and Liang, 1989, and Tenorio-Tagle *et al.*, 1991). The ejected material expands almost freely until it impacts with the wind-driven dense shell. This interaction generates optical, UV, and x-ray emission. If the mass of the shell is smaller than $\approx 50M_\odot$, the SN shock overruns the shell and proceeds to propagate through the undisturbed gas in the form of an adiabatic shock. Radiative losses during the temporal merging of shocks are not important in this case. For larger masses of shell the radiative losses are so great that the supernova shock loses considerable energy and cannot overrun the shell. The shock merges with the shell and they proceed to propagate as one radiative shock, carrying away all momentum.

Igumentshchev *et al.* (1992) have studied the dynamics of adiabatic supernova ejecta in a disklike envelope with the gas density distribution

$$\rho(r,\Theta)=\frac{\dot{M}}{4\pi r^2 V_w}\left[\frac{3}{2}\beta\sin^2\Theta+(1-\beta)\right] \qquad (3.132)$$

produced by nonspherical mass loss from a progenitor star. They have found a significant elongation of the remnant in the direction of the maximum density gradient during a relatively short ($\leq 400\,\mathrm{yr}$) initial phase of evolution.

A self-similar solution for the interaction region between a fast inner stellar wind and a slower outer one has been developed by Chevalier and Imamura (1983) in which both winds are assumed to be spherically symmetric and adiabatic.

Observations of narrow UV and optical emission lines indicate the presence of a circumstellar shell around SN 1987A that was ionized by the initial UV and x-ray flash from the supernova explosion. The $[OIII]\lambda 5007$ images (Wampler *et al.*, 1990; Jakobsen *et al.*, 1991) have revealed an elliptical ring around SN 1987A. Analysis of the Doppler velocity of the ring shows that the ellipse is actually a circular ring that is inclined at $\approx 45°$ and expands with $\approx 10\,\mathrm{km\,s^{-1}}$ velocity. Deeper ground-based observations by Crotts *et al.* (1989) and Wamper *et al.* (1990) have revealed two large loops which are connected with the expanding ring. Thus all the structure is interpreted as the projection of the hourglass-shaped shell (see for more details the reviews of Imshennik and Nadyozhin, 1989, and McCray, 1993). Luo and McCray (1991a, 1991b) and Wang and Mazzali (1992) have proposed that this unusual shell formation is the result of fast wind expansion from a blue supergiant in the relict, axially symmetric wind envelope of a red supergiant and have predicted the evolution of the x-ray, UV, infrared, and radio emission of the remnant. The bubble formation was simulated, using the thin-shell approximation. To reproduce an hourglass shape with the observed scales and velocities, Luo and McCray and Wang and Mazzali adopted the parameters of Lundqvist and Fransson (1991) for the stellar wind model. The steady, low-velocity red supergiant wind has the mass-loss rate $\dot{M}_R=10^{-5}M_\odot\ \mathrm{yr}^{-1}$, expansion velocity ($V_R=10\ \mathrm{km\,s^{-1}}$), and axially symmetric gas density distribution

$$\rho(r,\Theta)=\frac{3\dot{M}_R}{4\pi r^2 V_R}\frac{a+\cos 2\Theta}{3a-1}. \qquad (3.133)$$

The fast, isotropic blue supergiant wind has a mass-loss rate of $\dot{M}_B=3\times10^{-6}M_\odot\ \mathrm{yr}^{-1}$ and an expansion velocity $V_B=550\,\mathrm{km\,s^{-1}}$. Luo and McCray (1991b) assumed the constant $a=1.5$, which implies an equator-to-pole density contrast $\rho_e/\rho_p=5/1$, whereas Wang and Mazzali (1992) used a different form of asymmetry and suggested that this ratio is only 1.25.

The calculated contrast in the column density distribution from the pole to the equator of the shell is much greater than in the red supergiant envelope because of the convergence of the Lagrangian elements near the shell's equator. Thus the waist of the shell is much brighter than the lobes due to higher column densities. Figure 16 from Luo and McCray (1991b) shows the predicted

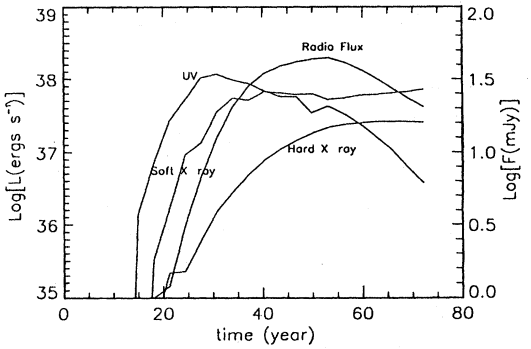

FIG. 16. The predicted luminosity of SNR 1987A in the different wavebands resulting from the interaction of supernova ejecta with an axially symmetric wind-driven shell. From Luo and McCray, 1991b.

UV, nonthermal radio, soft ($0.1\,\mathrm{keV} < h\nu < 3.5\,\mathrm{keV}$) and hard ($3.5\,\mathrm{keV} < h\nu < 10\,\mathrm{keV}$) x-ray luminosities of the SN 1987A remnant.

The collision of supernova ejecta of $V_t \simeq 3000\,\mathrm{km\,s^{-1}}$ and mass M_{ej} with a bubble outer shell of radius R_s is accompanied by the formation of forward and reverse shocks (Chevalier and Liang, 1989). If the mass of the hot low-density bubble interior is M_b, it must happen at $t \simeq 1.4(M_b/M_{\mathrm{ej}})^{1/6}(R_s/V_t)$ (Chevalier, 1982), about 15 yr after the explosion, i.e., at the beginning of the next century. Then UV and x-ray luminosities of the remnant should rise abruptly above $10^{37}\mathrm{ergs\,s^{-1}}$ (Luo and McCray, 1991a, 1991b).

A comprehensive model of the circumstellar shell around SN 1987A based on the full 2D hydrodynamic calculations has been developed by Blondin and Lundqvist (1993). The main difference between these calculations and those of Luo and McCray (1991b) is the absence of a cusp at the shell equator due to the pressure gradient within the cavity. This leads to a much faster (60–70 $\mathrm{km\,s^{-1}}$) ring expansion and suggests that the standard Lundqvist and Fransson (1991) model of the stellar wind cannot fit the observations. To get the observed parameters of the SN 1987A shell, Blondin and Lundqvist (1993) have been forced to adopt relatively extreme values for the progenitor wind parameters: a high concentration of the red supergiant wind near the equator of the progenitor star, an equator-to-pole density contrast of ≈ 20, and a low-energy, radiatively cooling blue supergiant wind with $\dot{M}_B = 3 \times 10^{-7} M_\odot\,\mathrm{yr^{-1}}$ and $V_B = 300\,\mathrm{km\,s^{-1}}$.

The nature of the red supergiant's wind asymmetry is not known, but it may be due to a binary companion of the progenitor star, as has been proposed for a planetary nebula by Morris (1981), and Kolesnik and Pilyugin (1986).

Two unprecedented and mysterious rings of H_α emission have been discovered in front of and behind the explosion point of SN 1987A by NASA's Hubble Space Telescope (Burrows *et al.*, 1994). These rings probably coincide with the surface of the hourglass shell whose origin has been discussed above.

Chu and Mac Low (1990) and Chu *et al.* (1993) have analyzed the archival data from the Einstein Observatory and new ROSAT observations to look for diffuse x-ray emission from regions containing OB associations in the Large Magellanic Cloud (LMC). Diffuse x-ray emissions were positively detected in ten OB associations concentrated in seven OB/H II systems. These systems are presented in Table II. Another five systems show enhanced soft x-ray emission with a low level of confidence. Most of these complexes have simple shell-like morphology in the H_α emission and may best be classified as an early stage of superbubble evolution.

The observed x-ray luminosities range from $7 \times 10^{34}\,\mathrm{ergs\,s^{-1}}$ to $7 \times 10^{36}\,\mathrm{ergs\,s^{-1}}$ across the Einstein 0.2–4 keV band and generally coincide well with the more careful analysis of Einstein data made by Wang *et al.* (1991). Chu and Mac Low (1990) have considered one of the complexes, the nebula N51D containing the OB associations LH51 and LH54. The shell diameters reach 75–150 pc. The contribution of early-type stars located within the systems to the total x-ray luminosities was estimated to be not greater than 1%. Thus the observed x-ray emission must be from a hot rarefied interstellar gas. But application of the theory described in Sec. II to the N51D and N44 nebulae shows that calculated x-ray luminosities fall an order of magnitude below that derived from the Einstein and ROSAT observations. A supernova explosion near the center of the bubble does not increase the total x-ray luminosity by much, since in a huge bubble the blastwave from a supernova explosion sweeps up enough mass and slows down to below x-ray-emitting speed in a relatively short time. Thus the enhancement of x-ray emission due to interaction of freely expanding ejecta with the preexisting shell is negligible (Chu and Mac Low, 1990).

TABLE II. X-ray emitting OB/H II systems in the Large Magellanic Cloud.

Neubla	OB association	X-ray luminosity (10^{35} $\mathrm{ergs\,s^{-1}}$)
N44	LH47, LH48	14
N51D	LH51, LH54	3.3
N57A	LH76	0.74
N70	LH114	1.8
N154	LH81, LH87	8.6
N157	LH100	70
N158	LH101, LH104	11

To overcome this inconsistency, Chu and Mac Low (1990) have proposed a mechanism for an off-center supernova explosion inside a preexisting wind-driven bubble. To simulate 2D shock expansion within the cavity they use a numerical code based on the thin-layer approximation that is similar to that described by Mac Low and McCray (1988) and Bisnovatyi-Kogan *et al.* (1989; for more detail, see Sec. III.B). Chu and Mac Low (1990) distinguish between mean pressure $P_{\mathrm{in}} = (\gamma - 1)E_{\mathrm{th}}/\Omega$ and post-shock pressure $P_s = \lambda P_{\mathrm{in}}$ [see Eq. (3.2)] in the adiabatic shock wave. They adopt the constant $\lambda = 1.53$ (see Koo and McKee, 1990, and our discussion of the Kompaneets approximation, Sec. III.A.4). To reproduce the pressure enhancement in the region between outgoing and reverse shocks during the impact of the SNR with the dense bubble shell, they increase the pressure behind the shock by the factor β, which was chosen as $\beta = 4.5$. This factor applies while the reverse shock propagates through the shell and then rapidly approaches the regular interior pressure. The gas density and the temperature distributions within the wind-driven cavity are assumed to follow the conductive evaporation profiles [see Eqs. (2.90) and (2.93)].

The final results are sensitive to the adopted density of the bubble shell. During impact with the cold ($T \approx 100\,\mathrm{K}$) neutral shell, the supernova blastwave de-

celerates almost immediately to below x-ray-emitting velocities, and growth of the x-ray luminosity is negligible. But young supershells have to be photoionized and heated by the hot early-type stars from the embedded OB associations. Thus it is appropriate to assume the shell boundary as that where the temperature falls to 10^4 K. After collision with such a shell, the supernova shock-wave velocity remains high enough to heat it to $\approx 10^6$ K for several thousand years. To compare this model with observation, Chu and Mac Low (1990) calculate the dynamics and x-ray emission of the nebula N51D. This is a bubble with radius 53 pc expanding at 30–35 $\mathrm{km\,s^{-1}}$ velocity. The application of the model of Weaver *et al.* (1977) to the expansion of this nebula gives an estimate of about 1 Myr for its age. The x-ray emission from N51D lies completely within the H II region, $L_x = 3.3 \times 10^{35}\,\mathrm{ergs\,s^{-1}}$. The ambient interstellar gas number density was estimated from the H_α observations of Meaburn and Terrett (1980) and from the dynamics of the nebula to be $n \simeq 0.5\,\mathrm{cm^{-3}}$. The expected x-ray luminosities display a variety of behaviors for models with different locations of the progenitor star within the cavity and are shown in Fig. 17. Thus an off-center SNR interacting with the inner photoionized edge of a shell driven by stellar wind from an OB association may produce the observed x-ray luminosity.

OB stars possess a strong stellar wind over the entire main sequence lifetime (de Jager *et al.*, 1988; Oey and Massey, 1994), so the age of a star exploded as a supernova cannot exceed essentially the dynamic time of the bubble, $\tau \approx 10^6$ yr, if simultaneous birth of all stars in the association is assumed. Choisi *et al.* (1978) have estimated the main sequence lifetime of stars within the mass range $30M_\odot \leq M \leq 80M_\odot$ as $\tau_{\mathrm{ms}} = 9 \times 10^6 (M/10M_\odot)^{-0.5}$ yr. The calculations of Maeder (1988) gave a lifetime of 3 Myr even for a 120-$M_\odot$ star. Therefore it seems likely that this nebula is still at the stellar-wind-driven stage of expansion and some special conditions are required for the early stages of supernova explosions.

A possible kinematic identification of the "hidden" supernova remnants inside the small Magellanic Cloud H II regions N19 and N66 is presented by Rosado *et al.* (1994). More detailed study of the stellar content of OB/H II systems and analysis of x-ray maps of higher sensitivity would greatly enhance our understanding of the problem.

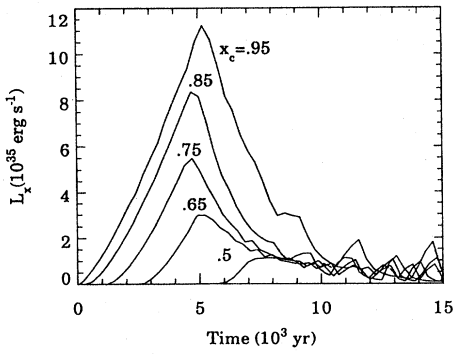

FIG. 17. X-ray luminosity of a supernova remnant produced by an off-center explosion inside a wind-driven bubble for different initial positions x_c of the progenitor star. From Chu and Mac Low, 1990.

G. Supershells in a plane-stratified interstellar medium

Sites of recent star formation show strong evidence of the collective effects of stellar winds and supernova interaction with the surrounding interstellar medium. Observations of our galaxy by Heiles (1979, 1984) and of the nearby spiral galaxies M31 and M33 by Brinks and Bajaja (1986) and Deul and Hartog (1990) have confirmed that shell-like structures are a common feature of the interstellar medium. Puche *et al.* (1992, 1995) have undertaken a program to study the neutral hydrogen component of the interstellar medium in dwarf galaxies, as an attempt to extract transient properties of bubble evolution which are difficult to observe in the massive spiral systems due to distortion effects of the galactic shear, and to provide an observational base for a comprehensive evolutionary scenario of the interstellar medium. All observed galaxies show a large amount of internal structure in the form of H I expanding shells. For example a detailed study of the almost face-on irregular galaxy Ho II (Puche *et al.*, 1992) has revealed 51 holes in the H I density distribution that typically range in size from 100 to 1700 pc and that provide evidence of expansion at a velocity $V \approx 10\,\mathrm{km\,s^{-1}}$. Deul and Hartog (1990) looked for ^{12}CO emission connected with the interior of the four H I holes in M33 to investigate the possibility that H I holes really are not empty but are filled with a molecular gas as dense as the surrounding H I. Their upper limits are much less than the expected mass of molecular gas if the conversion factor between the ^{12}CO surface brightness and H_2 surface density is of the same order of magnitude as the galactic one. For a detailed review of the observational aspects of the problem, see Tenorio-Tagle and Bodenheimer (1988), Brinks (1990), Silich (1990), and Heiles (1991).

The fundamental problem that arises in connection with these objects is the identification of the energy source of the shell expansion (Tenorio-Tagle and Bodenheimer, 1988). If the stellar wind and supernova explosions are the main sources of energy for bubble expansion (Bruhweiler *et al.*, 1980; Tomisaka and Ikeuchi, 1986; McCray and Kafatos, 1987), then the interior of the H I bubble should be filled with a hot ($\approx 10^6$) rarefied gas and should be observed as a source of extended soft x-ray emission. Until recent years there have been no positive observations of hot gas connected with H I holes or shells, with the exception of the Cash *et al.* (1980) x-ray feature known as the Cygnus Superbubble [see, however, Bochkarev and Sitnik (1985), who argued that this region is a projection of several physically separated sources at different distances from the sun in the direction of the Carina-Cygnus spiral arm, and Comeron and Torra (1994), who discuss the origin of the Cygnus OB1-OB9

associations].

Domgorgen *et al.* (1995) have analyzed the IUE (International Ultraviolet Explorer satellite) high-dispersion spectra of four stars located either inside or behind the LMC-4 region. They discovered absorption lines of highly ionized species in the spectra of all four stars, which was interpreted as evidence for the existence of a hot gas component in this region. The first detections of diffuse x-ray emission from the hot interior of superbubbles LMC-2 and LMC-4 were presented by Wang and Helfand (1991), Bomans *et al.* (1994), and Singh *et al.* (1987). The total x-ray luminosities were estimated as $L_x \approx 2\times10^{37}\,\mathrm{ergs\,s^{-1}}$ from the LMC-2 region in the Einstein Observatory 0.16–3.5-keV IPC broadband (Wang and Helfand, 1991), and $L_x \approx 1.4\times10^{37}\,\mathrm{ergs\,s^{-1}}$ from the LMC-4 region in the ROSAT 0.1–2.4-keV band (Bomans *et al.*, 1994). The temperatures of the hot x-ray-emitting gas are assumed to be $T \approx 5\times10^6$ K in the LMC-2 bubble and $T \approx 2.4\times10^6$ K in the LMC-4. The enhanced x-ray emission coincides well with the cavity seen in H I and IRAS maps. A comprehensive reanalysis of the Einstein IPC data on the LMC has been provided recently by Wang *et al.* (1991). A local (on the characteristic scale ~ 1 kpc) anticorrelation of diffuse x-ray emission with the H I surface density distribution has been revealed. These results are consistent with the coherent supernovae model of the interstellar medium in the LMC. Diffuse x-ray emission from young ionized bubbles containing OB associations has been discovered recently by Chu and Mac Low (1990; Chu *et al.*, 1993). As was shown in the previous section, they considered the evolution of the bubble to be still strongly influenced by a strong stellar wind from massive stars in OB associations as well as by the first supernova explosions.

The characteristic sizes of expanding shells often exceed the disk thickness of their host galaxies and reach 0.1–1 kpc, with estimated kinetic energies of up to 10^{53}–10^{54} ergs (Heiles, 1984; Tenorio-Tagle and Bodenheimer, 1988). Therefore the dynamics of the largest "supershells" depend strongly on the gas density distribution in the vertical direction, unless the galactic disk is very thick. Galactic shear is another very important dynamic factor which defines the late stages of superbubble evolution. Here we consider the action of these two agents separately, while the bubble evolution induced by their combined action is described in the next section.

The first fully two-dimensional calculations of superbubble evolution were provided by Tomisaka and Ikeuchi (1986) for Fuchs and Thielheim's (1979) two-component model of the interstellar medium with the gas density distribution

$$n(z) = n_0\left[0.22\exp\left(-\frac{\Phi(z)}{\sigma_i^2}\right) + 0.78\exp\left(-\frac{\Phi(z)}{\sigma_c^2}\right)\right] \tag{3.134}$$

and gravitational potential

$$\Phi(z) = 68.6\ln\left[1+0.9565\sinh^2\left(0.758\frac{z}{z_0}\right)\right](\mathrm{km\,s^{-1}})^2. \tag{3.135}$$

Here the constants $\sigma_i = 14.4\,\mathrm{km\,s^{-1}}$, $\sigma_c = 7.1\,\mathrm{km\,s^{-1}}$, and $z_0 = 124$ pc are the velocity dispersions of the interstellar gas and clouds and the scale height of the gravitational field. The two-dimensional MacCormack (1971) numerical scheme, with artificial viscosity and space resolution $\Delta r = \Delta z = 5$ pc or $\Delta r = \Delta z = 10$ pc, was employed. Each supernova was assumed to release energy $E_{\mathrm{SN}} = 10^{51}$ ergs and mass $m_{\mathrm{ej}} = 10M_\odot$. Classical thermal conductivity was included in one variant of the calculations. It plays an important role in the formation of the internal bubble structure. The temperature within the cavity becomes smoother and lower, whereas density increases (see, however, the discussion at the end of this section).

We shall treat the superbubble as a large stellar wind cavity (McCray and Kafatos, 1987; McCray and Mac Low, 1988) supported by continuous supernovae explosions. Mac Low and McCray (1988) have shown that once a cold dense shell with isobaric interior has formed, the mass of the interior becomes great enough for a single SNR to be subsonic before collision with the common huge shell. Thus the hot interior gas buffers the discrete supernovae explosions, allowing us to treat them as a continuous energy input rate. Mac Low and McCray (1988) also calculated the dynamics of a spherical bubble driven by discrete, Poisson-distributed supernova explosions. They concluded that bubble expansion becomes identical to the continuous-input case after 5–10 supernovae have occurred [see, however, Tenorio-Tagle *et al.* (1987), who found in this case more complicated internal structure dominated by some kind of instability, and discussion of this instability by Mac Low *et al.*, 1989]. The adiabatic phase of the bubble's evolution persists until radiative cooling becomes important in the hot gas behind the shock front, at time

$$t_c = \frac{3kT_s}{n_s\Lambda(T)}, \tag{3.136}$$

where T_s and n_s are the post-shock gas temperature and number density, and $\Lambda(T)$ is the cooling function. Then during a short time radiation takes away approximately half of the remnant's thermal energy (Chevalier, 1974; Falle, 1981; Blinnikov *et al.*, 1982), and almost all swept-up gas collapses into a thin, dense, cold shell with a low-density hot gas within the cavity. Taking

$$\Lambda(T) = 1\times10^{-22}T_6^{-0.7}\xi\ \mathrm{ergs\,cm^3\,s^{-1}}, \tag{3.137}$$

where T_6 is the temperature in 10^6 K units and ξ is the metallicity, and assuming a strong adiabatic shock wave, Mac Low and McCray (1988) estimated that the radiative phase begins after a short time of evolution,

$$t_c = 2.3\times10^4 n_0^{-0.71}\xi^{-1}L_{38}^{0.29}\ \mathrm{yr}, \tag{3.138}$$

where n_0 is the particle number density in the ambient interstellar medium and L_{38} is the energy input rate due to repeated supernovae explosions in $10^{38}\,\mathrm{ergs\,s^{-1}}$ units. Thin-shell formation in interstellar shocks associated with supernova explosions in an arbitrary power-law density distribution has been explored by Franco *et al.*

(1994).

The inner density of a radiative superbubble was considered to be dominated by the mass evaporated from the cold dense shell. Mac Low and McCray (1988) adapted the formula (2.92) for mass flux $\dot{M}_{\rm sh}$ to a nonspherical bubble as follows:

$$\dot{M}_{\rm sh} = \frac{4}{25}\frac{\mu_{\rm in}}{k} C T_c^{5/2} \int_{\lambda_{\rm min}}^{\lambda_{\rm max}} \frac{d\Sigma}{R}, \qquad (3.139)$$

where $\mu_{\rm in} = \frac{14}{23} m_H$ is the mean mass per particle in the hot bubble interior, $C = 6 \times 10^{-7}\,{\rm ergs\,s^{-1}\,cm^{-1}\,K^{-7/2}}$ is the coefficient of thermal conductivity, T_c is the temperature near the center of the bubble, $d\Sigma$ and $R = \sqrt{\omega^2 + z^2}$ are the surface area and the radius of the particular Lagrangian element (see Sec. III.B), k is the Boltzmann constant, and $\lambda_{\rm min}$ and $\lambda_{\rm max}$ are minimum and maximum values of the Lagrangian coordinates.

The energy budget for a radiative bubble includes the energy input rate from supernova explosions $L(t)$, work $P_{\rm in} d\Omega/dt$ done by the shell expansion, and radiative cooling of the rarefied hot bubble interior,

$$L_R = \int_{\lambda_{\rm min}}^{\lambda_{\rm max}} n_{\rm in}^2 \Lambda(T_{\rm in}) d\Omega, \qquad (3.140)$$

where Ω is the bubble volume. Therefore the equations of energy conservation (3.56) must be replaced by

$$\frac{dE_{\rm th}}{dt} = L(t) - L_R(t) - 2\pi \int_{\lambda_{\rm min}}^{\lambda_{\rm max}} P_{\rm in} U_n \frac{\partial \Sigma}{\partial \lambda} d\lambda, \quad (3.141)$$

where U_n is the component of the expansion velocity normal to the shock front.

A numerical scheme based on the thin-layer approximation, as described in Sec. III.B, has been developed by Mac Low and McCray (1988) and Bisnovatyi-Kogan *et al.* (1989). Bisnovatyi-Kogan *et al.* (1989) started from the adiabatic bubble and used the same density distribution (3.134) and z component of gravity $\Phi(z)$ (3.135) as in the previous paper of Tomisaka and Ikeuchi (1986), but did not take into account radiative loses from the hot bubble interior, whereas Mac Low and McCray (1988) allowed them. The above schemes show good agreement for bubble evolution in a pure exponential gas disk up to 6 Myr, but display a significant difference from those of Tomisaka and Ikeuchi (1986) in the case of relatively high gas number density in the midplane of the galaxy. This difference comes from the numerical mass diffusion across the contact discontinuity from the cold shell to the hot bubble interior in the Tomisaka and Ikeuchi (1986) scheme and overestimation of radiative cooling of the bubble interior (Bisnovatyi-Kogan *et al.*, 1989, Mac Low *et al.*, 1989).

Mac Low *et al.* (1989) compared fully two-dimensional calculations with the thin-layer approximation. The results of their calculations for a Gaussian atmosphere

$$\rho = \rho_0 \exp(-z^2/H^2) \qquad (3.142)$$

with characteristic scale height H=100 pc and energy input rate $L = 1.67 \times 10^{38}\,{\rm ergs\,s^{-1}}$ are shown in Fig. 18. One can see that the thin-layer approximation works surprisingly well until the shell begins to accelerate and becomes Rayleigh-Taylor unstable.

In a disk galaxy, bubbles have two possibilities for their final fates. Either they accelerate, become Rayleigh-Taylor unstable, and blow out hot gas into the galactic halo, or they fall back to the galactic plane under the in-

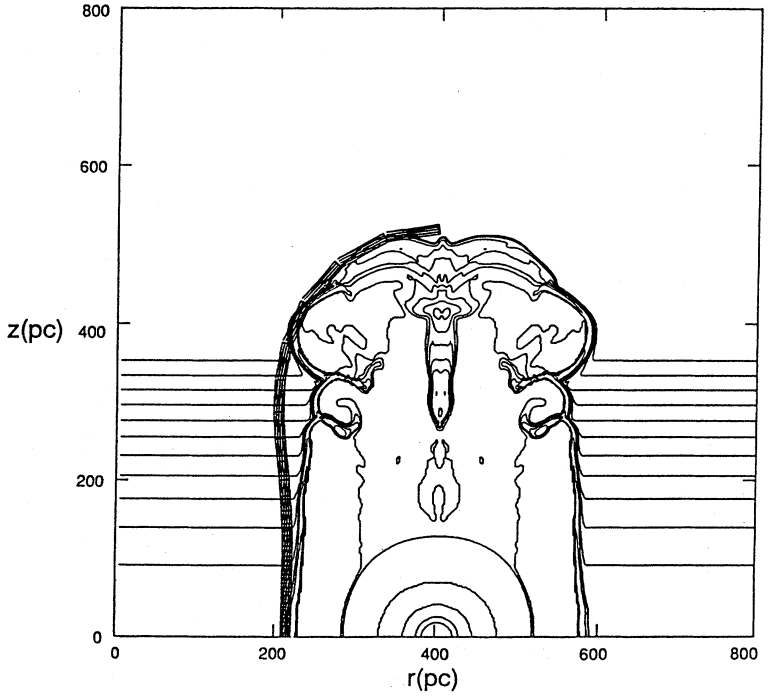

FIG. 18. Superbubble expansion in the Gaussian gas layer as follows from the full two-dimensional calculations and from the thin-layer method (left thick line). The age of the remnant $t = 5$ Myr, energy input rate $L_{38} = 1.67$. From Mac Low *et al.*, 1989.

fluence of interstellar gas pressure and the galactic gravitational field (Mac Low and McCray, 1988; Silich, 1991). The blowout phenomenon was considered with full two-dimensional simulations by Tomisaka and Ikeuchi (1986), Mac Low *et al.* (1989), Igumentshchev *et al.* (1990), and Tenorio-Tagle *et al.* (1990). The hybrid Fuchs and Thielheim (1979) or Dickey and Lockman (1990) (see Sec. IV) gas distribution seems to be less favorable for blowout. Superbubbles are prevented from accelerating by a dynamically important large-scale density component and actually do not blow hot gas out into a rarefied galactic halo unless unrealistically rich OB associations are assumed or the energy source is displaced from the galactic plane. Nevertheless continuous supernova explosions in OB associations may produce very large holes in the interstellar medium after pushing out the dense gas near the galactic plane.

Galactic-scale bipolar outflow from the nuclei of starburst galaxies (which have experienced a very high star formation rate in the recent past) was studied with full 2D numerical simulations by Tomisaka and Ikeuchi (1988), and Tomisaka and Bregman (1993). The extended (up to 10–50 kpc) x-ray emission around the starburst galaxy M82 was reproduced with an extremely high supernova explosion rate $\approx 0.1\,\mathrm{yr}^{-1}$ in the nuclear region of the galaxy. The evolutionary time of the event was estimated to be about 50 Myr. During this time the starburst emits $(3\times10^{39}$–$10^{40})\,\mathrm{ergs\,s}^{-1}$ in the GINGA LAC (1.56–8.265 keV) band and $\approx 10^{41}\,\mathrm{ergs\,s}^{-1}$ in the Einstein or ROSAT HRI band. The cool ring that is formed near the galactic plane seems to correspond to the CO spur extending to the halo region in the galaxy M82.

H. Supershells in a differentially rotating galactic disk

Interstellar matter is not sitting at rest, as was assumed in the previous section, but rather moves around the galactic center. The rotation velocities are defined by the mass distribution and reveal strong deviation from solid-body rotation except in the central parts of some galaxies. The characteristic lifetime of a superbubble (10^7–10^8 yr) is comparable with the period of galactic rotation, and therefore huge expanding shells have to be subject to a large-scale galactic shear. This effect was considered in two dimensions by Tenorio-Tagle and Palouš (1987; Palouš *et al.*, 1990). The galactic disk was modeled as a homogeneous slab, rotating with constant velocity $V_0(R) = 250\,\mathrm{km\,s}^{-1}$, with a thickness of $H = 200\,\mathrm{pc}$. The interstellar gas number n_0 was taken to be $n_0 = 3\,\mathrm{cm}^{-3}$ at $R = 5\,\mathrm{kpc}$ from the galactic center, $n_0 = 1\,\mathrm{cm}^{-3}$ at $R = 10\,\mathrm{kpc}$, and $n_0 = 0.3\,\mathrm{cm}^{-3}$ at $R = 20\,\mathrm{kpc}$. At the beginning of the calculations a cylindrical shell with full width $h = H$ was assumed. The total amount of energy, $E_0 = 10^{53}\,\mathrm{ergs}$, was released instantaneously and distributed as $2/3E_0$ in the form of thermal energy of the remnant interior, and $1/3E_0$ is the kinetic energy of the shell. The initial temperature T_0 was equal in all models ($T_0 = 10^7\,\mathrm{K}$) and thus defined the gas number density within the cavity. It was assumed that only half of the mass of the interstellar gas was concentrated in the cold thin shell, while the other half was pushed out through the top and the bottom of the remnant. Free expansion into the galactic halo with the sound velocity a_s was allowed, leading to a rapid adiabatic decrease in the internal pressure P_{in},

$$P_{\mathrm{in}}(t) = P_0\,[\Omega(t=0)/\Omega(t)]^{\gamma}\,, \tag{3.143}$$

and growth of the remnant's height h,

$$h(t) = H + 2\int_0^t a_s dt. \tag{3.144}$$

Here Ω is the remnant's volume, while $\gamma = 5/3$ is the ratio of the specific heats.

The cylindrical shell was approximated by a number of plane Lagrangian elements orientated parallel to the axis of symmetry Z. The mass of a particular Lagrangian element increases with time as

$$\mu(t) = \mu_0 + \int_0^t W(t)u_n(t)\rho_0 dt, \tag{3.145}$$

where $\mu(t)$ is the mass per unit shell thickness. $W(t)$ is the width of the element, which is defined as the distance between centers of adjacent elements, and u_n is the normal component of the expansion velocity. The motion of the Lagrangian elements was described in the galactocentric coordinate frame R, Θ corotating with the ambient interstellar medium (the angular velocity of the coordinate frame is $\omega_0 = V_0/R$). It was impossible to take into account the Z component of gravity in this approach, but in some variants of the calculations self-gravity (gravitational interaction between different Lagrangian elements) was allowed.

The number column density across any Lagrangian element may be expressed as

$$N = \frac{\mu}{W\eta}, \tag{3.146}$$

where mass per unit thickness is defined by Eq. (3.145) and η is the mean mass per particle. When column number density N exceeds the critical value (Arshutkin and Kolesnik, 1984; Franco and Cox, 1986)

$$N_c = 10^{21}(Z_\odot/Z)\ \mathrm{cm}^{-2}, \tag{3.147}$$

where Z is metallicity, the optical depth of the background UV radiation becomes greater than unity. A decrease in photoionizing radiation then allows for rapid molecule formation in the inner part of the shell. Thus we may expect molecular cloud formation during the late stages of superbubble evolution. Figure 19 (Tenorio-Tagle and Palouš, 1987) displays cross sections of supershells by the midplane of the galaxy at different evolutionary times. The effect of differential galactic rotation becomes apparent after 2×10^7 yr of evolution. The remnant ellipticity grows with time, which leads to in-

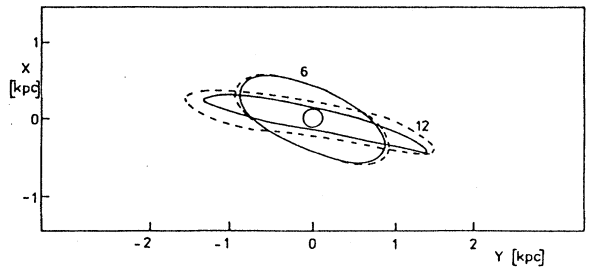

FIG. 19. Face-on view of a 2D bubble in a differentially rotating galactic disk after 6 and 12 Myr of evolution. Dashed lines are the same if the self-gravity of the shell has been taken into account. From Tenorio-Tagle and Palous, 1987.

homogeneous mass distribution along the shell. Most of the swept-up material streams towards opposite ends of the remnant, where conditions for molecular cloud formation are created. Thus while supernova explosions are usually considered as a disruptive agent in the interstellar medium, on a larger scale the combined action of multiple supernovae may have the opposite effect. They collect interstellar gas into giant molecular clouds and thus may trigger the process of new star formation, as has been proposed by Gerola and Seiden (1978) and Franco and Shore (1984). Palouš *et al.* (1990) have applied this algorithm to the limited sample of supershells in the galaxies M31 and M33. For two shells in M31, criterion (3.147) is satisfied and the swept-up matter accumulated at the ends is able to form giant molecular clouds. In contrast, there are no conditions for molecular cloud formation in any shells that have been considered in M33.

I. Bubble expansion in a uniform magnetic field

Although the strength of the magnetic field is not well defined, there is some evidence, due to Rand and Kulkarni (1989), that its value is close to a few μG. Thus the magnetic pressure $P_m \approx 10^{-12}\,(B/5\ \mu\mathrm{G})^2\,\mathrm{dyn\,cm^{-2}}$ may be comparable with the gas pressure in the galactic interstellar medium, $P_g \approx 4\times10^{-13}\ \mathrm{dyn\,cm^{-2}}$ (Jenkins *et al.*, 1983), or even with the ram pressure acting on the bubble shell, $P_{\mathrm{ram}} \approx 10^{-12}\ (\rho/2\times10^{-24}\,\mathrm{g\,cm^{-3}})\,(u/10\,\mathrm{km\,s^{-1}})^2\mathrm{dyn\,cm^{-2}}$. Thus it can play an essential role in bubble dynamics and influence the internal structure of a superbubble.

It is assumed that magnetic field is frozen into the fluid. Then the magnetic field lines are confined inside the shell, magnetic pressure within the cavity is negligible, and the total interior pressure P_{in} includes only the thermal contribution. Assuming the gas pressure inside the cavity to be uniform (the high temperature within the cavity and thus sound speed in the internal gas is higher than the blastwave velocity in the ambient interstellar gas), we get the interior energy of the remnant in the form

$$E_{\mathrm{th}} = \frac{2\pi P_{\mathrm{in}}}{3(\gamma-1)}\int_{-\pi/2}^{\pi/2} R_i^3 \sin\Theta d\Theta. \tag{3.148}$$

If L is the mechanical luminosity of the OB association, then E_{th} evolves according to

$$\frac{\partial E_{\mathrm{th}}}{\partial t} = L - 2\pi P_{\mathrm{in}}\int_{-\pi/2}^{\pi/2}\frac{\partial R_i}{\partial t}R_i^2\sin\Theta d\Theta. \tag{3.149}$$

We expect more pronounced action of the magnetic field at a later time, when the ratio of the external magnetic field pressure $B_0^2/8\pi$ to the ram pressure $\rho_0 V_{\mathrm{sn}}^2$ becomes greater. Then departure from the nonmagnetic case at the early stage of evolution may be described by the expansion of the governing equations in powers of the parameter

$$\varepsilon = \frac{B_0}{\sqrt{8\pi\rho_0 V_{\mathrm{sn}}^2}}. \tag{3.150}$$

Let us estimate now the shell thickness. Taking into account that all hydrodynamical variables vary only moderately across the shell (Ferriere *et al.*, 1991), we may approximate them by the values immediately behind the shock front. If mass redistribution along the shell may be neglected, then

$$\rho_s = \frac{1}{3}\frac{R_s}{\Delta R}\rho_0 \tag{3.151}$$

and

$$P_s = \frac{1}{3}\frac{R_s T_s}{\Delta R T_0}P_0, \tag{3.152}$$

where P_s, ρ_s, and T_s are the mean gas pressure, density, and temperature in the shell.

Neglecting for a crude estimation the departure of the unit normal to the shock front from the radial direction, we have from the Eq. (3.99)

$$B_{s\Theta} = \frac{R_s}{2\Delta R}B_0\sin\Theta. \tag{3.153}$$

Combining these equations with the Rankine-Hugoniot relations (3.103)–(3.107) on the shock front, Ferriere *et al.* (1991) have found an approximate equation for the shell thickness:

$$\frac{\Delta R}{R_s} = \frac{1}{2}\left[\frac{1}{3}\frac{T_s}{T_0}\varepsilon_p^2 + \sqrt{\left(\frac{1}{3}\frac{T_s}{T_0}\varepsilon_p^2\right)^2 + (\varepsilon\sin\Theta)^2}\right], \tag{3.154}$$

where ε_p is a small parameter,

$$\varepsilon_p = \sqrt{\frac{P_0}{\rho_0 V_{\mathrm{sn}}^2}}. \tag{3.155}$$

Within a narrow region near the magnetic poles ($\Theta \approx 0$)

$$\frac{\Delta R}{R_s} = \frac{1}{3}\frac{T_s}{T_0}\varepsilon_p^2. \tag{3.156}$$

Here the action of the magnetic field is negligible, the ram pressure is balanced by the thermal pressure of the swept-up gas, and the shell is thin. Away from the magnetic poles the magnetic pressure becomes the dominant agent to balance the ram pressure, and the shell thickness grows as

$$\frac{\Delta R}{R_s} = \frac{1}{2}\varepsilon \sin\Theta. \tag{3.157}$$

Thus we may expect the volume of a hot magnetized bubble interior to be reduced in comparison with bubble expansion in a nonmagnetic ambient medium.

Ferriere *et al.* (1991) have developed this approach to provide a numerical simulation of the evolution of a magnetized supershell. They have divided the shell into a number of pieces separated by cones with a constant Θ. The hydrodynamical evolution of each of these elements is described by equations for the inner radius R and outer radius R_s of the shell as functions of the control volume velocity, equations of mass, and radial and poloidal momentum conservation, which are similar to Eqs. (3.97) and (3.98). This set of major equations is accompanied by the equation of magnetic-field flux conservation (3.99), two boundary conditions at the inner shell surface (3.100)–(3.101), and five boundary conditions at the outer radiative shock (3.103)–(3.107).

The results of the numerical calculations have shown that magnetic tension in the shell causes the inner bubble boundary to be elongated in the direction of the external magnetic field, whereas the outer shock front tends to move faster in the perpendicular direction. The shell thickness is much greater than in the nonmagnetic case (with the exception of the bubble poles) and increases from the bubble pole to the equator. These main conclusions coincide well with the results of the full magnetohydrodynamical calculations provided by Tomisaka (1991, 1992), who used a "monotonic scheme" of van Leer (1977) and Norman and Winkler (1986) to solve the hydrodynamical equations and the "constrained transport method" (Evans and Hawley, 1988) to solve the induction equation for the magnetic field. He considered ten models with an energy input rate L from $3\times10^{36}\,\mathrm{ergs\,s^{-1}}$ to $3\times10^{37}\,\mathrm{ergs\,s^{-1}}$, interstellar gas number density n from $0.03\,\mathrm{cm^{-3}}$ to $0.3\,\mathrm{cm^{-3}}$, and regular galactic magnetic field $B_0 = (0-5)\ \mu\mathrm{G}$.

The volume of the hot bubble interior as a function of time is shown in the Fig. 20. Here model A is for $B_0 = 3\mu G$, $L = 3\times10^{37}\,\mathrm{ergs\,s^{-1}}$, and $n_0 = 0.3\,\mathrm{cm^{-3}}$; model B is the same, except for $B_0 = 5\,\mu\mathrm{G}$, and model F is for zero magnetic field, $B_0 = 0$. The dashed line presents the analytic results for a nonmagnetic bubble. It follows from this figure that the volume of a hot bubble interior is reduced to 45%–60% of that for a nonmagnetic bubble. This difference decreases with the increase of the OB-association mechanical luminosity and becomes small (only 2%) for superbubbles with $L = 3\times10^{38}\,\mathrm{ergs\,s^{-1}}$.

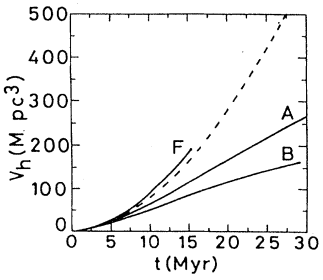

FIG. 20. Time evolution of a magnetized bubble volume filled with a hot interior gas. Numerical results for $B_0 = 0$ are presented as a dashed line. From Tomisaka, 1992.

Thus it seems likely that bubbles with a low energy deposition may be confined within a thin galactic disk layer by a regular magnetic field, but such a field does not exert a strong influence over the more active superbubbles. Nevertheless it seems likely that magnetic field action may partially reduce the filling factor of the hot rarefied phase of the interstellar medium and may restrict mass flow from the galactic disk to the halo.

IV. THREE-DIMENSIONAL SHOCKS

In this section we shall extend our analysis to three-dimensional shocks. We shall focus here on the relatively simple thin-layer approximation and its application to some astrophysical problems.

A. Thin-layer approximation

Three-dimensional numerical schemes based on the thin-layer approximation have been developed independently by Palouš (1990, 1992) and Bisnovatyi-Kogan and Silich (1991; Silich, 1992a, 1992b).

Let us introduce, following Bisnovatyi-Kogan and Silich (1991; Silich, 1992a, 1992b) the Cartesian coordinate system (x, y, z). The shock wave will be approximated by a number of Lagrangian elements which represent segments of the shock front and cover the surface of the remnant. If m is the mass, $\mathbf{r}$ is the radius vector, $\mathbf{u}$ is the velocity of the particular Lagrangian element, and $\rho(x,y,z) = \rho_0 f(x,y,z)$ is the ambient gas density, then the equations of mass and momentum conservation may be written as follows:

$$\frac{dm}{dt} = \rho(x,y,z)(\mathbf{u}-\mathbf{V})\mathbf{n}\Sigma, \tag{4.1}$$

$$\frac{d}{dt}(m\mathbf{u}) = \Delta P\mathbf{n}\Sigma + \mathbf{V}\frac{dm}{dt} + m\mathbf{g}, \tag{4.2}$$

$$\frac{d\mathbf{r}}{dt} = \mathbf{u}, \tag{4.3}$$

where $\mathbf{n}$ is the unit vector normal to the shock front, $\mathbf{g}$ is the acceleration of the external gravitational field, $\mathbf{V}$

is the velocity field of the undisturbed gas flow, Σ is the surface area of the Lagrangian element, $m = \sigma\Sigma$, σ is the surface density, and $\Delta P = P_{\rm in} - P_{\rm ext}$ is the pressure difference between the hot interior and the cooler external gas. The pressure $P_{\rm in}$ of the hot tenuous gas within the cavity is a function of the bubble's thermal energy $E_{\rm th}$ and volume Ω:

$$P_{\rm in} = (\gamma - 1)E_{\rm th}/\Omega. \tag{4.4}$$

To describe the expansion of the shock we must be able to specify its surface area and define the volume of any closed three-dimensional region. It is well known from differential geometry that any surface may be specified parametrically, with Cartesian coordinates at any point on the surface being a function of two parameters, λ_1 and λ_2: $x = x(\lambda_1, \lambda_2)$, $y = y(\lambda_1, \lambda_2)$, $z = z(\lambda_1, \lambda_2)$. Then the surface area element may be defined by the expression (Budak and Fomin, 1965):

$$d\Sigma = S(\lambda_1, \lambda_2)d\lambda_1 d\lambda_2, \tag{4.5}$$

$$S(\lambda_1, \lambda_2) = \left\{ \left[\frac{\partial(y,z)}{\partial(\lambda_1,\lambda_2)}\right]^2 + \left[\frac{\partial(z,x)}{\partial(\lambda_1,\lambda_2)}\right]^2 + \left[\frac{\partial(x,y)}{\partial(\lambda_1,\lambda_2)}\right]^2 \right\}^{1/2}, \tag{4.6}$$

where $\partial(x_i, x_j)/\partial(\lambda_1, \lambda_2) \equiv \det[\partial(x_i, x_j)/\partial(\lambda_1, \lambda_2)]$ are the appropriate Jacobians. The most numerically tractable expression for the volume of a 3D remnant follows from the Ostrogradskii-Gauss theorem and the definition of the surface integral of second kind (Budak and Fomin, 1965):

$$\Omega = \frac{1}{3}\int_{\lambda_{1,\min}}^{\lambda_{1,\max}}\int_{\lambda_{2,\min}}^{\lambda_{2,\max}} \left[z\frac{\partial(x,y)}{\partial(\lambda_1,\lambda_2)} + y\frac{\partial(z,y)}{\partial(\lambda_1,\lambda_2)} - x\frac{\partial(y,z)}{\partial(\lambda_1,\lambda_2)} \right] d\lambda_1 d\lambda_2. \tag{4.7}$$

The components of the unit vector normal to the remnant surface are (Budak and Fomin, 1965):

$$n_x = \frac{1}{S}\frac{\partial(y,z)}{\partial(\lambda_1 d\lambda_2)}, \tag{4.8}$$

$$n_y = \frac{1}{S}\frac{\partial(z,x)}{\partial(\lambda_1 d\lambda_2)},$$

$$n_z = \frac{1}{S}\frac{\partial(x,y)}{\partial(\lambda_1 d\lambda_2)}.$$

If parameters λ_1 and λ_2 are considered as the Lagrangian coordinates of the shock front, then Eqs. (4.1)–(4.3) may be rewritten for the mass $\mu = \sigma S(\lambda_1, \lambda_2)$ per unit of Lagrangian area, in the very compact form (convenient for numerical integration)

$$\frac{d\mu}{dt} = \rho\chi, \tag{4.9}$$

$$\frac{du_x}{dt} = \frac{\Delta P}{\mu}\frac{\partial(y,z)}{\partial(\lambda_1\lambda_2)} - \frac{u_x - V_x}{\mu}\rho\chi + g_x, \tag{4.10}$$

$$\frac{du_y}{dt} = \frac{\Delta P}{\mu}\frac{\partial(z,x)}{\partial(\lambda_1\lambda_2)} - \frac{u_y - V_y}{\mu}\rho\chi + g_y, \tag{4.11}$$

$$\frac{du_z}{dt} = \frac{\Delta P}{\mu}\frac{\partial(x,y)}{\partial(\lambda_1\lambda_2)} - \frac{u_z - V_z}{\mu}\rho\chi + g_z, \tag{4.12}$$

$$\frac{dx}{dt} = u_x, \quad \frac{dy}{dt} = u_y, \quad \frac{dz}{dt} = u_z. \tag{4.13}$$

Here the function χ is defined as

$$\chi = (u_x - V_x)\frac{\partial(y,z)}{\partial(\lambda_1,\lambda_2)} + (u_y - V_y)\frac{\partial(z,x)}{\partial(\lambda_1,\lambda_2)} + (U_z - V_z)\frac{\partial(x,y)}{\partial(\lambda_1,\lambda_2)}. \tag{4.14}$$

The motion of any Lagrangian element is then described by seven ordinary differential equations Eqs. (4.9)–(4.13). Approximating the shock front by a number N of Lagrangian elements, one gets a system of $7N$ differential equations of mass and momentum conservation. This set of equations is coupled by Eq. (4.4), for the gas pressure within the cavity, and the equation of energy conservation, valid for an adiabatic shock:

$$E_{\rm tot} = E_{\rm th} + E_k + E_g, \tag{4.15}$$

where $E_{\rm th}$, E_k, and E_g are the thermal energy of the hot bubble interior and the kinetic and gravitational energies of the shell, respectively. Variations of the total energy $E_{\rm tot}$ of the remnant throughout the adiabatic stage of evolution are defined by the energy input rate $L(t)$ and the kinetic and thermal energies of the swept-up interstellar gas with temperature $T(x, y, z)$:

$$E_{\rm tot} = E_0 + \int_0^t \left[L(t) + \frac{1}{2}\int_{\lambda_{1,\min}}^{\lambda_{1,\max}}\int_{\lambda_{2,\min}}^{\lambda_{2,\max}} \dot{\mu}(V^2 + 3kT/\eta) \times d\lambda_1 d\lambda_2 \right] dt, \tag{4.16}$$

where E_0 is the initially deposited energy and η is the mean mass per particle. The kinetic energy of the remnant is assumed to be concentrated in the thin shell behind the shock front:

$$E_k = \frac{1}{2}\int_{\lambda_{1,\min}}^{\lambda_{1,\max}}\int_{\lambda_{2,\min}}^{\lambda_{2,\max}} \mu(u_x^2 + u_y^2 + u_z^2)d\lambda_1 d\lambda_2. \tag{4.17}$$

The work done against gravity is

$$E_g = -\int_0^t \left[\int_{\lambda_{1,\min}}^{\lambda_{1,\max}}\int_{\lambda_{2,\min}}^{\lambda_{2,\max}} \mu\mathbf{u}\mathbf{g}d\lambda_1 d\lambda_2 \right] dt. \tag{4.18}$$

During the radiative phase of expansion, the gas behind

the shock front cools so quickly that it does not add to the total energy of the remnant. Rarefied hot gas inside the cavity expands adiabatically and accelerates the surrounding dense shell. The time derivative of the thermal energy of the remnant is then defined by the equation [used instead of Eq. (4.15)]:

$$\frac{dE_{\rm th}}{dt} = L(t) - \int_{\lambda_{1,\min}}^{\lambda_{1,\max}} \int_{\lambda_{2,\min}}^{\lambda_{2,\max}} P_{\rm in} u_n \times S(\lambda_1,\lambda_2) d\lambda_1 d\lambda_2, \tag{4.19}$$

where u_n is the velocity component normal to the shock front.

Numerical integration of the full set of equations [Eqs. (4.9)–(4.13) for every Lagrangian element; the equation of state (4.4) and equation of energy conservation (4.15) for an adiabatic shock; or Eq. (4.19) for an isothermal shock] then determines the shape, expansion velocities, and distribution of surface density $\sigma = \mu/S(\lambda_1,\lambda_2)$ along the shell.

B. 3D adiabatic supernova remnants

The evolution of three-dimensional adiabatic supernova remnants has been considered by Bisnovatyi-Kogan and Silich (1991). An instantaneous point explosion with the energy $E_0 = 10^{51}$ ergs was assumed. Then Eq. (4.16) could be rewritten in differential form,

$$\frac{dE_{\rm tot}}{dt} = \frac{1}{2} \int_{\lambda_{1,\min}}^{\lambda_{1,\max}} \int_{\lambda_{2,\min}}^{\lambda_{2,\max}} \dot{\mu}[V^2 + 3kT/\eta] d\lambda_1 d\lambda_2. \tag{4.20}$$

Calculations were performed for two sets of initial conditions. First was an initially spherical supernova remnant, which expands in the medium with an ellipsoidal density distribution

$$\rho = \rho_0 \left[\frac{1-\alpha_0}{1+(x/x_0)^2+(y/y_0)^2+(z/z_0)^2} + \alpha_0 \right], \tag{4.21}$$

where x_0, y_0, and z_0 are the characteristic inhomogeneity scales in the x, y, and z directions, $\alpha_0 = \rho_\infty/\rho_0$. The Lagrangian coordinates were defined so that at the beginning of the calculations

$$\begin{aligned} x &= R_e \sin\lambda_1 \cos\lambda_2, \\ y &= R_e \sin\lambda_1 \sin\lambda_2, \\ z &= R_e \cos\lambda_1, \end{aligned} \tag{4.22}$$

i.e., as spherical coordinates at the surface of an initially spherical bubble. The initial radius R_e and expansion velocity U_0 were determined by the Sedov (1959) solution,

$$R_e = (\xi_0 E_0/\rho_0)^{1/5} t_0^{2/5}, \tag{4.23}$$

$$U_0 = \frac{0.8}{\gamma+1} \left(\frac{\xi_0 E_0}{\rho_0 t_0^3} \right)^{1/5}, \tag{4.24}$$

where the constant ξ_0 is defined

$$\xi_0 = \left[\frac{75(\gamma-1)}{8\pi} \right]^{1/5}. \tag{4.25}$$

This definition gives better coincidence with the exact Sedov values for different γ than does the approximate formula (2.63) (Bisnovatyi-Kogan and Blinnikov, 1982). The initial mass of the remnant was assumed to be equal to the mass of the swept-up interstellar gas. Then the initial surface density was

$$\sigma = \frac{M_g}{4\pi R_e^2} = \frac{1}{3}\rho_0 R_e, \tag{4.26}$$

and the initial mass per unit Lagrangian coordinate was defined by the expression

$$\mu = \frac{1}{3}\rho_0 R_e S(\lambda_1,\lambda_2) = \frac{1}{3}\rho_0 R_e^3 \sin\lambda_1. \tag{4.27}$$

The temperature of the surrounding gas was taken constant, $T_g = 10^4$ K. Figure 21 shows the results of calculations for the initial radius $R_e = 1$ pc of the remnant, the particle number density in the center of the

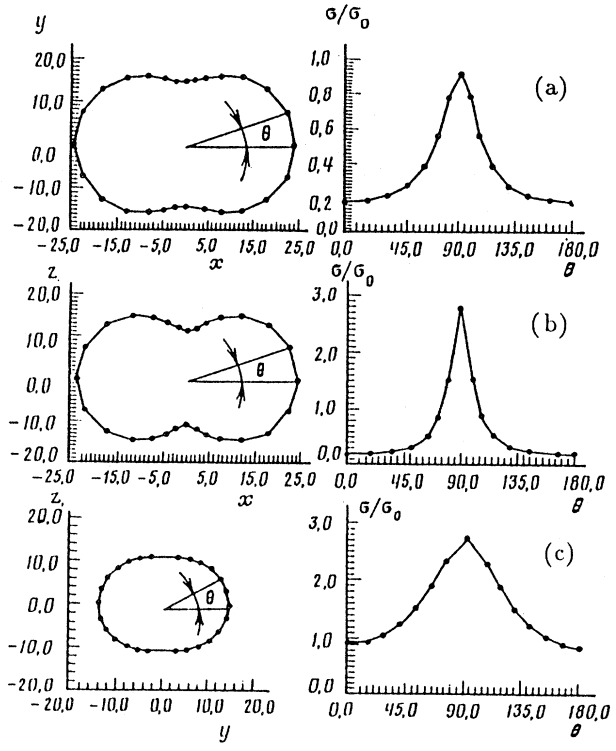

FIG. 21. Sections and surface density distributions of an adiabatic shock wave formed from a point explosion in a medium with ellipsoidal density distribution. The remnant age $t = 9500$ yrs. (a) Section by the plane $z = 0$; (b) section by the plane $y = 0$; (c) section by the plane $x = 0$. From Bisnovatyi-Kogan and Silich, 1991.

ambient gas density distribution $n_0 = \rho_0/\eta = 1\,\mathrm{cm}^{-3}$ (η is the mean mass per particle), the ratio α_0 of the gas density at infinity to the central gas density $\alpha_0 = 0.01$, and the characteristic scale of the gas density distribution, $x_0 = 2\,\mathrm{pc}$, $y_0 = 4\,\mathrm{pc}$, and $z_0 = 8\,\mathrm{pc}$. The spherical shell eventually evolved into a dumbbell-shaped remnant. The direction of the largest elongation coincides with the direction of the highest density gradient (x axis). The surface density distribution is highly anisotropic and reaches maximum near the remnant waist. The expansion velocities along x, y, and z axes after 9500 years are equal to $u_x = 1420\,\mathrm{km\,s}^{-1}$, $u_y = 770\,\mathrm{km\,s}^{-1}$, and $u_z = 490\,\mathrm{km\,s}^{-1}$.

Expansion of a supernova remnant that was initially a triaxial ellipsoid, in a homogeneous ambient gas distribution, was considered as an another example of 3D remnant evolution. The Lagrangian coordinates were taken from the relations

$$x = R_x \sin\lambda_1 \cos\lambda_2,$$

$$y = R_y \sin\lambda_1 \sin\lambda_2, \tag{4.28}$$

$$z = R_z \cos\lambda_1$$

with $R_y = \alpha R_x$, $R_z = \beta R_x$ and $\alpha, \beta < 1$. Here x, y, z are coordinates of the shock front at the beginning of the calculations. The major axis R_x is expressed through the ratio of the ejected mass M_{ej} and swept-up mass M_g, the density of the surrounding gas ρ_g, and the constants α and β:

$$R_x = \left(\frac{3}{4\pi\alpha\beta}\frac{M_{\mathrm{ej}}}{\rho_g}\frac{M_g}{M_{ej}}\right)^{1/3}. \tag{4.29}$$

The expansion velocity at the beginning of the calculations was taken as constant along the remnant,

$$U_0 = (2E_k/M_{\mathrm{ej}})^{1/2}, \tag{4.30}$$

directed normal to the shell.

The constant initial surface density σ was defined by

$$\sigma = \frac{M_g + M_{\mathrm{ej}}}{\int S(\lambda_1,\lambda_2)d\lambda_1 d\lambda_2} = \frac{2}{3}\frac{\beta\rho_g R_x}{S_0}\left(1 + \frac{M_{\mathrm{ej}}}{M_g}\right), \tag{4.31}$$

where

$$S_0 = 1 + \frac{\beta}{4\pi}\int_0^{2\pi} \frac{\delta^2}{\sqrt{\beta^{-2} - \delta^2}} \ln\left|\frac{\beta^{-1} + \sqrt{\beta^{-2} - \delta^2}}{\beta^{-1} - \sqrt{\beta^{-2} - \delta^2}}\right| d\lambda_2, \tag{4.32}$$

$$\delta^2 = 1 + (\alpha^{-2} - 1)\sin^2\lambda_2. \tag{4.33}$$

The total released energy E_0 and the fraction of it that is converted into kinetic energy of the shell motion E_k, the mass of ejecta M_{ej} and its ratio to the swept-up mass M_g, the density of the ambient gas ρ_g, and the ellipsoid parameters α and β were taken as the initial parameters. The results of calculations for an ejected mass $M_{\mathrm{ej}} = 3M_\odot$, explosion energy $E_0 = 10^{51}$ ergs, with 73% in the form of kinetic energy, and ellipsoid axes ratios $R_x : R_y : R_z = 1 : 2 : 4$ are presented in Fig. 22. The most interesting evolutionary feature of the adiabatic triaxial remnant is the change in the direction of elongation. The largest axis R_x at the beginning of the calculations becomes the smallest, and the smallest axis R_z becomes the largest. The shock, which was initially highly elongated in the x direction, is converted into an ellipsoidal body elongated in the direction of the z axis. The surface density distribution remains almost homogeneous over the whole remnant.

C. Supershells in a plane-stratified differentially rotating galactic disk

Numerical simulations of superbubble expansion in a plane-stratified, differentially rotating galactic disk have

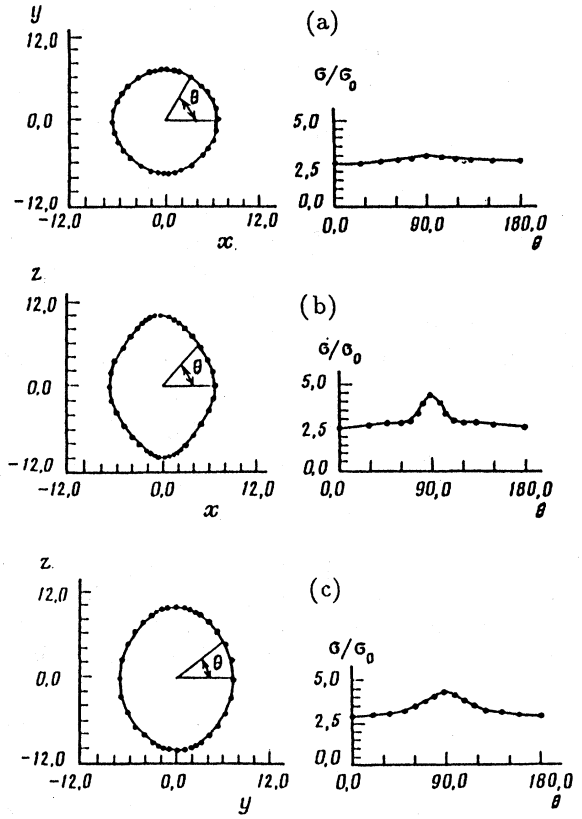

FIG. 22. Sections and surface density distributions of an initially triaxial, ellipsoidal, adiabatic shock wave in a homogeneous interstellar medium. The remnant age $t = 4100$ yrs. (a) Section in the plane $z = 0$; (b) section in the plane $y = 0$; (c) section in the plane $x = 0$. From Bisnovatyi-Kogan and Silich, 1991.

been provided by Palouš (1990, 1992; Silich, 1991, 1992a, 1992b; Mashchenko and Silich, 1994).

Let us introduce a galactocentric coordinate system (x, y, z) with the initial bubble location at a distance R_0 from the galactic center and z_0 above the galactic plane. Then the Lagrangian coordinates λ_1 and λ_2 may be introduced by

$$\begin{aligned} x &= R_0 + R_e \sin\lambda_1 \cos\lambda_2, \\ y &= R_e \sin\lambda_1 \sin\lambda_2, \\ z &= z_0 + R_e \cos\lambda_1, \end{aligned} \tag{4.34}$$

where $-\pi/2 \le \lambda_1 \le \pi/2$ and $0 \le \lambda_2 \le 2\pi$. The initial radius of the remnant R_e was taken to be much smaller than the characteristic scale of the gas density gradients in the galactic disk. As was estimated in Sec. III.G, galactic bubbles enter the radiative phase at an early time in their expansion. Therefore the analytic solution [Eqs. (2.100–(2.102)] of Weaver *et al.* (1977) for the expansion velocity U_0 and thermal energy $E_{\rm th,0}$, depending on the initial time t_H, were used as initial conditions:

$$U_0 = 0.6 \left(\frac{125}{154\pi}\frac{L_0}{\rho_0}\right)^{1/5} t_H^{-2/5}, \tag{4.35}$$

$$E_{\rm th,0} = \frac{5}{11} L_0 t_H, \tag{4.36}$$

$$t_H = \left(\frac{154\pi}{125}\frac{\rho_0 R_e^5}{L_0}\right)^{1/3}. \tag{4.37}$$

Here ρ_0 is the undisturbed interstellar gas density at a point with coordinates of the bubble center, while L_0 is the energy input rate due to winds from massive stars and supernova explosions in an OB association. Taking into account galactic rotation $V_{\rm rot}$, one obtains the components of the expansion velocity at an initial time t_H:

$$\begin{aligned} U_x &= U_0 \sin\lambda_1 \cos\lambda_2 - V_{\rm rot}\frac{y}{R}, \\ U_y &= U_0 \sin\lambda_1 \sin\lambda_2 + V_{\rm rot}\frac{x}{R}, \\ U_z &= U_0 \cos\lambda_1, \end{aligned} \tag{4.38}$$

where $R = \sqrt{x^2 + y^2}$ is the cylindrical galactocentric radius of the particular Lagrangian element. It was assumed that interstellar gas rotates around the center of the galaxy under the action of a gravitational field,

$$g_x = -\frac{V_{\rm rot}^2}{R^2} x, \tag{4.39}$$

$$g_y = -\frac{V_{\rm rot}^2}{R^2} y, \tag{4.40}$$

where the rotation curve of Wouterloot *et al.* (1990)

$$V_{\rm rot}(R) = 220(R/8.5\ {\rm kpc})^{0.0382}\ {\rm km\,s^{-1}} \tag{4.41}$$

was adopted.

The average structure of the gaseous disk in the z direction is approximated with the three-component density distribution discussed by Dickey and Lockman (1990):

$$\begin{aligned} n(z) = n_1 \exp(-z^2/H_1^2) + n_2 \exp(-z^2/H_2^2) \\ + n_3 \exp(-\mid z \mid /H_3) = n_t(0) f(z), \end{aligned} \tag{4.42}$$

where $n_t(0) = n_1 + n_2 + n_3$ is the total gas number density in the midplane of the galaxy and $f(z=0) = 1$. In the solar vicinity $n_1 = 0.395\,{\rm cm^{-3}}$, $H_1 = 127\,{\rm pc}$; $n_2 = 0.107\,{\rm cm^{-3}}$, $H_2 = 318\,{\rm pc}$; $n_3 = 0.064\,{\rm cm^{-3}}$, $H_3 = 403\,{\rm pc}$. Some calculations have been carried out (Silich, 1992b) for a composite Lockman *et al.* (1986), and Reynolds (1989) gas density distribution with a widespread ionized component. The characteristic scale heights H_i in Eq. (4.42) for explosions happening at different places in the galaxy were taken proportional to the half-width $H_{1/2}$ of the H I layer in the galactic plane:

$$H_i(R) = \alpha H_i(R_\odot), \quad \alpha = H_{1/2}(R)/H_{1/2}(R_\odot), \tag{4.43}$$

along with the coherent change of all three components in the gas density distribution,

$$n_i(R) = \beta n_i(R_\odot), \quad i = 1,2,3. \tag{4.44}$$

Here

$$\beta = \alpha^{-1}\frac{\sigma_{\rm HI}(R)}{\sigma_{\rm HI}(R_\odot)}, \tag{4.45}$$

where $\sigma_{\rm HI}$ is the surface density of a neutral hydrogen disk. The parameters $H_{1/2}$ and $\sigma_{\rm HI}$ were taken from the Wouterloot *et al.* (1990) model. In the solar vicinity $H_{1/2}(R_\odot) = 150\,{\rm pc}$, $\sigma_{\rm HI}(R_\odot) = 8.57 M_\odot/{\rm pc}^2$. The z component of gravity g_z was approximated by the linear interpolation of Allen's (1976) data or was specified by the analytic formula of Kuijken and Gilmore (1989):

$$g_z = -2\pi G\sigma_d \frac{z}{\sqrt{z^2 + z_d^2}} - 4\pi G\rho_H z, \tag{4.46}$$

where σ_d and z_d are the surface density and scale height of the stellar disk. The parameter ρ_H is the effective density of the galactic halo. For a uniform spherical halo with density ρ_{h0} we have $\rho_H = \rho_{h0}/3$. To fit the observed rotation curve, parameters ρ_H and σ_d had to be coupled with the relation (Kuijken and Gilmore, 1989)

$$\rho_H = 0.015 - 0.0047\left(\frac{\sigma_d}{50 M_\odot/{\rm pc}^2}\right) M_\odot/{\rm pc}^3. \tag{4.47}$$

Finally Caldwell and Ostriker's (1981) exponential distribution of the stellar component surface density along the galactic disk was adopted,

$$\sigma_d(R) = \sigma_d(R_\odot)\exp\left(\frac{R_\odot - R}{L}\right), \tag{4.48}$$

with the characteristic scale of inhomogeneity $L = 4.5\,{\rm kpc}$ and $\sigma_d(R_\odot) = 46 M_\odot/{\rm pc}^2$.

The temperature distribution in the gaseous disc of our galaxy is poorly known. But measurements of the soft-

x-ray background and OVI absorption lines by Burstein *et al.* (1976) and Jenkins and Meloy (1974) indicate the existence of a hot galactic halo. To include this effect it was tentatively assumed that temperature grows with the distance to the galactic plane as

$$T(z) = \frac{n_0^2 T_0}{n^2(z)} \tag{4.49}$$

or

$$T(z) = \frac{n_0 T_0}{n(z)}, \tag{4.50}$$

where the gas temperature in the midplane of the galaxy was taken to be $T_0 = 6000\,\mathrm{K}$.

It was assumed that the mass accumulation stops for those Lagrangian elements which reach the regions where sound speed a_s begins to exceed the expansion velocity. Note that the thin-layer approximation is no longer valid under such conditions. The motion of these elements proceeds without collisions.

The thin-layer approximation [Eqs. (4.9)–(4.14) and Eq. (4.4)] was used by Silich (1992a, 1992b; Silich *et al.*, 1994) to investigate galactic superbubble evolution in three dimensions.

Figure 23 shows a multisupernova remenant in the shape of an hourglass, with a noticeable degree of deformation by the galactic shear. After the bubble takes such a shape, both gravity and pressure within the cavity combine to decelerate the lower parts of the shell.

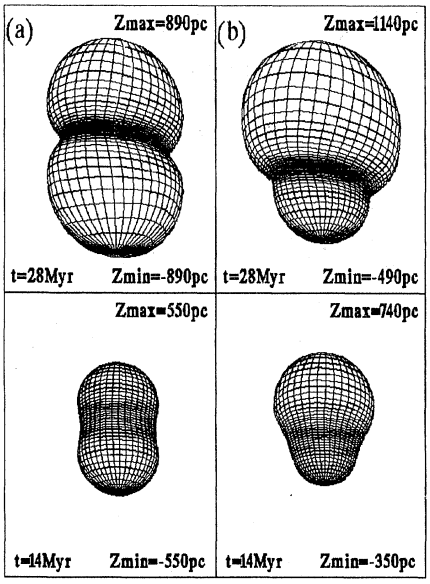

FIG. 23. Galactic superbubble morphology for different locations of the parent OB association relative to the galactic plane. Left: the OB association is at the midplane of the galaxy. Right: the OB association is 50 pc above the galactic plane. From Silich *et al.*, 1994.

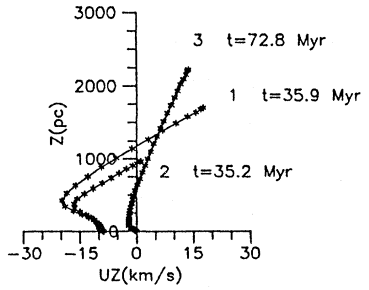

FIG. 24. Variation of the z component of the bubble expansion velocity with the position of the Lagrangian element above the galactic plane. Curves 1 and 2 correspond to the energy input rates $L_{38} = 2$ and $L_{38} = 0.5$ and a z component of the gravity as in the solar vicinity. Curve 3 is the bubble's evolution with an energy input rate of $L_{38} = 0.5$ and weak gravity like that at 15 kpc from the galactic center. From Silich, 1992b.

The z component of the expansion velocity slows down and changes direction near the plane of symmetry $z = 0$. This process is illustrated in Fig. 24, where distribution of the z component of expansion velocity over the remnant surface is shown for supershells located at different distances from the galactic center. An expanding cusp, i.e., an expanding dense ring, is formed in the equatorial plane of the remnant. This is, as we might expect, the onset of destruction of the shell as a coherent structure. In the inner part of the Galaxy up to 50% of the swept-up interstellar gas is concentrated near the galactic midplane after 35 Myr of evolution (Silich, 1992b). Figure 25 displays a cross section of the supershell cross section by the midplane of the Galaxy at different times. The action of the z component of the gravity restricts the lifetime of the superbubble and does not allow development of highly elongated structures. The ratio of the major to the minor axis of the supershell does not exceed 2–3 during the time of cusp formation. A displacement of the energy source from the plane of symmetry in the

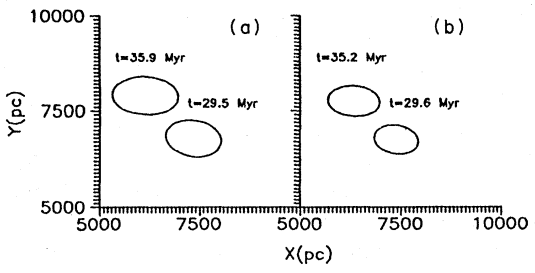

FIG. 25. Sections of superbubbles in the galactic plane $z = 0$ at different times. The bubble centers lie at 10 kpc from the galactic center. (a) Energy input rate $L_{38} = 2$; (b) energy input rate $L_{38} = 0.5$. From Silich, 1992b.

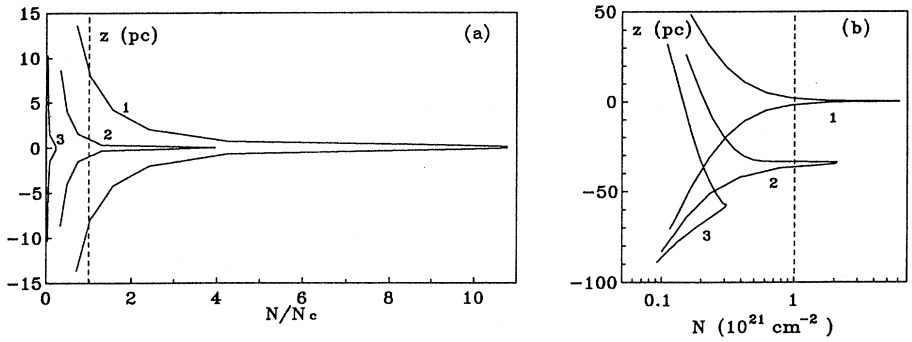

FIG. 26. Distribution of the relative column density along the shell. (a) OB association is in the midplane of the galaxy. Curves 1,2,3 correspond to the galactocentric radii $R = 5$, 8.5, and 15 kpc. (b) OB association lies above the galactic plane. Curves 1,2,3 correspond to 0, 50, and 100 pc distance from the OB association to the galactic plane. Energy input rate $L_{38} = 1.05$, $R = 8.5$ kpc. From Mashchenko and Silich, 1994.

z direction generates a strongly asymmetrical structure, and the bubble may break out of the galactic disk (Silich *et al.*, 1994).

Palouš (1992) has made a realistic matching of the H I distribution in a particular region of the Milky Way Galaxy, $55° \leq l \leq 75°$, $-5° \leq b \leq 5°$, within the radial velocity interval $97\,\mathrm{km\,s^{-1}} \leq V_{\mathrm{LSR}} \leq 75\,\mathrm{km\,s^{-1}}$, which corresponds to the galactocentric distance $R = 17$ kpc and contains an expanding supershell GS064-01-97. He found that he could reproduce observations if at this distance the fraction of H I in the thick exponential component [the third term in Eq. (4.42)] is 3 to 5 times greater than near the Sun. So numerical models based on the thin-layer approximation have predictive capabilities that may be quite useful.

The organizing role of supershells in molecular cloud formation has been reexamined for three-dimensional remnants by Mashchenko and Silich (1994). They used the galactic model, as described above, and performed calculations for three galactocentric radii (5 kpc, 8.5 kpc, and 15 kpc) and three position of the parent OB association above the galactic plane (0, 50 pc, and 100 pc). The energy input rate was assumed to be constant, with three different values $L = (0.315;\ 1.05,\ \text{or}\ 3.15)\times 10^{38}\,\mathrm{ergs\,s^{-1}}$, which corresponds to 30–300 supernova explosions during 30 Myr, the lifetime of an OB association.

The time evolution of a superbubble shape in a differentially rotating galactic disk is illustrated in Fig. 23. The OB association located in the midplane of the galaxy (left in Fig. 23) generates a superbubble that differs strongly from the remnant produced by the same association located 50 pc above the galactic plane (right in Fig. 23). In any case, during the late stages of expansion near the galactic plane, a typical "belt" with enhanced surface density develops.

The distribution of the relative column density N/N_c, near the waist of a supershell for different bubble locations in the galaxy is presented in Fig. 26. Here the critical value N_c which shields the internal shell layers from the background UV radiation is defined by Eq. (3.147). The column number densities across some segments of the remnant may exceed the critical value N_c. This may happen in the inner parts of the Milky Way ($R < 15$ kpc) only, if the OB association is located fewer than 100 pc from the galactic plane. It was estimated that the molecular layer is likely to be developed within a very narrow (in the z direction) parts of the shell. This newly formed molecular gas layer is confined to a slab with a half-width smaller than one hundred parsecs, in agreement with the observed distribution of molecular clouds in the Milky Way Galaxy (Solomon and Sanders, 1980). The mass of the shell, which can be transformed into molecular form, may reach about $10^6 M_\odot$ (see Fig. 27), despite the small thickness of the molecular layer. Most of the molecular gas is concentrated on opposite ends of the remnant, as was expected from the two-dimensional calculations of Tenorio-Tagle and Palouš (1987; Palouš *et al.*, 1990). It seems, therefore, very likely that supershells may play an important role in molecular cloud formation and thus stimulate the process of star formation in the galaxy.

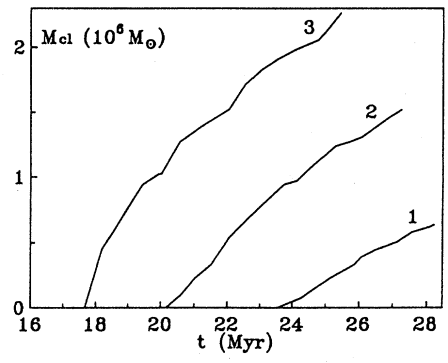

FIG. 27. The mass of the shell material that can be transformed into molecular form. Curves 1,2,3 correspond to the energy release rates $L_{38} = 0.315$, 1.05, and 3.15. The bubble center is 5 kpc from the galactic center. From Mashchenko and Silich, 1994.

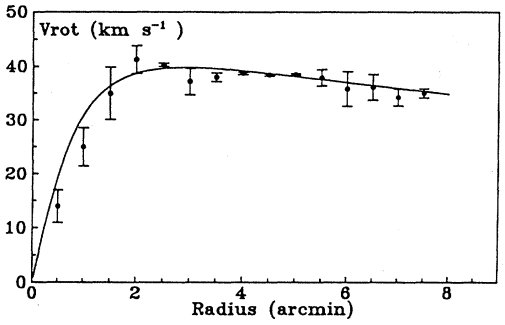

FIG. 28. The rotation curve of the Ho II galaxy and its analytic approximation. From Puche *et al.*, 1992.

D. Superbubbles in the HoII galaxy

The galaxy Ho II (Puche *et al.*, 1992) is the dwarf irregular companion of the M81 group, which lies at a mean distance of 3.2 Mpc. The total kinematic mass of the galaxy was estimated as $M_{\rm tot} \approx 2 \times 10^9 M_\odot$ with approximately 30% of this mass in the form of neutral hydrogen ($M_{\rm HI} \approx 7 \times 10^8 M_\odot$). The scale height of the H I layer derived from measurements of the velocity dispersion is $H = 625$ pc. This value is much greater than the thickness of the gaseous disk in a normal spiral galaxy. The vertical distribution of the H I gas number density is approximated by the Gaussian law

$$n(r,z) = \frac{N(r)}{\sqrt{2\pi}H} \exp(-z/H)^2, \qquad (4.51)$$

with the radial H I column density distribution tabulated by Puche *et al.* (1992). The orientation parameters, inclination i and position angle PA, were estimated to be $i \approx 40°$, $PA \approx 177°$. The rotation curve (Fig. 28) displays a fast, almost linear, growth in the inner part of the galaxy and then almost flat behavior up to a distance of 7.5 kpc from the galactic center.

The VLA observations (Puche *et al.*, 1992) of the HoII galaxy have revealed 51 objects, with characteristic sizes ranging from 100 pc to 1700 pc, which may be considered as expanding shells or holes in the H I column density distribution. Massive stars in the centers of large holes and H_α emission from the interior of small structures and boundary regions of the larger ones provide observational evidence for the mechanism of multiple correlated supernova explosions within rich OB associations, as has been discussed earlier.

Location and orientation of the H I holes in the plane of view are shown in Fig. 29 from Puche *et al.* (1992).

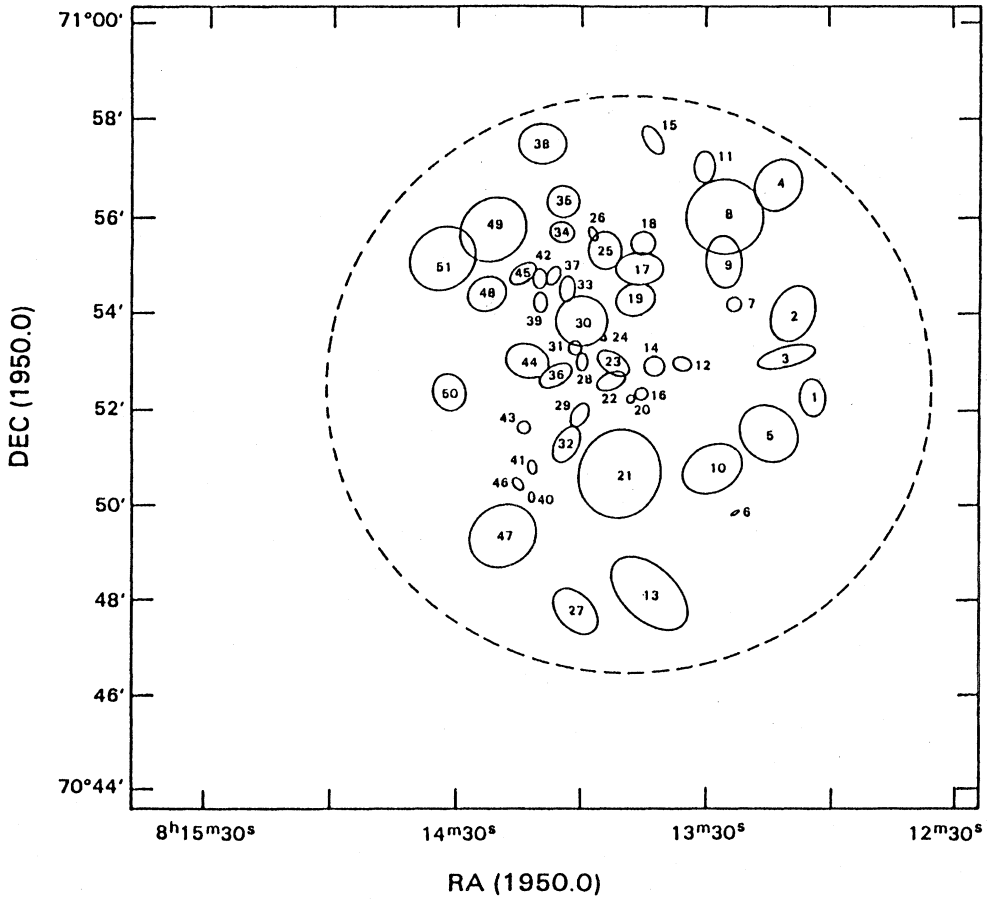

FIG. 29. Location and orientation of the H I holes in the Ho II galaxy. From Puche *et al.*, 1991.

There are some examples of almost radial orientation of the major axis of the remnant which seem difficult to understand from the theory developed in Sec. III. To determine evolutionary differences between superbubbles in massive disk galaxies and those in dwarf, low-mass systems, Mashchenko and Silich (1995) have provided numerical simulations of superbubble evolution in the Ho II galaxy.

It was tentatively assumed that density of the stellar component obeys the King distribution and is the dominant agent in the gravity field, i.e., the self-gravity of the gas component was ignored. Then the z component of the gravitational field g_z and rotational velocity $V_{\rm rot}(r)$ may be expressed as follows (Tomisaka and Ikeuchi, 1988):

$$g_z = -GM_c\frac{z}{\omega^3}\left[\ln\left(\frac{\omega}{r_c}+\sqrt{1+\left(\frac{\omega}{r_c}\right)^2}\right) - \frac{\omega}{r_c\sqrt{1+(\frac{\omega}{r_c})^2}}\right], \tag{4.52}$$

$$V_{\rm rot}(r) = \left(\frac{GM_c}{r}\right)^{1/2}\left[\ln\left(\frac{r}{r_c}+\sqrt{1+\left(\frac{r}{r_c}\right)^2}\right) - \frac{r}{r_c\sqrt{1+(\frac{r}{r_c})^2}}\right]^{1/2}, \tag{4.53}$$

where G is the gravity constant, $r=\sqrt{x^2+y^2}$ is the cylindrical radius, and $\omega=\sqrt{x^2+y^2+z^2}$ is the spherical radius. To fit the rotation curve, the parameters M_c and r_c were determined as follows: $M_c = 1.179\times10^9 M_\odot$ and $r_c = 929\,\mathrm{pc}$. Thermal evaporation of the cold dense shell and radiative cooling from the hot bubble interior were allowed.

The numerical model described at the beginning of this section generates the three-dimensional shape, surface density distribution, and expansion velocity field of the remnant. To compare the results of numerical calculations with observations, we must project the shells onto the plane of the sky.

Let us introduce a galactic coordinate system x, y, z, with its origin at the center of Ho II, and the coordinates x', y', z', with the x' and y' axes located in the plane of the sky and the z' axis directed towards the observer. If one assumes the x' axis to be common and coinciding with the line which is the intersection between the plane of the galaxy and the plane of view, then the observed coordinates x', y', z' are defined as follows:

$$x' = x, \tag{4.54}$$

$$y' = y\cos i + z\sin i, \tag{4.55}$$

$$z' = -y\sin i + z\cos i, \tag{4.56}$$

where i is inclination angle. Note that as a rule analysis of the galactic rotation curve alone does not allow us to distinguish between i and $(180^\circ - i)$, i.e., between two possible directions of the angular momentum of the galaxy.

The H I column density along any line of sight which intersects with the remnant surface may then be expressed as

$$N(x',y') = \sum_j \frac{N_j}{|\cos\xi_j|} + \int n(x',y',z')dz', \tag{4.57}$$

where the index j denotes intersection with different Lagrangian layers, $N_j = \sigma_j/\eta$ is the column number density of the shell, σ_j is the surface mass density, η is the mean mass per particle, ξ_j is the angle between line of sight and the unit vector normal to the shell surface. The last term in Eq. (4.57) gives the total column density outside the remnant. The column number density goes to infinity for those Lagrangian elements in which $\xi_j \to 90^\circ$. To exclude this effect, which is due to an infinitely small shell thickness, it was assumed the projected column number density for Lagrangian elements with $\xi_j > 60^\circ$ would be the same as for the angle $\xi_j = 60^\circ$. This somewhat arbitrary procedure smoothed the column density distribution near the edge of the H I hole in the plane of the sky, but did not provide a significant influence on the later analysis. Approximating the column density isodense with the 10% contrast relative to the surrounding gas by an elliptical hole, one gets then the position of the hole center, its major and minor axes, and their orientation.

Superbubble evolution was simulated for three galactocentric radii: R=1.5 kpc, 4.17 kpc, and 6 kpc. The parent OB association was assumed to be located in the midplane of the galaxy and to provide an energy input rate $3.4\times10^{37}\,\mathrm{ergs\,s^{-1}}$ which corresponds to approximately 30 supernova explosions during 30 Myrs, lifetime of the OB association. For every galactocentric radius nineteen polar angles, Θ_i, $\Theta_{i+1} = \Theta_i + 10^\circ$ were considered, where

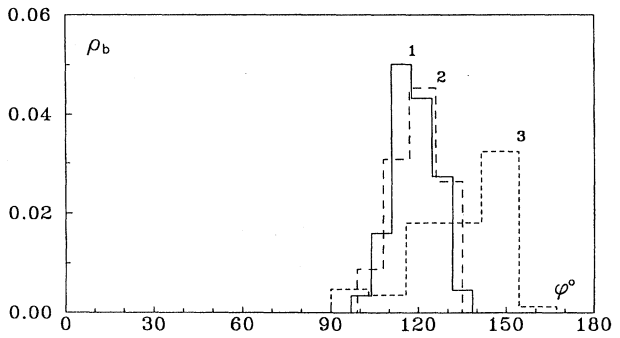

FIG. 30. The density of distribution for the main axis of the H I hole to be oriented in the ϕ direction. From Mashchenko and Silich, 1995.

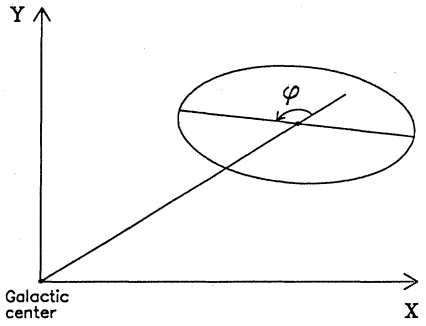

FIG. 31. Scheme of H I holes orientation in the plane of sky. From Mashchenko and Silich, 1995.

Θ is the angle between the x axis and the radius vector of the shell's center in the plane of the galaxy. The value of Θ_0 was adopted to be $-90°$.

For inner galactic regions with $R < 1.5$ kpc, calculations were continued up to 70 Myr. The theoretical maps of the column density distribution and parameters of the holes were calculated with the interval 10 Myr for every value of the polar angle Θ. For galactocentric radii $R = 4.17$ kpc and $R = 6$ kpc, calculations were stopped after 80 Myrs, and the time interval was equal to 20 Myr. Thus the H I maps and main observational parameters of each H I hole (its major and minor axes and their orientation) were generated for 285 supershells with different ages and different locations in the galaxy.

The results of the numerical calculations are presented in Fig. 30 in the form of histograms for the density of distribution ρ_b of H I holes with major axes in the different directions ϕ:

$$\rho_b = \frac{1}{n}\frac{\Delta n_\phi}{\Delta\phi}. \tag{4.58}$$

Here n is the total number of holes for which calculations were done at the particular galactocentric radius R, Δn_ϕ is the number of holes with the main axis in the interval $\Delta\phi$, and ϕ is the angle between the line which connects the center of the galaxy with the center of the H I hole and the observed main axis of the ellipse, which represents this hole (see scheme in Fig. 31). The tangential orientation of the main axis corresponds to $\phi = 90°$. The histograms 1,2,3 are for galactocentric radii $R = 1.5$ kpc, 4.17 kpc, and 6 kpc. Thus for the adopted direction of the galactic spin $i \approx 40°$, all major axes of the H I holes have to be within the range $90° \le \phi \le 180°$. Were the vector of the galactic angular momentum to be directed away from the observer ($i' = 180° - i = 140°$), the angle ϕ should fall in the interval $0° \le \phi \le 90°$. Thus we get a simple method which allows us to distinguish between two possible directions of galactic spin. If the major axes of the H I holes are concentrated in the third quadrant ($90° \le \phi \le 180°$), then $i' < 90°$. If the major axes of the holes are in the second quadrant ($0° \le \phi \le 90°$), then angle i' should be greater than 90°.

An observed value for the angle ϕ may be extracted from the Puche *et al.* (1992) observations as follows:

$$\phi = PA_h - \beta + 90°, \tag{4.59}$$

where PA_h is the position angle of the hole's major axis, while β is the polar angle of the hole's center. Analysis of the observational data shows that major axes of the H I holes in the Ho II galaxy are really concentrated in the third quadrant (see Table III), but only in the outer part of the galaxy ($R > 3.4$ kpc). Here the χ^2 criterion rejects equipartition of the main axes between the second and third quadrants with the probability $\alpha = 95\%$. In the inner part of the galaxy, distribution of the main axes of the holes between second and third quadrants is more homogeneous. Here the χ^2 criterion rejects the homogeneous distribution of the main axes between second and third quadrants with the probability $\alpha = 70\%$ only. This analysis gives evidence in favor of the Ho II spin's being directed away from the observer ($i' \approx 140°$). This conclusion is in contradiction with the results of Karachentsev (1989), who predicts ($i' = 43° \pm 8°$) from an analysis of the distribution of the dust clouds. We are uncertain about the reasons for this discrepancy. Either Karachentsev's method does not work well for the almost-face-on galaxies, or some physical reason restricts the action of the galactic shear on supershell evolution.

We assume the different orientations of the H I holes come from interaction of the shell with large-scale interstellar clouds or from supershell collisions, which are more frequent in the inner part of the galaxy as a result of their higher density in this region. Thus analysis of the statistical properties of superbubble ensembles and comparison with the numerical models may provide a good opportunity to study the structure and global properties of the interstellar medium in the nearby galaxies.

TABLE III. The orientation of H I holes in the Ho II galaxy.

Galactocentric distance (kpc)	Number of holes with $0° \le \phi \le 90°$	Number of holes with $90° \le \phi \le 180°$	α
0–7.5	24	20	45%
0–3.4	9	14	70%
3.4–7.5	15	6	95%

V. CONCLUDING REMARKS

Observations of shell-like structures in galaxies have revealed considerable deviations from spherical symmetry, prompting the development of theories dealing with nonspherical, mainly axisymmetrical gas flows. We have described here models based mainly on the thin-layer approximation, which permits us to calculate not only 2D, but also 3D, models (in fact, they are called 1.5D and

2.5D hydrodynamics, because of the negligible thickness of the shell and the use of an averaged value of the inner gas pressure in the calculations). The interpretation and models of different astrophysical objects observed during the last decade are presented here on the basis of these calculations.

This approach remains approximate, but the precision of the calculations is rather high, because the parameter Δ/R is really small, whereas the temperature and the sound speed within the cavity are high in most cases of application. It is not clear how much the models could be improved by the use of full 2D and 3D calculations. Three-dimensional calculations require such powerful computers and so much time to reach reasonable precision, that they cannot be used for a great number of observed objects. This is true of 3D calculations with barotropic equations of state, as well as for calculations taking account of thermal processes.

The existence of the small parameter Δ/R produces difficulties even for 2D calculations, especially those taking account of thermal processes. The sensitivity of the radiation processes to temperature in combination with large gradients in the shell makes necessary a very fine grid in the shell and around, which must be adaptive because of continuous joining of matter to the shell. These difficulties probably could be solved by using mixed Eulerian-Lagrangian schemes with adaptation, but the results of 2D calculations made up to the present time by less sophisticated methods in many cases do not exceed in precision the calculations made by the thin-shell approximation.

In our opinion, the methods described here can be widely applied for construction of models interpreting numerous observations of supernova remnants, superbubbles, and other shell objects. The full 2D and 3D calculations can in principle reach higher precision and give more complete information, but complications connected with the development of numerical schemes and consuming of numerical time would not, in our opinion, permit their use for interpretation of numerous observations, but only for more detailed study of the most interesting objects.

ACKNOWLEDGMENTS

This work was supported, in part, by Grant No. 93-02-17106 from the Russian Foundation of Fundamental Research and Grant No. 3-169 from the Astronomy Program of the Russian Ministry of Science. G.S.B.-K. acknowledges the partial support of the Kapitza Fellowship of the Royal Society and International Sciences Foundation Grant No. M3400. S.A.S. acknowledges the support of the International Sciences Foundation through Grant No. UC9000 and partial support from the National Space Agency of the Ukraine.

REFERENCES

Allen, C. W., 1986, *Astrophysical Quantities* (Athlone, London).

Andriankin, E. I., A. M. Kogan, A. S. Kompaneets, and V. P. Krainov, 1962, Zh. Prikl. Mekh. Tekh. Fiz. N6, 3.

Ardelian, N. V., G. S. Bisnovatyi-Kogan, and Yu. P. Popov, 1979, Astron. Zh. **56**, 1244 [Sov. Astron. **23**, 705 (1979)].

Arnett, D., B. Fryxell, and E. Muller, 1989, Astrophys. J. Lett. **341**, L63.

Arshutkin, L. N., and I. G. Kolesnik, 1984, Astrofizika **21**, 147.

Avedisova, V. S., 1971, Astron. Zh. **48**, 894 [Sov. Astron. **15**, 708 (1972)].

Balick, B., 1987, Astron. J. **94**, 671.

Baranov, V. B., K. V. Krasnobaev, and A. G. Kulikovskii, 1970, Dokl. Akad. Nauk SSSR **194**, 41 [Sov. Phys. Dokl. **15**, 745 (1971)].

Bisnovatyi-Kogan, G. S., 1967, Appl. Math. Mech. **31**, 762.

Bisnovatyi-Kogan, G. S., 1970, Astron. Zh. **47**, 813 [Sov. Astron. **14**, 652 (1971)].

Bisnovatyi-Kogan, G. S., and S. I. Blinnikov, 1982, Astron. Zh. **59**, 876 [Sov. Astron. **26**, 530 (1982)].

Bisnovatyi-Kogan, G. S., S. I. Blinnikov, and S. A. Silich, 1989, Astrophys. Space. Sci. **154**, 229.

Bisnovatyi-Kogan, G. S., T. A. Lozinskaya, and S. A. Silich, 1990, Astrophys. Space Sci. **166**, 277.

Bisnovatyi-Kogan, G. S., and M. V. Murzina, 1995, Astron. Astrophys., in press.

Bisnovatyi-Kogan, G. S., and D. K. Nadyozhin, 1972, Astrophys. Space Sci. **15**, 353.

Bisnovatyi-Kogan, G. S., and S. A. Silich, 1991, Astron. Zh. **68**, 749 [Sov. Astron. **35**, 370 (1991)].

Blinnikov, S. I., V. S. Imshennik, and V. P. Utrobin, 1982, Pis'ma Astron. Zh. **8**, 671 [Sov. Astron. Lett. **8**, 361 (1982)].

Blondin, J. M., and P. Lundqvist, 1993, Astrophys. J. **405**, 337.

Bochkarev, N. G., 1985, Astron. Zh. **62**, 875 [Sov. Astron. **29**, 509 (1985)].

Bochkarev, N. G., 1988, Nature **332**, 518.

Bochkarev, N. G., and T. A. Lozinskaya, 1985, Astron. Zh. **62**, 103 [Sov. Astron. **29**, 60 (1985)].

Bochkarev, N. G., and T. G. Sitnik, 1985, Astrophys. Space Sci. **108**, 237.

Bochkarev, N. G., and S. A. Zhekov, 1990, Astron. Zh. **67**, 274 [Sov. Astron. **34**, 138 (1990)].

Bodenheimer, P., G. Tenorio-Tagle, and H. W. Yorke, 1979, Astrophys. J. **233**, 85.

Bodenheimer, P., and S. E. Woosley, 1983, Astrophys. J. **269**, 281.

Bomans, D. J., K. Dennert, and M. Kurster, 1994, Astron. Astrophys. **283**, L21.

Brinks, E., 1990, in *The Interstellar Medium in Galaxies*, edited by H. A. Thonson and J. M. Shull (Kluwer Academic, Netherlands), p. 39.

Brinks, E., and E. Bajaja, 1986, Astron. Astrophys. **169**, 14.

Bruhweiler, F. C., T. Gull, M. Kafatos, and S. Sofia, 1980, Astrophys. J. Lett. **238**, L27.

Budak, B. M., and S. V. Fomin, 1965, *Multiple Integrals and Series* (Nauka, Moscow).

Burrows, C., 1994, Hubble Space Telescope News, May, 19.

Burstein, P., R. J. Borken, W. L. Kraushaar, and W. T. Sanders, 1976, Astrophys. J. **213**, 405.

Bychkov, K. V., and S. B. Pikel'ner, 1975, Pis'ma Astron. Zh. **1**, 29 [Sov. Astron. Lett. **1**, 14 (1975)].

Caldwell, J. A. P., and J. P. Ostriker, 1981, Astrophys. J. **251**, 61.

Cash, W., P. Charles, S. Bowyer, F. Walter, G. Garmire, and

G. Riegler, 1980, Astrophys. J. Lett. **238**, L71.
Castor, J., R. McCray, and R. Weaver, 1975, Astrophys. J. Lett. **200**, L107.
Chechetkin, V. M., A. A. Denisov, and Yu. P. Popov, 1989 in *Supernovae, 10 the Santa Cruz Summer Workshop in Astronomy and Astrophysics*, edited by S. E. Woosley (Springer, Heidelberg), p. 375.
Chernyi, G. G., 1957, Dokl. Akad. Nauk SSSR **112**, 213.
Chevalier, R. A., 1974, Astrophys. J. **188**, 501.
Chevalier, R. A., 1982, Astrophys. J. **259**, 302.
Chevalier, R. A., and J. N. Imamura, 1983, Astrophys. J. **270**, 554.
Chevalier, R. A., and E. P. Liang, 1989, Astrophys. J. **344**, 332.
Chevalier, R. A., and D. Luo, 1994, Astrophys. J. **421**, 225.
Chieze, I. P., and B. Lazareff, 1981, Astron. Astrophys. **95**, 194.
Chiosi, C., E. Nasi, and S. P. Sreenivasan, 1978, Astron. Astrophys. **63**, 103.
Chu, Y.-H., 1981, Astrophys. J. **249**, 195.
Chu, Y.-H., and M.-M. Mac Low, 1990, Astrophys. J. **365**, 510.
Chu, Y.-H., M.-M. Mac Low, G. Garcia-Segura, B. Wakker, and R. C. Kennicutt, 1993, Astrophys. J. **414**, 213.
Chugai, N. N., 1993, Astrophys. J. Lett. **414**, L101.
Comerón, F., and J. Torra, 1992, Astron. Astrophys. **261**, 94.
Comerón, F., and J. Torra, 1994, Astrophys. J. **423**, 652.
Cowie, L. L., and C. F. McKee, 1977, Astrophys. J. **211**, 135.
Cowie, L. L., C. F. McKee, and J. P. Ostriker, 1981, Astrophys. J. **247**, 908.
Cox, D. R., 1972, Astrophys. J. **178**, 159.
Cox, D. P., and J. Franco, 1981, Astrophys. J. **251**, 681.
Cox, D. P., and R. Edgar, 1983, Astrophys. J. **265**, 443.
Crotts, A. P. S., W. E. Kunkee, and P. J. McCarthy, 1989, Astrophys. J. Lett. **347**, L61.
Dalton, W. W., and S. A. Balbus, 1993, Astrophys. J. **404**, 625.
Danziger, I. J., and P. Bouchet, 1989, in *Evolutionary Phenomena in Galaxies*, edited by B. Pagel and J. Beckman (Cambridge University, Cambridge, England), p. 283.
de Jager, C., H. Niewenhuijzen, and K. A. van der Hucht, 1988, Astron. Astrophys. Suppl. Ser. **72**, 259.
Deul, E. R., and R. H. Hartog, 1990, Astron. Astrophys. **229**, 362.
Dickey, J., and F. Lockman, 1990, Annu. Rev. Astron. Astrophys. **28**, 215.
Domgorgen, H., D. J. Bomans, and K.S. de Boer, 1995, Astron. Astrophys. **296**, 523.
Dopita, M. A., J. F. Bell, Y.-H. Chu, and T. A. Lozinskaya, 1994, Astrophys. J. Suppl. Ser. **93**, 455.
Dopita, M. A., D. S. Mathewson, and V. L. Ford, 1985, Astrophys. J. **297**, 599.
Doroshkevich, A. G., and Ya. B. Zeldovich, 1981, Zh. Eksp. Teor. Fiz. **80**, N3, 801 [Sov. Phys. JETP **53**, 405 (1981)].
Draine, B. T., and C. F. McKee, 1993 Annu. Rev. Astron. Astrophys. **31**, 373.
Dufour, R. J., 1989, Rev. Mex. Astr. Astrof. **18**, 87.
Dyson, J. E., 1973, Astron. Astrophys. **23**, 381.
Dyson, J. E., 1975, Astrophys. Space Sci. **35**, 299.
Dyson, J. E., and J. de Vries 1972, Astron. Astrophys. **20**, 223.
Eilek, J. A., and P. A. Hughes, 1990, in *Astrophysical Jets*, edited by P. E. Hughes (Cambridge University, Cambridge, England), p. 428.
Elmegreen, B. G., 1992, in *Evolution of Interstellar Matter and Dynamics of Galaxies*, edited by J. Palouš, W. B. Burton, and P. O. Lindblad (Cambridge University, Cambridge, England), p. 178.
Elmegreen, B. G., and W.-H. Chiang, 1982, Astrophys. J. **253**, 666.
Evans, C. R., and J. F. Hawley, 1988, Astrophys. J. **332**, 659.
Fabian, A. C., R. Willingale, J. P. Pye, S. S. Murray, and G. Fabbiano, 1980, Mon. Not. R. Astron. Soc. **193**, 175.
Falle, S. A. E. G., 1981, Mon. Not. R. Astron. Soc. **195**, 1011.
Falle, S. A. E. G., A. R. Garlick, and P. H. Pidsley, 1984, Mon. Not. R. Astron. Soc. **208**, 925.
Fedorenko, V. N., 1983, Astrophys. Space. Sci. **98**, 25.
Ferriere, K., M.-M. Mac Low, and E. Zweibel, 1991, Astrophys. J. **375**, 239.
Franco, J., and D. P. Cox, 1986, Publ. Astron. Soc. Pac. **98**, 1076.
Franco, I., A. Ferrara, M. Rozyczka, G. Tenorio-Tagle, and D. P. Cox, 1993, Astrophys. J. **407**, 100.
Franco. J., W. W. Miller III, S. J. Arthur, G. Tenorio-Tagle, and R. Terlevich, 1994, Astrophys. J. **435**, 805.
Franco, J., and S. N. Shore, 1984, Astrophys. J. **285**, 813.
Franco, J., G. Tenorio-Tagle, P. Bodenheimer, and M. N. Różyczka, 1991, Publ. Astron. Soc. Pac. **103**, 803.
Fuchs, B., and K. O. Thielheim, 1979, Astrophys. J. **227**, 801.
Gaffet, B., 1978, Astrophys. J. **225**, 442.
Garay, G., L. F. Rodrigues, and J. H. Gorkom, 1986, Astrophys. J. **309**, 553.
Gaume, R. A., and R. L. Mutel, 1987, Astrophys. J. Suppl. Ser. **65**, 193.
Gerola, H., and P. E. Seiden, 1978, Astrophys. J. **223**, 129.
Gershberg, R. E., and P. V. Scheglov, 1964, Astron. Zh. **41**, 425 [Sov. Astron. **8**, 337 (1964)].
Graham, J. A., and D. G. Lawrie, 1982, Astrophys. J. Lett. **253**, L73.
Giuliani, J. L., Jr., 1982, Astrophys. J. **256**, 624.
Hamilton, A. J. S., 1985, Astrophys. J. **291**, 523.
Hamilton, A. J. S., C. L. Sarazin, and A.E. Szymkowiak, 1986, Astrophys. J. **300**, 698.
Heiles, C., 1979, Astrophys. J. **229**, 533.
Heiles, C., 1984, Astrophys. J. Suppl. Ser. **55**, 585.
Heiles, C., 1987, Astrophys. J. **315**, 555.
Heiles, C., 1991, in *The Interstellar Disk-halo Connection in Galaxies: Proceedings of the 144th Symposium of the IAU*, edited by H. Bloemen (Kluwer Academic, Boston), p. 433.
Helfand, D. J., and R. H. Becker, 1984, Nature **307**, 215.
Hindman, J. V., 1967, Aust. J. Phys. **20**, 147.
Hnatyk, B. I., 1987, Astrophysics **22**, 66.
Hnatyk, B. I., 1988, Pis'ma Astron. Zh. **14**, 724 [Sov. Astron. Lett. **14**, 309 (1988)].
Igumentshchev, I. V., B. M. Shustov, and A. V. Tutukov, 1990, Astron. Astrophys. **234**, 396.
Igumentshchev, I. V., A. V. Tutukov, and B. M. Shustov, 1992, Astron. Zh. **69**, 479 [Sov. Astron. **36**, 241 (1992)].
Imshennik, V. S., 1977, in *Numerical Methods of Plasma Physics*, edited by A. A. Samarsky, in Russian (Nauka, Moscow), p. 100.
Imshennik, V. S., and D. K. Nadezhin, 1989, Sov. Astrophys. Phys. Rev. **8**, 1.
Izotov, Yu., N. Guseva, V. Lipovetsky, and A. Kniazev, 1994, in *Panchromatic View of Galaxies—Their Evolutionary Puzzle*, edited by G. Hensler, C. Theis, and J. Gallagher (Editions Frontiéres, Gif Sur Yvette, France), p. 192.
Jakobsen, P., R. Albrecht, C. Barbieri, J. C. Blades, A. Bok-

senberg, *et al.*, 1991, Astrophys. J. Lett. **369**, L63.
Jenkins, E. B., and D. A. Meloy, 1974, Astrophys. J. Lett. **193**, L121.
Jenkins, E. B., M. Jura, and M. Loewenstein, 1983, Astrophys. J. **270**, 88.
Johnson, H. M., and D. E. Hogg, 1965, Astrophys. J. **142**, 1033.
Karachentsev, I.D., 1989, Astron. Zh. **66**, 907 [Sov. Astron. **33**, 470 (1989)].
Kesteven, M. J., and J. L. Caswell, 1987, Astron. Astrophys. **183**, 118.
Kestenboim, Kh. S., G. S. Roslyakov, and L. A. Chudov, 1974, *Point Explosion. Methods of Calculations. Tables* (Nauka, Moscow).
Kirshner, R. R., P. F. Winkler, and R. A. Chevalier, 1987, Astrophys. J. Lett. **315**, L135.
Klein, R. I., C. F. McKee, and P. Colella, 1990, in *The Evolution of the Interstellar Medium*, Astronomical Society of the Pacific Conference No. 12, edited by L. Blitz (ASP, San Francisco), p. 117.
Klein, R. I., C. F. McKee, and P. Colella, 1994, Astrophys. J. **420**, 213.
Klimishin, I. A., 1984, *Shock Waves in the Star Envelopes* (Nauka, Moscow).
Klimishin, I. A., and B. I. Hnatyk, 1981, Astrofisika **17**, 547.
Kolesnik, I. G., and L. S. Pilyugin, 1986, Astron. Zh. **63**, 279 [Sov. Astron. **30**, 169 (1986)].
Kompaneets, A. S., 1960, Dokl. Akad. Nauk SSSR **130**, 1001 [Sov. Phys. Dokl. **5**, 46 (1960)].
Kontorovich, V. M., and S. F. Pimenov, 1995, unpublished.
Koo, B.-C., and C. F. McKee, 1990, Astrophys. J. **354**, 513.
Korobeinikov, V. P., 1985, *Problems of the Theory of the Point Explosion* (Nauka, Moscow).
Korycansky, D. G., 1992, Astrophys. J. **398**, 184.
Kovalenko, I. G., 1987, Kinematika i Fizika Nebes. Tel **3**, N5, 78 [Kinematics and Physics of Celestial Bodies **3**, N5, 88 (1987)].
Krol', V. A., and P. I. Fomin, 1978, Astrom Astrofiz. **36**, 13.
Kuijken, K., and G. Gilmore, 1989, Mon. Not. R. Astron. Soc. **239**, 571.
Kulikovskyi, A. G., and G. A. Lyubimov, 1962, *Magnetohydrodynamics* (Nauka, Moscow).
Kunze, R., H. W. Yorke, and R. Spurzem, 1992, in *Evolution of Interstellar Matter and Dynamics of Galaxies*, edited by J. Palouš, W. B. Burton, and P. O. Lindblad (Cambridge University, Cambridge, England), p. 77.
Lada, C. J., 1985, Annu. Rev. Astron. Astrophys. **23**, 267.
Landau, L. D., and E. Lifshitz, 1959, *Fluid Mechanics* (Pergamon, London).
Laumbach, D. D., and R. F. Probstein, 1969, J. Fluid Mech. **35**, 53.
Laval, A., M. Rosado, J. Boulesteix, Y. P. Georgelin, E. L. Coarer, M. Marcelin, and A. Viale, 1992, Astron. Astrophys. **253**, 213.
Leontovich, M. A., and S. M. Osovetz, 1956, Atom. Energia **3**, 81.
Lockman, F. J., L. M. Hobbs, and J. M. Shull, 1986, Astrophys. J. **301**, 380.
Long, K. S., and D. J. Helfand, 1979, Astrophys. J. Lett. **234**, L77.
Long, K. S., W. P. Blair, R. L. White, and Y. Matsui, 1991, Astrophys. J. **373**, 567.
Lozinskaya, T. A., 1979, Astron. Astrophys. **71**, 29.
Lozinskaya, T. A., 1992, *Supernovae and Stellar Winds in the Interstellar Medium* (AIP, New York).
Lozinskaya, T. A., and S. V. Repin, 1990, Astron. Zh. **67**, 1152 [Sov. Astron. **34**, 580 (1990)].
Lozinskaya, T. A., and T. G. Sitnik 1988, Astron. Zh. Lett. **14**, 240 [Sov. Astron. Lett. **14**, 100 (1988)].
Lundqvist, P., and C. Fransson, 1991, Astrophys. J. **380**, 575.
Luo, D., and R. McCray, 1991a, Astrophys. J. **372**, 194.
Luo, D., and R. McCray, 1991b, Astrophys. J. **379**, 659.
MacCormack, R. W., 1971, in *Proceedings of the 2nd International Conference on Numerical Methods in Fluid Dynamics*, Lecture Notes in Physics No. 8, edited by Maurice Holt (Springer, Heidelberg/Berlin), p. 151.
Mac Low M.-M., and R. McCray, 1988, Astrophys. J. **324**, 776.
Mac Low, M.-M., R. McCray, and M. L. Norman, 1989, Astrophys. J. **337**, 141.
Mac Low, M.-M., C. F. McKee, R. I. Klein, J. M. Stone, and M. L. Norman, 1994, Astrophys. J. **433**, 757.
Mac Low, M.-M., D. van Buren, D. O. S. Wood, and E. Churchwell, 1991, Astrophys. J. **369**, 395.
Maeder, A., 1988, Astron. Astrophys. Suppl. Ser. **76**, 411.
Manchester, R. N., 1987, Astron. Astrophys. **171**, 205.
Markert, T. H., C. R. Canizares, G. W. Clark, and P. F. Winkler, 1983, Astrophys. J. **268**, 134.
Mashchenko, S. Ya., and S. A. Silich, 1994, Astron. Zh. **71**, 237.
Mashchenko, S. Ya. and S. A. Silich, 1995, Astron. Zh., in press.
Mathews, W. G., and J. C. Baker, 1971, Astrophys. J. **170**, 241.
McCray, R., 1993 Annu. Rev. Astron. Astrophys. **31**, 175.
McCray, R., and M. Kafatos, 1987, Astrophys. J. **317**, 190.
McKee, C. F., 1982, in *Supernovae. A Survey of Current Research*, edited by M. Rees and R. Stoneham (Reidel, Dordrecht), p. 433.
McKee, C. F., and L. L. Cowie, 1977, Astrophys. J. **215**, 213.
McKee, C. F., and J. P. Ostriker, 1977, Astrophys. J. **218**, 148.
Meaburn, J., 1980, Mon. Not. R. Astron. Soc. **192**, 365.
Meaburn, J., and D. C. Terrett, 1980, Astron. Astrophys. **89**, 126.
Morris, M., 1981, Astrophys. J. **249**, 572.
Morton, D. C., 1967, Astrophys. J. **150**, 535.
Nadyozhin, D. K., 1985, Astrophys. Space Sci. **112**, 225.
Norman, M. L., and K.-H. A. Winkler, 1986, in *Astrophysical Radiation Hydrodynamics*, edited by K.-H. A. Winkler and M. L. Norman (Reidel, Dordrecht), p. 187.
Oey, M. S., and P. Massey, 1994, Astrophys. J. **425**, 635.
Oort, J. H., 1977, Annu. Rev. Astron. Astrophys. **15**, 295.
Oort, J. H., 1978, Phys. Scr. **17**, 175.
Ostriker, J. P., and C. F. McKee, 1988, Rev. Mod. Phys. **60**, 1.
Paczynski, B., 1986, Astrophys. J. Lett. **308**, L43.
Palouš, J., 1990, in *The Interstellar Disk-Halo Connection in Galaxies*, edited by H. Bloemen (Srerrewacht, Leiden), p. 101.
Palouš, J., 1992, in *Evolution of Interstellar Matter and Dynamics of Galaxies*, edited by J. Palouš, W. B. Burton, and P. O. Lindblad (Cambridge University, Cambridge, England) p. 65.
Palouš, J., J. Franco, and G. Tenorio-Tagle, 1990, Astron. Astrophys. **227**, 175.
Panagia, N., K. Gilmozzi, F. Macchetto, H.-M. Adorf, and R. P. Kirshner, 1991, Astrophys. J. Lett. **380**, L23.

Pas'ko, V. P., and S. A. Silich, 1986, Kinematika i Fizika Nebes. Tel **2**, N3, 15 [Kinematics and Physics of Celestial Bodies **2**, N3, 15 (1986)].
Pas'ko, V. P., and S. A. Silich, 1988, Kinematika i Fizika Nebes. Tel **4**, N2, 85 [Kinematics and Physics of Celestial Bodies **4**, N2, 88 (1988)].
Pikel'ner, S. B., 1968, Astrophys. Lett. **2**, 97.
Pikel'ner, S. B., and P. V. Shcheglov, 1968, Astron. Zh. **45**, 953 [Sov. Astron. **12**, 757 (1969)].
Prilutski, O. F., and V. V. Usov, 1975, Astrophys. Space Sci. **34**, 395.
Puche, D., D. Westpfahl, E. Brinks, and J-R. Roy, 1992, Astron. J. **103**, N6, 1841.
Puche, D., and D. Westpfahl, 1995, unpublished.
Pye, J. P., K. A. Pounds, D. P. Rolf, F. D. Seward, A. G. Smith, and R. Willingale, 1981, Mon. Not. R. Astron. Soc. **194**, 569.
Raga, A., 1986, Astrophys. J. **300**, 745.
Rand, R. J., and S. Kulkarni, 1989, Astrophys. J. **343**, 760.
Raymond, I. C., and B. W. Smith, 1977, Astrophys. J. Suppl. Ser. **35**, 419.
Reid, M. J., and P. T. P. Ho, 1985, Astrophys. J. Lett. **288**, L17.
Reynolds, R. J., 1989, Astrophys. J. **339**, L29.
Ride, S. K., and A. B. Walker, 1977, Astron. Astrophys. **61**, 339.
Roger, R. S., D. K. Milne, M. J. Kesteven, K. J. Wellington, and R. F. Haynes, 1988, Astrophys. J. **332**, 940.
Rosado, M., 1989, Rev. Mex. Astron. Astrof. **18**, 105.
Rosado, M., E. Le Coarer, and Y. P. Georgelin, 1994, Rev. Mex. Astron. Astrofis. **29**, 97.
Sakashita, S., and H. Hanami, 1986, Publ. Astron. Soc. Jpn. **38**, 879.
Schiano, A.K.R., 1985, Astrophys. J. **299**, 24.
Sedov, L. I., 1946, Dokl. Akad. Nauk SSSR **42**, 17.
Sedov, L. I., 1959, *Similarity and Dimensional Methods in Mechanics* (Academic, New York).
Seward, F. D., 1990, Astrophys. J. Suppl. Ser. **73**, 781.
Shapiro, P.R., 1979, Astrophys. J. **233**, 831.
Shostak, G. S., and H. van Woerden, 1983, in *Proceedings of the 1983 International Symposium on Kinematics and Dynamics of Galaxies*, edited by E. Athanassoula (Reidel, Dordrecht), p. 33.
Silich, S. A., 1985, Kinematika i Fizika Nebes. Tel **1**, N6, 37 [Kinematics and Physics of Celestial Bodies **1**, N6, 36 (1985)].
Silich, S. A., 1990, in *Structure and Evolution of the Regions of Star Formation*, edited by I. G. Kolesnik (Naukova Dumka, Kiev), p. 161.
Silich, S. A., 1992a, in *Evolution of Interstellar Matter and Dynamics of Galaxies*, edited by J. Palouš, W. B. Burton, and P. O. Lindblad (Cambridge University, Cambridge, England) p. 72.
Silich, S. A., 1992b, Astrophys. Space. Sci. **195**, 317.
Silich, S. A., and P. I. Fomin, 1983, Dokl. Akad. Nauk SSSR **268**, 861 [Sov. Phys. Dokl. **28**, 157 (1983)].
Silich, S. A., J. Franco, J. Palouš, and G. Tenorio-Tagle, 1994, in *Violent Star Formation from 30 Doradus to QSOs*, edited by G. Tenorio-Tagle (Cambridge University, Cambridge, England), p. 162.
Singh, R. P., D. N. Nousek, D. N. Burrows, and G. P. Garmire, 1987, Astrophys. J. **313**, 185.
Solomon, P. M., and D. B. Sanders, 1980, in *Giant Molecular Clouds in the Galaxy. Third Gregynog Astrophysics Workshop*, edited by P. M. Solomon and M. G. Edmunds (Pergamon New York), p. 41.
Spitzer, L., 1962, *Physics of Fully Ionized Gases* (Interscience, New York).
Spitzer, L., 1978, *Physical Processes in the Interstellar Medium* (Wiley, New York).
Stepanov, V. V., 1958, *A Course of Differential Equations* (Nauka, Moscow).
Storey, M. C., L. Stavelley-Smith, R. N. Manchester, and M. J. Kesteven, 1992, Astron. Astrophys. **265**, 752.
Stothers, R., 1972, Astrophys. J. **175**, 431.
Suzuki, T., T. Shigeyama, and K. Nomoto, 1993, Astron. Astrophys. **274**, 883.
Taylor, G. I., 1950, Proc. R. Soc. London, Ser. A **201**, N1065, 159.
Tenorio-Tagle, G., 1979, Astron. Astrophys. **71**, 59.
Tenorio-Tagle, G., 1980, Astron. Astrophys. **88**, 61.
Tenorio-Tagle, G., 1981, Astron. Astrophys. **94**, 338.
Tenorio-Tagle, G., and P. Bodenheimer, 1988, Annu. Rev. Astron. Astrophys. **26**, 145.
Tenorio-Tagle, G., P. Bodenheimer, and M. Różyczka, 1987, Astron. Astrophys. **182**, 120.
Tenorio-Tagle, G., P. Bodenheimer, M. Różyczka, and J. Franco, 1986, Astron. Astrophys. **170**, 107.
Tenorio-Tagle, G., and J. Palouš, 1987, Astron. Astrophys. **186**, 287.
Tenorio-Tagle, G., M. Różyczka, J. Franco, and P. Bodenheimer, 1991, Mon. Not. R. Astron. Soc. **251**, 318.
Tenorio-Tagle, G., M. Różyczka, and P. Bodenheimer, 1990, Astron. Astrophys. **237**, 207.
Timochin, A. N., and G. S. Bisnovatyi-Kogan, 1995, Astrophys. Space. Sci., in press.
Tomisaka, K., 1991, Astrophys. J. Lett. **361**, L5.
Tomisaka, K., 1992, Publ. Astron. Soc. Jpn. **44**, 177.
Tomisaka, K., and J. N. Bregman, 1993, Publ. Astron. Soc. Jpn. **45**, 513.
Tomisaka, K., A. Habe, and S. Ikeuchi, 1981, Astrophys. Space Sci. **78**, 273.
Tomisaka, K., and S. Ikeuchi, 1986, Publ. Astron. Soc. Jpn. **38**, 697.
Tomisaka, K., and S. Ikeuchi, 1988, Astrophys. J. **330**, 695.
Tsunemi, H., and H. Inoue, 1980, Publ. Astron. Soc. Jpn. **32**, 247.
Tuohy, I. R., D. H. Clark, and W. M. Burton, 1982, Astrophys. J. Lett. **260**, L65.
van Buren, D., and R. McCray, 1988, Astrophys. J. Lett. **239**, L93.
van Buren, D., M.-M. Mac Low, D. O. S. Wood, and E. Churchwell, 1990, Astrophys. J. **353**, 570.
van Leer, B., 1977, J. Comp. Phys. **23**, 276.
Veilleux, S., G. Cecil, J. Bland-Hawthorn, and R. B. Tully, 1994, Astrophys. J. **433**, 48.
Wampler, E. J., L. Wang, D. Baade, K. Banse, S. D'Odorico, C. Gouiffes, and M. Tarenghi, 1990, Astrophys. J. **362**, 13.
Wang, L., and P. A. Mazzali, 1992, Nature **355**, 58.
Wang, Q., and D. J. Helfand, 1991, Astrophys. J. **379**, 327.
Wang, Q., T. Hamilton, D. J. Helfand, and X. Wu, 1991, Astrophys. J. **374**, 475.
Weaver, R., R. McCray, J. Castor, P. Shapiro, and R. Moore, 1977, Astrophys. J. **218**, 377.
Weigert, A., and H. J. Wendker, 1989, *Astronomie und Astrophysik ein Grundkurs* (VCH, Weinheim, Germany).
White, R. L., and K. S. Long, 1991, Astrophys. J. **373**, 543.
Wouterloot, J. G. A., J. Brand, W. B. Burton, and K. K.

Kwee, 1990, Astron. Astrophys. **230**, 21.
Wu, C. C., M. Leventhal, C. L. Sarazin, and T. R. Gull, 1983, Astrophys. J. Lett. **269**, L5.
Yorke, H. W., G. Tenorio-Tagle, and P. Bodenheimer, 1983, Astron. Astrophys. **127**, 313.
Zeldovich, Ya. B., and Yu. P. Raizer, 1966, *Physics of Shock Waves and High Temperature Phenomena* (Academic, New York).